Design of ballasted railway track foundations using numerical modelling

Part II: Applications

Md. Abu Sayeed

PhD Candidate, Department of Civil Engineering,

Curtin University, WA 6845, Australia

Mobile: +61404214238

E-mail: sayeed.ce00@yahoo.com

Mohamed A. Shahin*

Associate Professor, Department of Civil Engineering,

Curtin University, WA 6845, Australia

Phone: +61-8-9266 1822; Fax: +61-8-9266 2681

E-mail: M.Shahin@curtin.edu.au

*Corresponding author

SUBMITTED TO: **CANADIAN GEOTECHNICAL JOURNAL**

Design of ballasted railway track foundations using numerical modelling

Part II: Applications

Abstract: This paper is the second of two companion papers in relation to a new design method for ballasted railway track foundations. The development of the new design method has been explained in the first paper (i.e., Part I: Development), and the procedures for using the method and its practical application on some field case studies are presented in this paper. Special feature of the proposed design method is that it considers the true impact of train dynamic moving loads and number of repeated applications of the traffic tonnage. The proposed method is then applied to four case studies of actual tracks and the results are compared with field measurements and found to be in good agreement. It should be noted that, although the proposed design method is able to overcome most shortcomings of the existing methods and found to provide excellent outcomes, further verification for more field case studies is highly desirable.

Keywords: Finite elements, numerical modelling, ballasted railway track foundations, dynamic amplification factor, high-speed trains.

Introduction

A new method is developed for design of ballasted railway track foundations for determining the granular ballast layer thickness required to prevent the railway track failures induced by the repeated train (dynamic) moving loads. Two common track failure criteria are considered to govern the new design method, namely the subgrade progressive shear failure and excessive plastic deformation of track substructure. The process leading to development of the new design method, including all affecting design parameters, are studied in detail and presented in a separate companion paper, i.e., Part I: Development (Sayeed and Shahin 2017). In this paper, the design procedures that need to be followed for using the new design method is described and the applicability of the method is verified by conducting a comparison between the method outcomes and field measurements, for some well-documented case studies. The results obtained from the new design method are found to be in good agreement with the field measurements, thus, the method can be used with confident in routine design by practitioners.

Description of design procedures of new proposed method

This section presents detailed procedures for using the new design method of selecting a granular layer thickness with the aid of the design charts developed in the companion paper (i.e., Part I: Development). The method has two design procedures corresponding to two different criteria of preventing railway track failures. One procedure is meant for preventing the progressive shear failure at the top subgrade surface, while the other focusses on preventing the excessive plastic deformation of the track. The thickness of the granular layer that should be used for design should be the maximum thickness obtained from applying the two procedures. It should be noted that if the subgrade is very stiff and dynamic wheel load is low, the obtained design thickness might be very small and in such a case it is suggested to use a standard minimum thickness of granular layer equal to 0.45 m, including 0.30 m of ballast plus 0.15 m of sub-ballast, as suggested by Li et al. (2016). However, if the subgrade is soft (e.g., E_s = 15 MPa, i.e., shear wave speed ≈ 54 m/s), before proceeding to calculate the granular layer thickness using the design charts, the practitioner needs to double check whether the design speed is higher than the critical speed of the train-track-ground condition at hand. To quantify the critical speed of the train-track-ground condition, readers are referred to Sayeed and Shahin (2016). If the design train speed is higher than the critical speed, the soft subgrade will be susceptible to failure and it is thus recommended to improve the subgrade (e.g., by chemical additives) so that the subgrade modulus can be increased and in turn the critical speed becomes higher than the train design speed.

Design procedure for preventing progressive shear failure

The design procedure for preventing the progressive shear failure is based on limiting the cumulative plastic strain at the subgrade surface below a threshold value. As discussed earlier, limiting the cumulative plastic strain is achieved automatically by limiting the deviatoric stress induced by the dynamic train moving loads. Li and Selig (1998a, b) developed a design procedure for preventing this mode of track failure; however, their method has several limitations discussed in the companion paper (i.e., Part I: Development). The intention of the proposed new design method is to overcome most of the current limitations of the available design methods including Li-Selig's method, by providing a methodology that suits the modern railway traffics.

Fig. 1 shows a flowchart that can be used for calculating the granular layer thickness needed to prevent the progressive shear failure. The flowchart has four main steps: (1) data collection and preparation; (2) determination of allowable deviatoric stress; (3) determination of allowable strain influence factor; and (4) selection of the granular layer thickness using the developed design charts. The above steps are described in some detail below.

Step 1: The designer should collect and prepare the following information:

- *Loading conditions*: this requires calculation of the design dynamic wheel load, P_d, and number of equivalent repeated application of wheel load in the subgrade layer, N_s, for a given design traffic tonnage. In order to establish the dynamic wheel load, P_d, it is required to determine the wheel spacing factor (WSF) corresponding to the wheel spacing, which can be obtained from Fig. 12(b) of the companion paper (i.e., Part I: Development). It is also required to determine the dynamic amplification factor (DAF) corresponding to the train speed, which can be obtained from Fig. 13 of the companion paper (i.e., Part I: Development) and best corresponds to the track-ground condition under consideration. The dynamic wheel load, P_d, can then be estimated using Equation (7) of the companion paper (Part I: Development), and the number of load repetitions in the subgrade layer can be calculated using Equation (9) of the companion paper (i.e., Part I: Development). If there are some major groups of wheel loads, the corresponding groups of dynamic wheel loads and number of repeated loads should be determined separately. Equations (10) and (13) of the companion paper (i.e., Part I: Development) have then to be employed to determine the total number of equivalent load applications in the subgrade, Ns, of the wheel load, P_s.

- *Design criterion*: the design proceeds by selecting an acceptable level of the cumulative plastic strain at the subgrade surface, $\varepsilon_{(p\_s)a}$, for certain number of repeated loads (i.e., for the design traffic tonnage).

- *Subgrade characteristics*: this design item requires selection of the subgrade soil type and determination of the soil monotonic strength, σ_{s_s}, from the unconfined compressive strength (UCS) test and soil modulus, E_s, obtained from the cyclic triaxial compression test under a confining pressure equal to 100 kPa.

- *Granular material characteristics*: the mechanical properties of the granular materials in the form of the ballast modulus, E_b, need to be determined from the cyclic triaxial compression test under a confining pressure equal to 100 kPa.

Step 2: The allowable deviatoric stress at the subgrade surface is determined using the following equation developed in the companion paper (i.e., Part I: Development)**:**

$$\sigma_{(d\_s)a} = \left(\frac{\varepsilon_{(p\_s)a}}{aN_s^{\ b}} \right)^{\frac{1}{m}} \sigma_{s\_s} \times 100 \qquad (1)$$

where, $\sigma_{(d\_s)a}$ is the allowable deviatoric stress at the subgrade surface; $\varepsilon_{(p\_s)a}$ is the allowable cumulative plastic strain at the subgrade surface needed to prevent the progressive shear failure; σ_{s_s} is the soil unconfined compressive strength; a, b and m are material parameters pertinent to the subgrade soil type (see Table 2 of the companion paper, i.e., Part I: Development); N_s is the total equivalent number of repeated applications of the design load obtained from Step 1.

Step 3: The allowable strain influence factor at the subgrade surface is determined, using the following equation derived in the companion paper (i.e., Part I: Development):

$$I_{(\varepsilon\_s)a} = \frac{\sigma_{(d\_s)a} \times A}{P_d} \qquad (2)$$

where, $I_{(\varepsilon\_s)a}$ is the allowable strain influence factor based on the allowable deviatoric stress, $\sigma_{(d\_s)a}$, obtained from Step 2; P_d is the design dynamic wheel load obtained from Step 1; and the area coefficient, A = 1 m^2.

Step 4: The required granular layer thickness needed to prevent the progressive shear failure at the subgrade surface is determined, as follows:

- Select a design chart from *Appendix A* (e.g., Fig. 2) that best corresponds to the ballast modulus; and

- Using the design chart, calculate the granular layer thickness corresponding to the modulus of subgrade soil, E_s, and allowable strain influence factor, $I_{(\varepsilon\_s)a}$, obtained from Step 3.

Design procedure for preventing excessive plastic deformation

The design procedure for preventing the excessive plastic deformation of ballast layer is developed in this section. It should be noted that most exiting methods are limited to determination of the subgrade deformation only, although about 40% of the total track deformation may occur from the granular layer (Li et al. 2016; Stewart 1982). The key advantage of the current proposed design method is that the design procedure for preventing the excessive plastic deformation is based on limiting the total plastic deformation including both the ballast and subgrade layers. According to this design criterion and the above procedure, a flowchart for calculating the granular layer thickness is presented in Fig. 3. As it is difficult to assume the exact value of the granular layer thickness initially, this procedure provides an optimum granular layer thickness after several repetitions following Steps 2-4, as follows:

Step 1: Initially, the designer should collect and prepare the required design information, as presented in the previous section, and some other information such as the thickness of the deformable subgrade layer, H_s, ballast type, compressive strength of ballast at 50 kPa confining pressure, σ_{s_b}, and number of load repetitions in the ballast layer, N_b. The number of load repetitions in the ballast layer can be calculated using Equation (8) of the companion paper (i.e., Part I: Development). Similar to the load repetitions in the subgrade soil, if there are some major groups of wheel loads, the corresponding groups of the dynamic wheel loads and number of repeated loads should be determined separately. Afterwards, Equations (11) and (12) of the companion paper (i.e., Part I: Development) can be employed to determine the total number of equivalent repeated load applications of the wheel load on the ballast layer. The design criterion for preventing the progressive shear failure (i.e., allowable plastic strain at the subgrade surface, $\varepsilon_{(p\_s)a}$) is thus substituted by enforcing the allowable total plastic deformation of the track substructure layers, ρ_{ta}.

Step 2: This step is to determine the deformation of granular ballast layer, as follows:

- Assume a granular layer thickness, H_b, equal to the granular layer thickness obtained from the design procedure used earlier for preventing the progressive shear failure.

- Select a suitable chart from *Appendix B* for estimating the distribution of the dimensionless strain influence factor, I_{ε_b}, with depth for the granular the ballast layer (e.g., Fig. 4) that best corresponds to the elastic modulus of the ballast and subgrade, and the granular layer thickness.

- Determine the deformation of the granular ballast layer, ρ_b, using the following equation developed in the companion paper (i.e., Part I: Development):

$$\rho_b = \frac{x[1+\ln(N_b)]^z}{100}\left(\frac{P_d}{A\sigma_{s\_b}}\right)^y \int_0^{H_b} \left(I_{\varepsilon\_b}\right)^y dh \qquad (3)$$

where, P_d is the design dynamic wheel load; σ_{s_b} is the static strength of ballast; N_b is the total number of equivalent repeated load applications of the wheel load for the ballast layer; x, y and z are material parameters for a particular ballast type (see Table 1 of the companion paper, i.e., Part I: Development); H_b is the granular ballast thickness; I_{ε_b} is the distribution of strain influence factor with ballast depth; and A is the area coefficient (= 1 m^2). All corresponding information are obtained from Step 1.

Step 3: This step is to determine the allowable subgrade deformation influence factor, $I_{(\rho\_s)a}$, using the information obtained from Steps 1 and 2 and applying the following equation developed in the companion paper (i.e., Part I: Development):

$$I_{(\rho\_s)a} = \frac{\rho_{ta} - \rho_b}{\frac{aLN_s^{\,b}}{100}\left(\frac{P_d}{A\sigma_{s\_s}}\right)^m} \qquad (4)$$

where, ρ_{ta} is the allowable track deformation; ρ_b is the contribution to track deformation by the ballast layer; N_s is the total equivalent number of load repetitions in the subgrade for the design traffic tonnage; P_d is the design dynamic wheel load; σ_{s_s} is the unconfined compressive strength of the soil; *a, b* and *m* are material parameters dependent on the soil type (see Table 2 of the companion paper, i.e., Part I: Development); A is the area coefficient (= 1 m^2); and L is the length coefficient (= 1 m).

Step 4: Finally, determine the required granular layer thickness, H_b, needed to prevent the excessive plastic deformation of the track, as follows:

- Select a suitable design chart from *Appendix C* (e.g., Fig. 5) that best corresponds to the ballast modulus, existing subgrade soil type, and modulus.

- Calculate the granular layer thickness, H_b, corresponding to the allowable deformation influence factor of subgrade and thickness of deformable subgrade layer using the selected design charts.

- Compare the design thickness obtained in this step with the thickness assumed in the calculation of the granular layer deformation in Step 2. If the obtained thickness from Step 4 is not equal to the assumed thickness, then repeat Steps 2-4 until the assumed H_b converges with the design thickness obtained in Step 4. In each iteration, the calculated thickness can be assumed for the next iteration to achieve faster convergence.

Design applications

To validate the proposed design method, it is applied to four well-documented case studies found in the literature and the results obtained are compared with field measurements. These two case studies are for test tracks reported by Li and Selig (1998b), including the Association of American Railroads (AAR) low track modulus (LTM) and trial low track modulus (TLTM). Another two case studies of real track sites at the Northeast Corridor (NC) between Baltimore and Philadelphia are also considered for additional validation of the proposed design method, and results obtained are again compared with field measurements and found to be in good agreement.

LTM and TLTM tracks

In 1991, a 183 m long low track modulus (LTM) test track was built on a fat clay type subgrade at the Association of American Railroads (AAR) Heavy Tonnage Loop (HTL) in Pueblo, Colorado. The information needed for design of these ballasted tracks are given in Table 1. Prior to the construction of the LTM, a 30 m long trial low track modulus (TLTM) test track was constructed to examine the practicality of building a longer LTM track. The key objective of constructing the LTM test track was to investigate the impact of soft subgrade on track performance under repeated heavy axle train (HAT) moving loads (Li and Selig 1996). The subgrade soil at the Pueblo test track site was originally silty sand, which does not represent a soft subgrade soil. To construct a track on soft subgrade soil, a 3.66 m wide and 1.5 m deep trench was dug in the natural subgrade and filled with the Mississippi buckshot clay of liquid limit (*LL* = 60~70) and plasticity index (*PI* = 40~45). To achieve a subgrade of low stiffness, the filled material within the trench was compacted with the water content (30%) and dry density at 90% of its maximum dry density, which according to the ASTM D698 was found to be 14.91 kN/m^3. Although the water content for both the LTM and TLTM subgrades was targeted to be 30%, the average water contents in the LTM and TLTM subgrades were actually 33% and 29%, respectively (Li and Selig 1996). Hence, the corresponding unconfined compressive strength of subgrade soil was about 90 kPa for the LTM track and 166 kPa for the TLTM track. The relevant soil modulus of the LTM track subgrade varied from 14 MPa to 21 MPa, while it was in the range of 41MPa to 55 MPa for the TLTM track. The difference between these two track sites was in their subgrade modulus and unconfined compressive strength (see Table 1). Accordingly, the design thickness for each track is expected to be different.

Step-by-step calculation for preventing progressive shear failure

Step 1: At first, the information needed for design of ballasted railway track foundations (i.e., loading condition, design criteria, ballast and subgrade material characteristics) are specified and listed in Table 1. For train geometry, the value of wheel spacing factor (WSF) corresponding to a wheel spacing of 1.8 m is found to be 1.38 (obtained from Fig. 12b of the companion paper, i.e., Part I: Development). Also, for this particular track-ground condition, the value of dynamic amplification factor (DAF) corresponding to the train speed is obtained to be 1.04, using Fig. 13 of the companion paper (i.e., Part I: Development). Afterwards, the design dynamic wheel load, P_d, is calculated to be 250 kN using Equation (7) of the companion paper (i.e., Part I: Development). The equivalent number of load repetitions in the subgrade layer is determined using Equation (9) of the companion paper (i.e., Part I: Development) to be N_s = 386,000.

Step 2: Considering the appropriate respective design parameters and number of load repetitions, N_s, obtained in Step 1, the allowable deviatoric stress at the subgrade surface, $\sigma_{(d\_s)a}$, is calculated using Equation (1) to be 41 kPa and 76 kPa for the LTM and TLTM tracks, respectively.

Step 3: The allowable strain influence factors corresponding to the allowable deviatoric stresses, $\sigma_{(d\_s)a}$, and design dynamic wheel load, P_d, are determined using Equation (2) to be $I_{(\varepsilon\_s)a}$ = 0.16 for the LTM track and 0.31 for the TLTM track.

Step 4: The design chart A2 of *Appendix A* is selected as it corresponds to ballast modulus E_b = 270 MPa, for both the LTM and TLTM tracks (see Fig. 2). The required granular layer thickness for the LTM track needed to prevent the progressive shear failure is determined for I_{ε_s} = 0.16 and E_s = 15 MPa, and is found to be H_b = 0.53 m. Similarly, using the same design chart, the required granular layer thickness for the TLTM track is found to be H_b = 0.40 m considering I_{ε_s} = 0.31, E_s = 41 MPa and E_b = 270 MPa.

Step-by-step calculation for preventing excessive plastic deformation

Step 1: This step is similar to Step 1 in the design procedure for preventing the progressive shear failure. Therefore, the design dynamic wheel load is obtained to be P_d = 250 kN and the equivalent number of load repetitions in the subgrade to be N_s = 386,000. Moreover, the number of load repetitions in the ballast layer is determined using Equation (8) of the companion paper (i.e., Part I: Development) to be N_b = 772000.

Step 2: At first, the granular layer thickness is assumed to be equal to the thickness obtained from the design procedure for preventing the progressive shear failure (i.e., H_b = 0.53 m for the LTM track and H_b = 0.40 m for the TLTM track). For the LTM track with E_b = 270 MPa, H_b = 0.53 m and E_s = 15 MPa, the distribution of the dimensionless strain influence factor, I_{ε_b}, with the ballast depth is obtained from *Appendix* B (Charts B7 and B8). Afterwards, for the granite ballast (assumed), the deformation of the ballast layer, ρ_b, is determined using Equation (3) to be 0.011 m, considering σ_{s_b} = 307 kPa, P_d = 250 kN and N_b = 772,000. Similarly, for the TLTM track with E_b = 270 MPa, H_b = 0.40 m and E_s = 41 MPa, the distribution of dimensionless strain influence factor, I_{ε_b}, with ballast depth is obtained from *Appendix* B (Charts B6 and B7). Afterwards, the deformation of the ballast layer is determined using Equation (3) to be 0.006 m.

Step 3: For the LTM track loading and subgrade conditions (i.e., P_d = 250 kN, N_s = 386000, CH type subgrade and σ_{s_s} = 90 kPa) and the design criterion of ρ_{ta} = 0.025 m, the allowable subgrade deformation influence factor, $I_{(\rho\_s)a}$, is obtained to be 0.01 using

Equation (4). Likewise, for the TLTM track, the allowable subgrade deformation influence factor is obtained using Equation (4) to be $I_{(\rho\_s)a}$ = 0.06 for P_d = 250 kN, N_s = 386000, CH type subgrade, and σ_{s_s} = 165 kPa.

Step 4: To determine the design thickness, chart C21 from *Appendix C* [see Fig. 5(a)] is selected which best corresponds to the LTM track substructure conditions (i.e., E_b = 270 MPa, E_s = 15 MPa, and CH soil). From this chart, the required granular layer thickness corresponding to the deformable subgrade layer (i.e., H_s = 1.5 m and $I_{(\rho\_s)a}$ = 0.01 obtained in Step 3), is found to be H_b = 0.66 m. As the obtained thickness is not equal to assumed thickness (i.e. obtained $H_b \neq H_b$ of Step 1), Step 2 (i.e., calculation of granular ballast deformation, ρ_b) is repeated considering the granular ballast thickness obtained in Step 4 (i.e., H_b = 0.66 m). After several repetitions of Steps 2−4, the granular layer thickness for the LTM track is obtained to be H_b = 0.70 m. Similarly, for the TLTM track with E_b = 270 MPa, E_s = 41 MPa, and CH soil, Fig. 5(b) is selected from *Appendix C.* Employing the selected design chart, the required granular layer thickness is determined corresponding to the deformable subgrade layer (i.e., H_s = 1.5 m and $I_{(\rho\_s)a}$ = 0.06) to be H_b = 0.25 m. Again, as the obtained $H_b \neq H_b$ of Step 1, Steps 2-4 are repeated. Finally, the required granular layer thickness needed to prevent the excessive plastic deformation is calculated to be H_b = 0.30 m.

Design thickness

As presented above, the granular layer thickness required to prevent the excessive plastic deformation (i.e., H_b = 0.70 m) for the LTM track is higher than that needed to prevent the progressive shear failure (i.e., H_b = 0.53 m). Thus, the design thickness is the maximum of the two obtained results (i.e., H_b = 0.70 m). On the other hand, for the TLTM track, the granular layer thickness required to prevent the excessive plastic deformation (i.e., H_b = 0.30

m) is less than that needed to prevent the progressive shear failure (i.e., H_b = 0.40 m). Hence, the design thickness to be used is H_b = 0.40 m.

Comparisons between proposed design method and field measurements

Based on the design criteria for preventing the progressive shear failure (i.e., $\varepsilon_{(p\_s)a} \leq 2\%$) and for preventing the excessive plastic deformation (i.e., $\rho_{ta} \leq 0.025$ m), the required granular layer thickness for the LTM and TLTM tracks are determined to be H_b = 0.70 m and 0.40 m, respectively, as calculated in the earlier section. In reality, during the construction of both the LTM and TLTM tracks, a granular layer of 0.45 m thickness (0.30 m ballast and 0.15 m sub-ballast) was adopted based on an assumption of 30% water content in the subgrade soil and minimum density of 90% of the standard maximum dry density. Afterwards, the track response in these sites was measured and the subgrade conditions were evaluated experimentally, which provide an excellent opportunity to assess the proposed design method. From the field measurements, it was found that the LTM track with the adopted granular layer thickness of 0.45 m was unable to bear the HAL for design traffic of 60 MGT, and thus had difficulty in sustaining the required track surface geometry. The LTM track subgrade suffered rapid progressive shear failure and excessive plastic deformation. Therefore, the test track needed frequent rail lifting by ballast tamping. Fig. 6 shows the cumulative track settlement with the traffic loading for the LTM track (Li 1994). It can be seen that the track actually required frequent ballast tamping and surfacing (rail lift up) following 12.4 MGT, and finally, the traffic along the track had to be stopped after approximately 62.3 MGT and the test track was then rebuilt. On the other hand, the TLTM track with the same granular layer thickness of 0.45 m was able to carry the HAL for design traffic of 60 MGT without any track failure. Consequently, no major track maintenance was invoked during the design life of this track.

A comparison between the originally adopted H_b and that obtained from design (see Table 2) indicates that the adopted thickness for the LTM track of 0.45 m was much less than the required thickness of 0.70 m, but the adopted thickness for the TLTM track of 0.45 m was higher than the required thickness of 0.40 m. Therefore, the LTM track was unable to maintain the track geometry and invoked maintenance, whereas the TLTM track was able to sustain the required track geometry without any maintenance. In other words, the proposed design method was successful in predicting the failure of the LTM track and the proper thickness of the TLTM track. These results are extremely encouraging for the proposed design method.

As an additional validation tool, the actual LTM track-subgrade condition with the adopted 0.45 m granular layer thickness is simulated using the 3D FE modelling and the distribution of the strain influence factor with depth in the ballast and subgrade layers is obtained. Then, the cumulative vertical track deflections for the ballast and subgrade layers at different traffic loads are computed using the results obtained from the 3D FE modelling as well as the following equation developed in the companion paper (i.e., Part I: Development):

$$\rho_t = \frac{x\left[1+\ln(N_b)\right]^z}{100}\left(\frac{P_d}{A\sigma_{s\_b}}\right)^y \int_0^{H_b}\left(I_{\varepsilon\_b}\right)^y dh + \frac{aLN_s^{\,b}}{100}\left(\frac{P_d}{A\sigma_{s\_s}}\right)^m \int_0^{H_s}\left(I_{\varepsilon\_s}\right)^m \frac{dh}{L} \quad (5)$$

The cumulative track deflections are then plotted against the traffic load in MGT and compared with the field measurements available in the literature (Li 1994), as shown in Fig. 7. It can be clearly seen that good agreement exists between the FE predictions and field measurements, which confirms that the validity of the FE modelling process and improved empirical models for predicting the cumulative plastic deformation of ballast and subgrade adopted in this study. This indicates that the design method developed in this study based on the combined FE modelling and improved empirical models is reliable and can be used with confidence to predict the railway track behavior.

Northeast Corridor track

In this section, two more case studies of real track sites at the Northeast Corridor (NC) between Baltimore and Philadelphia are used for further validation of the proposed method. One of the two sites is located at Edgewood, Maryland, and the other site is located at Aberdeen, Maryland, some 16 km apart from the Edgewood site. The track in Edgewood site suffered frequent bouts of differential settlements over a distance of approximately 10 km. This track site needed frequent maintenance by ballast tamping at least twice a year. Moreover, remedy measures such as application of geotextiles and lime slurry injection were taken since 1984; however, such remedies were not fruitful. For the other site at Aberdeen, only a small portion of the track (about 60 m long) suffered a problem of mud pumping; however, the geometry deterioration was not a concern (Li and Selig 1998b).

To investigate the key reasons for track failures at both sites, the loading characteristics and material properties were studied by Li and Selig (1994). Based on the information available in the literature, the minimum required granular layer thickness for both sites are determined using the current proposed design method. At the Edgewood site, the subgrade soil was lean clay (LC) with unconfined compressive strength of approximately 48-83 kPa. On the other hand, the subgrade soil at the Aberdeen site was also lean clay but its unconfined compressive strength was in the range of 97−290 kPa. The subgrade soil properties and other information required for design of tracks at both sites are given in Table 3. As both sites were parts of the NC and not far away from each other, the traffic was the same. The traffic along the NC track was mixed (50% passenger trains and 50% freight trains). Table 4 gives the loading characteristics used for design of these two tracks. As the traffic was mixed, the number of equivalent load applications in the ballast and subgrade layers is determined using Equations (7-13) of the companion paper (i.e., Part I: Development).

Based on the design criteria of preventing the progressive shear failure (i.e. $\varepsilon_{pa} \leq 2\%$) and for preventing the excessive plastic deformation (i.e. $\rho_{ta} \leq 0.025$ m), the required granular layer thicknesses, H_b , for the Edgewood site are determined to be 1.08 m and 1.16 m, respectively. Consequently, the design thickness for this site should be taken as 1.20 m. However, the actual granular layer thickness at the Edgewood site was varied from 0.30 to 0.50 m (from the cone penetration tests and cross trench measurements of the track site), as reported by Li and Selig (1994). This thickness is significantly less than the obtained design thickness of 1.20 m required to reduce the dynamic train induced stresses transmitted to the subgrade to prevent the progressive shear failure and excessive plastic deformation. As a result, it is not surprising that the track of this site has suffered a significant progressive shear failure at the subgrade surface, and deep ballast pockets have also occurred. Moreover, the non-uniform compressive strength of the subgrade (48 kPa to 83 kPa) caused excessive differential track settlement.

For the Aberdeen site, the required granular layer thickness calculated from the proposed design method is H_b = 0.66 m for preventing the progressive shear failure and H_b = 0.60 m for preventing the excessive plastic deformation. Therefore, the design thickness of this site should be $H_b \approx 0.70$ m. From the field measurements reported by Li and Selig (1994), the actual granular layer thickness at this site was varied between 0.70 and 1.0 m, which is equal or larger than the required design thickness. As the dynamic train induced stresses in the subgrade were lower than the allowable value, this track was able to carry the design load without any geometry deterioration. Comparison of the design thickness obtained from the proposed design method and actual thickness at both the Edgewood and Aberdeen sites is summarized in Table 5, which also includes the track conditions for both sites. Evidently, the results of the proposed design method are consistent with the field measurements.

Summary and conclusions

In this paper, step-by-step design procedures were presented for a new design method of ballasted railway track foundations. The new proposed method has substantial benefits over the existing methods in the way at which the railway traffic was characterized and stress was analyzed. In addition, the new method has taken into account the deformation of both the ballast and subgrade layers. The main parameters considered in design include the train speed, track-ground condition, geometry and magnitude of train wheel loads, number of load repetition, as well as modulus, thickness and type of ballast and subgrade. All these parameters considerably affect a safe design for preventing track failures. Design predictions obtained from the developed design method were examined against field measurements for four different case studies and the results were found to be in good agreement. Consequently, the proposed design method can be used with confidence and it is expected to provide a significant contribution to the current railway track code of practice. To facilitate the use of the new design method by practitioners, a user friendly software will be developed in the near future and will be made available upon request.

References

Li, D. 1994. Railway track granular layer thickness design based on subgrade performance under repeated loading. PhD Thesis, Department of Civil and Environmental Engineering. University of Massachusetts, Amherst, Massachusetts, USA.

Li, D., Hyslip, J., Sussmann, T., and Chrismer, S. 2016. Railway Geotechnics. CRC Press, Tailor & Francis Group, Broken Sound Parkway NW, USA.

Li, D., and Selig, E.T. 1994. Investigation of AMTRAK track foundation problems in Edgewood and Aberdeen, MD. Internal Rep. to the Assoc. of Am. Railroads and Amtrak.

Li, D., and Selig, E.T. 1996. Cumulative plastic deformation for fine-grained subgrade soils. Journal of Geotechnical Engineering **122**(12): 1006-1013.

Li, D., and Selig, E.T. 1998a. Method for railroad track foundation design. I: Development. Journal of Geotechnical and Geoenvironmental Engineering **124**(4): 316.

Li, D., and Selig, E.T. 1998b. Method for railroad track foundation design. II: Applications. Journal of Geotechnical and Geoenvironmental Engineering **124**(4): 323.

Li, D., Sussmann, T.R., and Selig, E.T. 1996. Procedure for railway track granular layer thickness determination. Association of American Railroads, Transportation Technology Center. Report No. R-898.

Sayeed, M.A., and Shahin, M.A. 2016. Three-dimensional numerical modelling of ballasted railway track foundations for high-speed trains with special reference to critical speed. Transportation Geotechnics **6**: 55-65. doi: http://dx.doi.org/10.1016/j.trgeo.2016.01.003.

Sayeed, M.A., and Shahin, M.A. 2017. Design of ballasted railway track foundations using numerical modelling: Part I-Development. Canadian Geotechnical Journal, doi: 10.1139/cgj-2016-0633.

Stewart, H.E. 1982. The prediction of track performance under dynamic traffic loading. *In* Department of Civil Engineering. University of Massachusetts, Amherst, Massachusetts, USA.

List of symbols

a	material parameter pertinent to the subgrade soil type
b	material parameter pertinent to the subgrade soil type
m	material parameter pertinent to the subgrade soil type
x	material parameter dependent on ballast type
y	material parameter dependent on ballast type
z	material parameter dependent on ballast type
A	area coefficient
E_b	ballast modulus
E_s	subgrade soil modulus
H_b	granular layer thickness
H_s	subgrade thicknesses
L	length coefficient
L_a	wheel spacing
N_b	number of load applications in the ballast layer
N_s	number of load applications in the subgrade layer
P_d	design dynamic wheel load
P_s	maximum static wheel load
$\varepsilon_{(p\_s)a}$	allowable subgrade surface cumulative plastic strain
$\sigma_{(d\_s)a}$	allowable deviatoric stress at the subgrade surface
σ_{s_b}	compressive strength of ballast at 50 kPa confining pressure
σ_{s_s}	unconfined compressive strength of the soil
ρ_b	deformation of granular ballast layer
ρ_{ta}	allowable total plastic deformation of the track
I_{ε_b}	strain influence factor in the granular layer
$I_{(\varepsilon\_s)a}$	allowable subgrade surface strain influence factor
$I_{(\rho\_s)a}$	allowable subgrade deformation influence factor

Figure captions

Fig. 1. Flowchart of design of railway track foundations for preventing the progressive shear failure of track subgrade.

Fig. 2. Typical example of design chart to calculate the granular layer thickness for preventing the progressive shear failure of track subgrade (obtained from *Appendix* A, Chart A2).

Fig. 3. Flowchart of design of railway track foundations for preventing the excessive track deformation.

Fig. 4. Distribution of strain influence factor with depth for the ballast layer.

Fig. 5. Typical examples of design charts to calculate the granular layer thickness for preventing the excessive track deformation (obtained from *Appendix* C, Charts C21 and C25).

Fig. 6. Field measurements of average settlement and lift-up of rail with traffic load for the LTM test track (redrawn from Li 1994).

Fig. 7. Comparison between new design method and field measurements.

Table captions

Table 1. Design parameters for the LTM and TLTM test tracks (adapted from Li et al. 1996).

Table 2. Design results and track conditions for the LTM and TLTM test tracks.

Table 3. Design parameters for tracks at Edgewood and Aberdeen sites (adapted from Li and Selig 1998b).

Table 4. Traffic characteristics at the Northeast Corridor between Baltimore and Philadelphia (adapted from Li and Selig 1998b).

Table 5. Comparison of results between new design method and site conditions for tracks at Edgewood and Aberdeen sites.

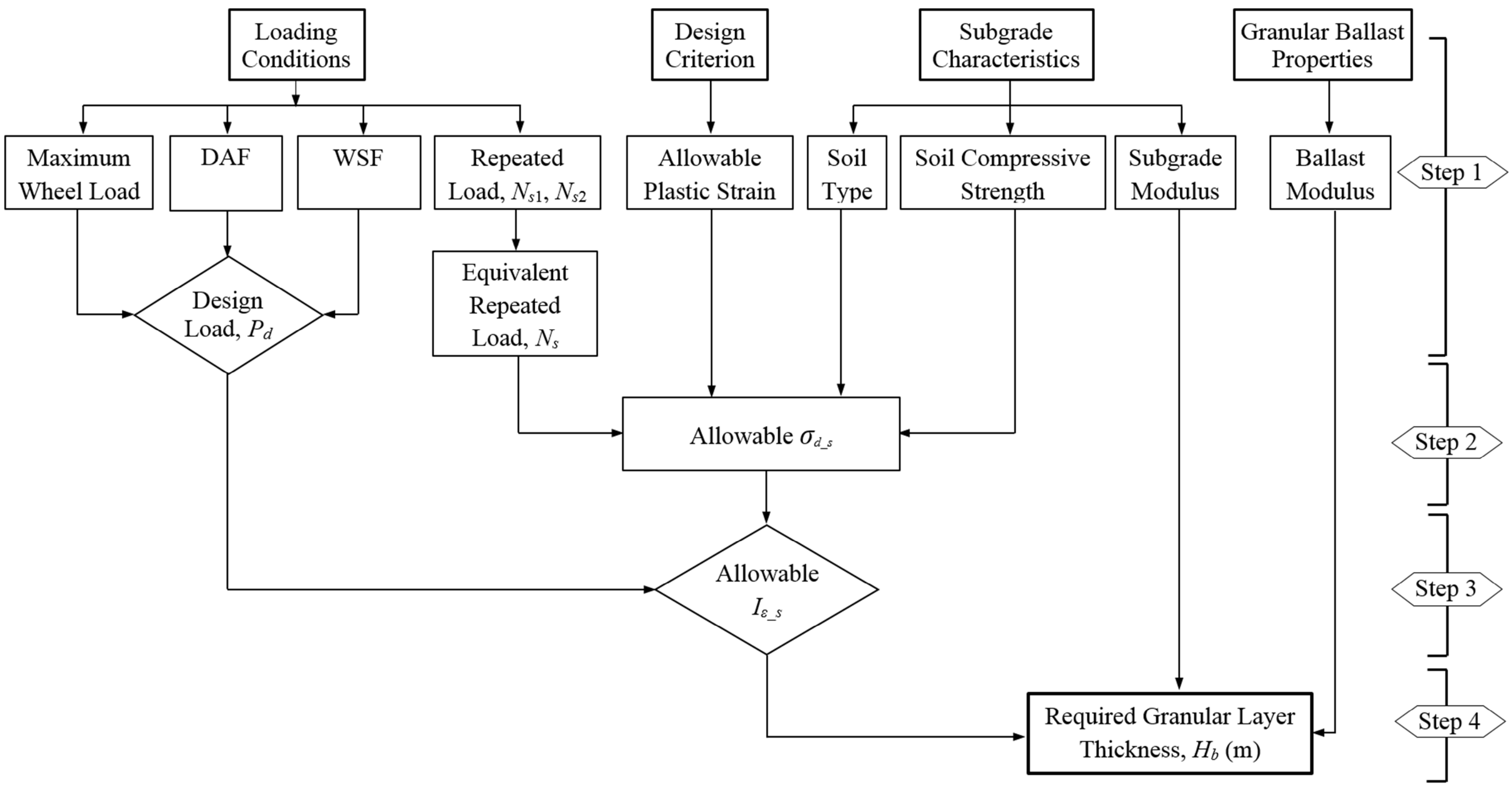

Fig. 1. Flowchart of design of railway track foundations for preventing the progressive shear failure of track subgrade.

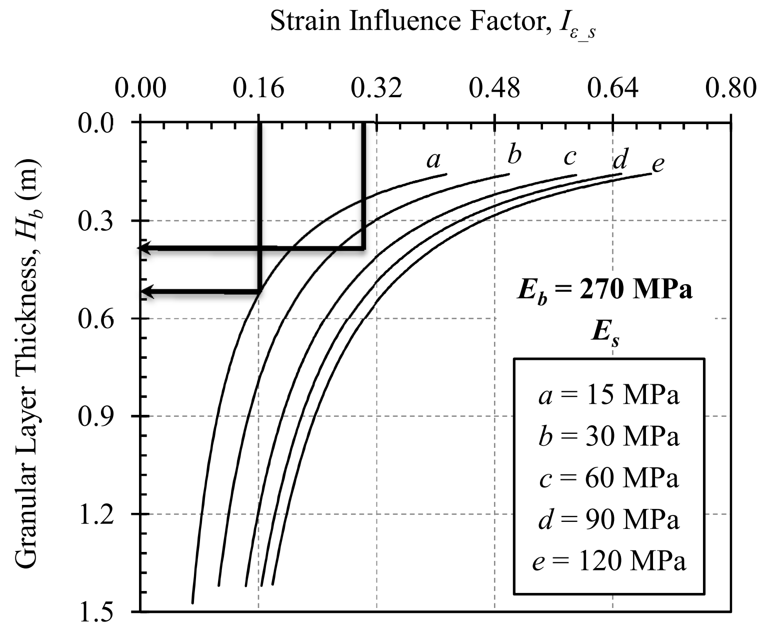

Fig. 2. Typical example of design chart to calculate the granular layer thickness for preventing the progressive shear failure of track subgrade (obtained from *Appendix A*, Chart A2).

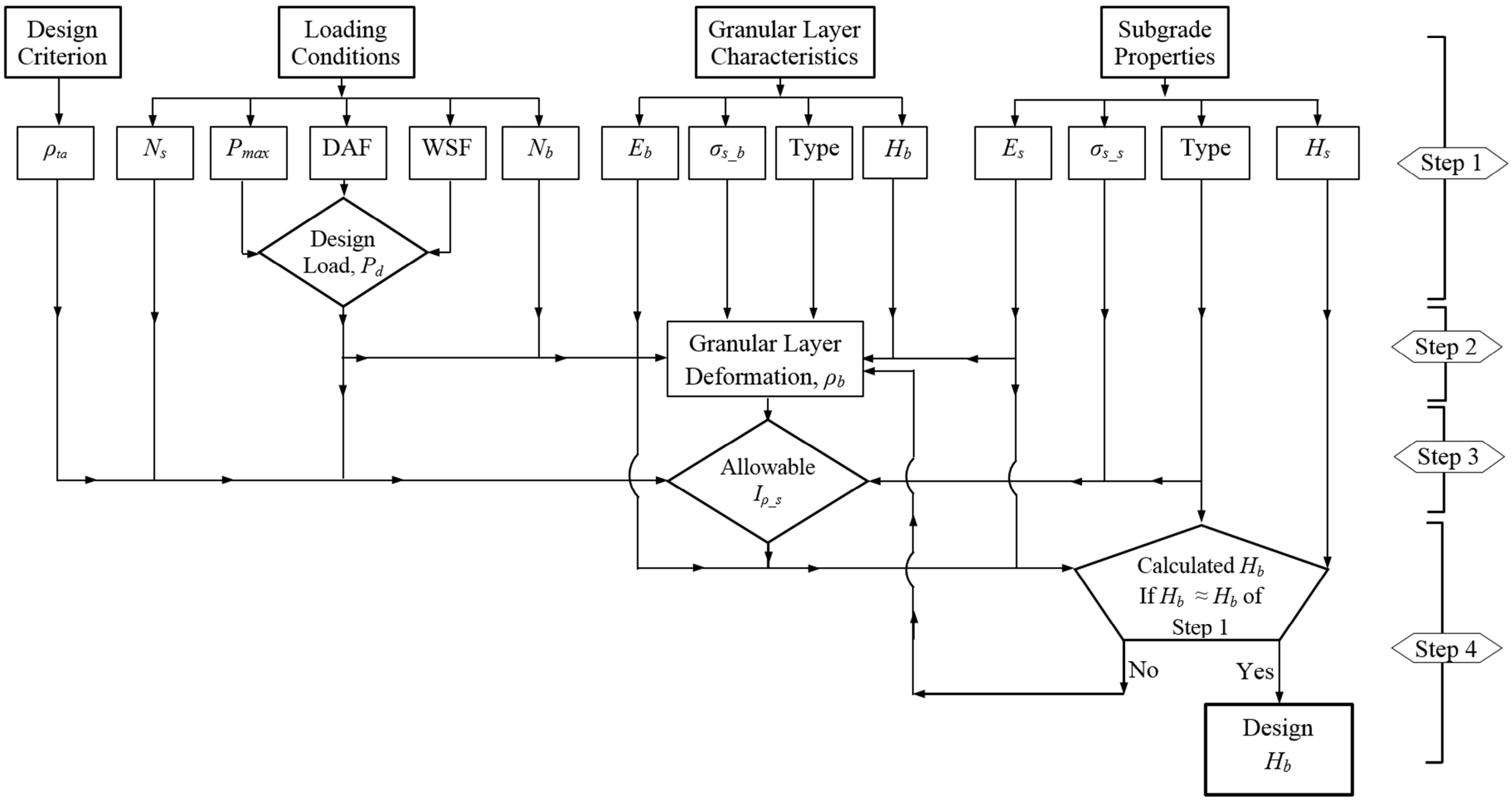

Fig. 3. Flowchart of design of railway track foundations for preventing the excessive track deformation.

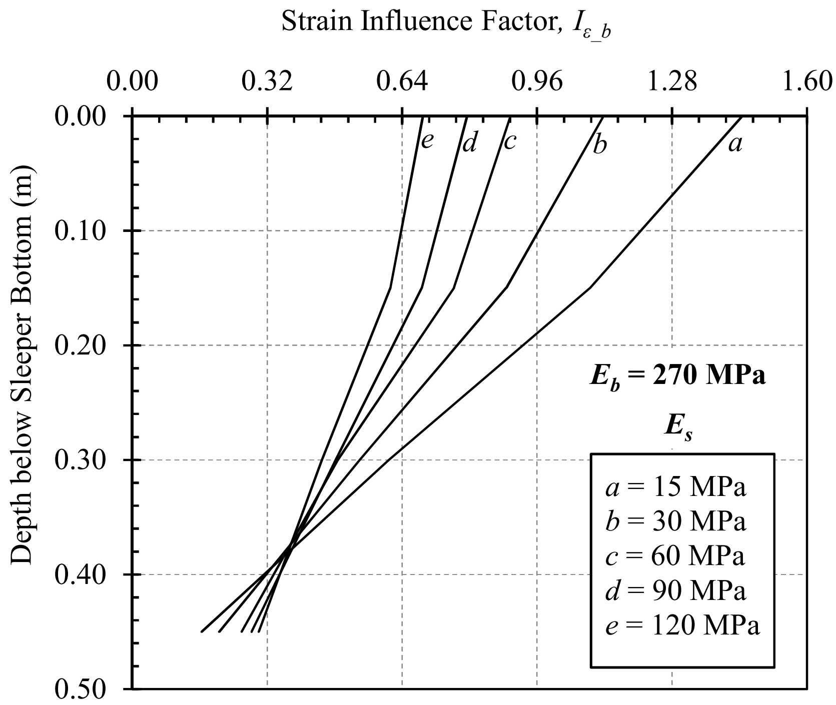

Fig. 4. Distribution of strain influence factor with depth for the ballast layer.

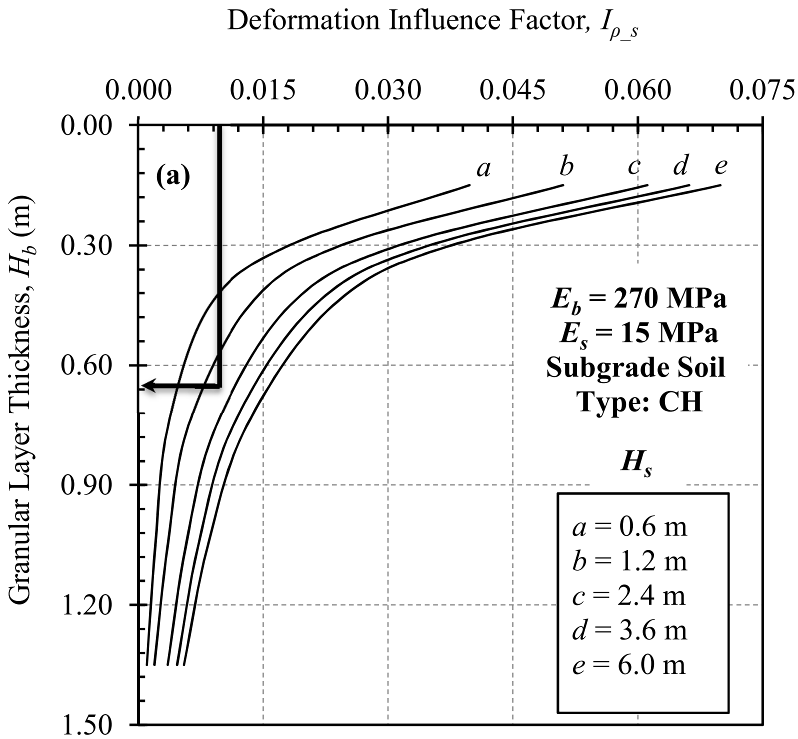

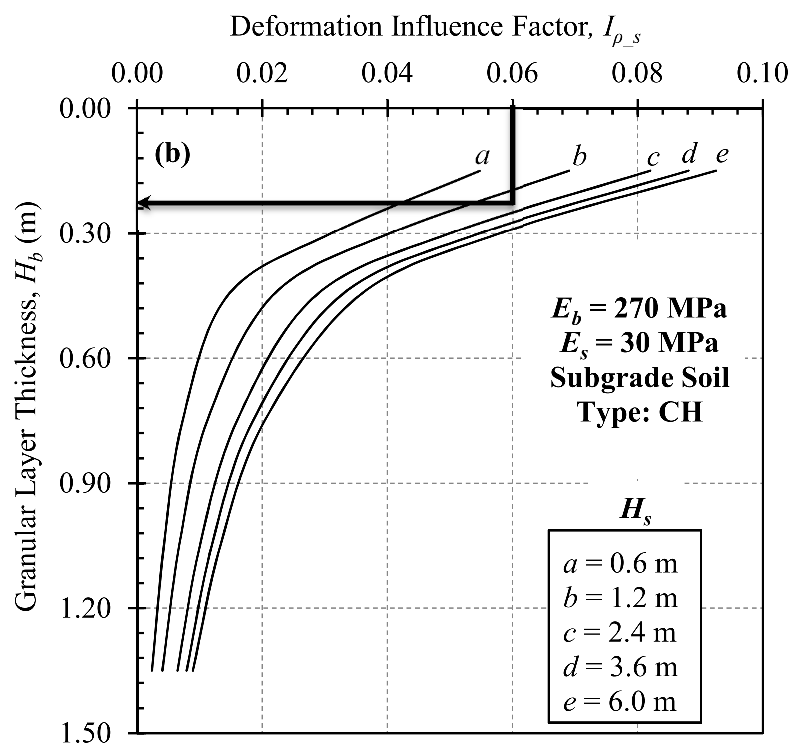

Fig. 5. Typical examples of design charts to calculate the granular layer thickness for preventing the excessive track deformation (obtained from *Appendix C*, Charts C21 and C25).

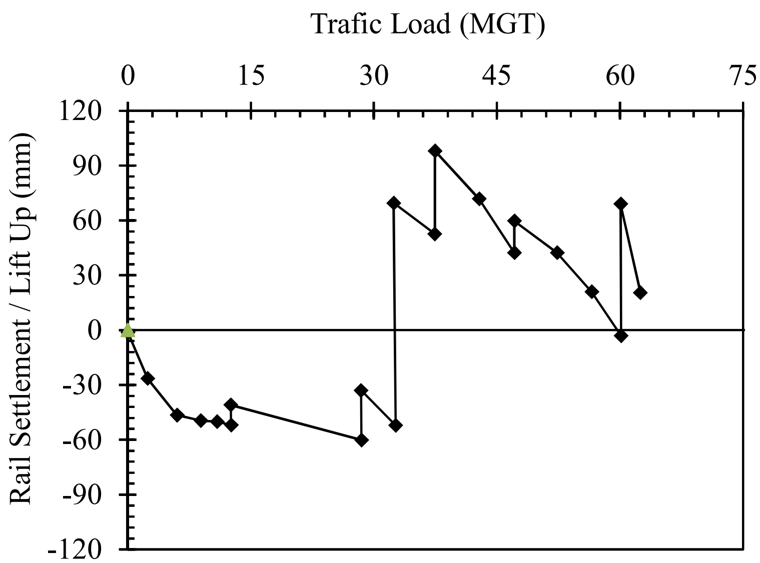

Fig. 6. Field measurements of average settlement and lift-up of rail with traffic load for the LTM test track (redrawn from Li 1994).

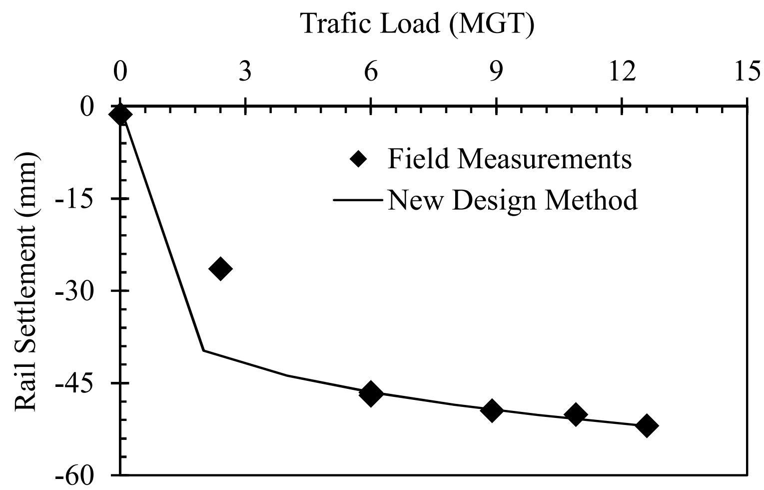

Fig. 7. Comparison between new design method and field measurements.

Table 1. Design parameters for the LTM and TLTM test tracks (adapted from Li et al. 1996).

Design parameters	LTM	TLTM
Loading condition		
Static wheel load, P_s (kN)	173	173
Wheel spacing, L_a (m)	1.8	1.8
Train speed, (m/s)	18	18
Design tonnage (MGT)	60	60
Design criteria		
Cumulative plastic strain, $\varepsilon_{(p\_s)a}$ (%)	2%	2%
Cumulative plastic deformation, ρ_{ta} (mm)	25	25
Subgrade characteristics		
Soil type	Fat clay (CH)	Fat clay (CH)
Thickness, H_s (m)	1.50	1.50
Subgrade modulus, E_s (MPa)	15	41
Unconfined compressive strength, σ_{s_s} (kPa)	90	165
Ballast characteristics		
Ballast type (assumed)	Granite (G)	Granite (G)
Ballast modulus, E_b (MPa)	270	270
Compressive strength, σ_{s_b} (kPa)	307	307

Table 2. Design results and track conditions for the LTM and TLTM test tracks.

Comparison parameters	LTM	TLTM
Unconfined compressive strength, σ_{s_s} (kPa)	90	165
Subgrade modulus, E_s (MPa)	14	41
Adopted granular layer thickness, H_b (m)	0.45	0.45
Required granular layer thickness, H_b (m)	0.70	0.40
Track condition with the adopted granular layer thickness	Track excessive plastic deformation and progressive shear failure	No track failures

Table 3. Design parameters for tracks at Edgewood and Aberdeen sites (adapted from Li and Selig 1998b).

Design parameters	Edgewood site	Aberdeen site
Subgrade characteristics		
Soil type	Lean clay (CL)	Lean clay (CL)
Thickness, H_s (m)	1.5	1.5
Subgrade modulus, E_s (MPa)	15	30
Unconfined compressive strength, σ_{s_s} (kPa)	48-83	97-290
Ballast characteristics		
Ballast type (assumed)	Granite (G)	Granite (G)
Ballast modulus, E_b (MPa)	270	270
Compressive strength, σ_{s_b} (kPa)	307	307
Design criteria (for 10 years)		
Cumulative plastic strain, $\varepsilon_{(p\_s)a}$ (%)	2%	2%
Cumulative plastic deformation, ρ_{ta} (mm)	25	25

Table 4. Traffic characteristics at the Northeast Corridor between Baltimore and Philadelphia (adapted from Li and Selig 1998b).

Loading condition	Annual traffic tonnage (MGT)	Static wheel load (kN)	Speed (km/h)	Wheel spacing (m)
Freight train				
Wheel 1	15	156	60	2.2
Wheel 2	22	44	60	2.2
Passenger train				
Wheel 1	15	70	190	2.9

Table 5. Comparison of results between new design method and site conditions for tracks at Edgewood and Aberdeen sites.

Comparison parameters	Edgewood site	Aberdeen site
Design thickness, H_b (m)	1.20	0.70
Existing thickness, H_b (m)	0.3-0.5	0.70-1.0
Remark	Existing thickness is less than design thickness.	Existing thickness is more than design thickness.
Track failure condition for the adopted thickness	Subgrade progressive shear failure, deep ballast pocket and differential settlement	No track failures

Appendix A: Design Charts to Calculate the Granular Layer Thickness for Preventing the Progressive Shear Failure.

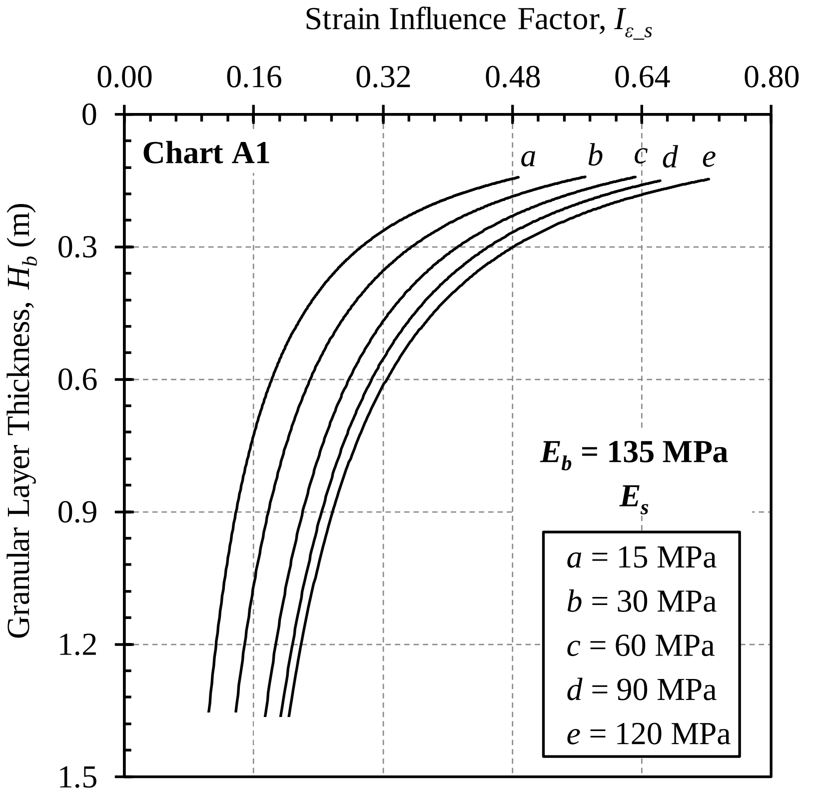

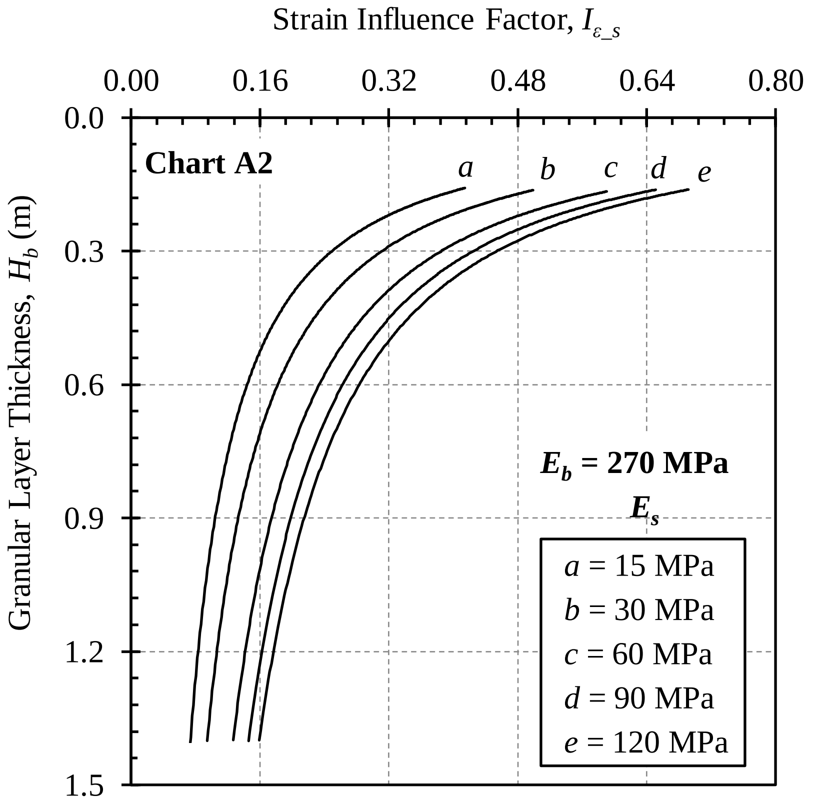

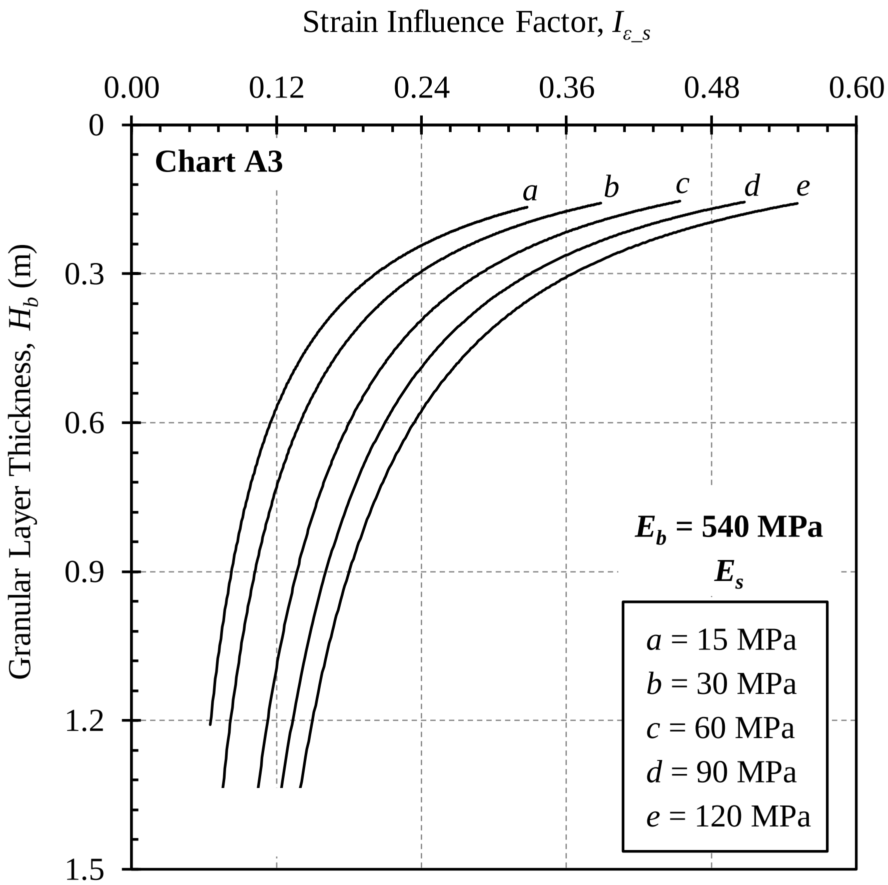
Strain Influence Factor, I_{ε_s}
0.00
0.12
0.24
0.36
0.48
0.60
0
0.3
0.6
0.9
1.2
1.5
Granular Layer Thickness, H_b (m)
Chart A3
a
b
c
d
e
E_b = 540 MPa
E_s
a = 15 MPa
b = 30 MPa
c = 60 MPa
d = 90 MPa
e = 120 MPa

Appendix B: Distribution of Strain Influence Factor with Depth for the Ballast Layer.

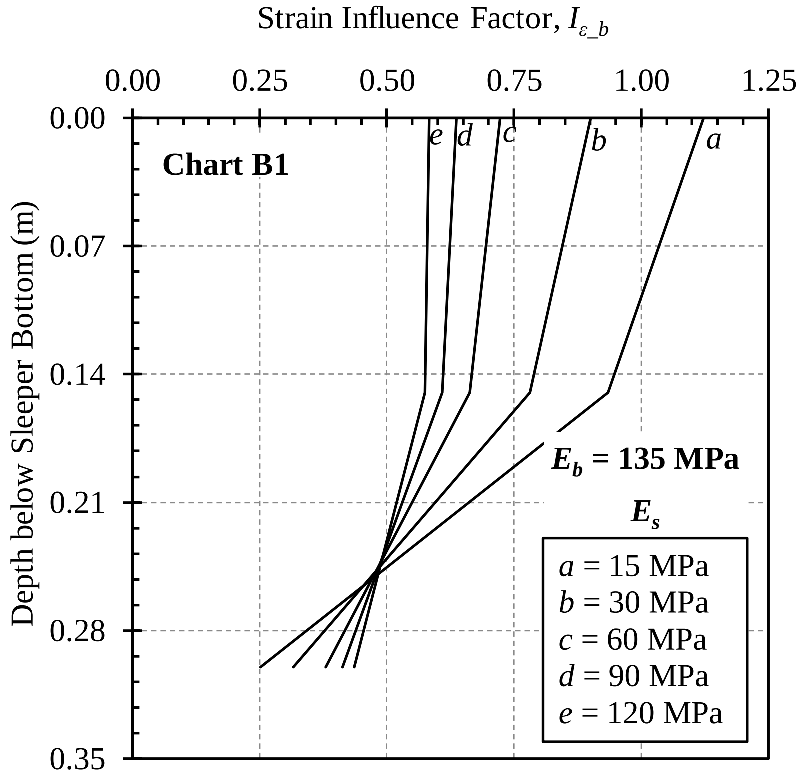

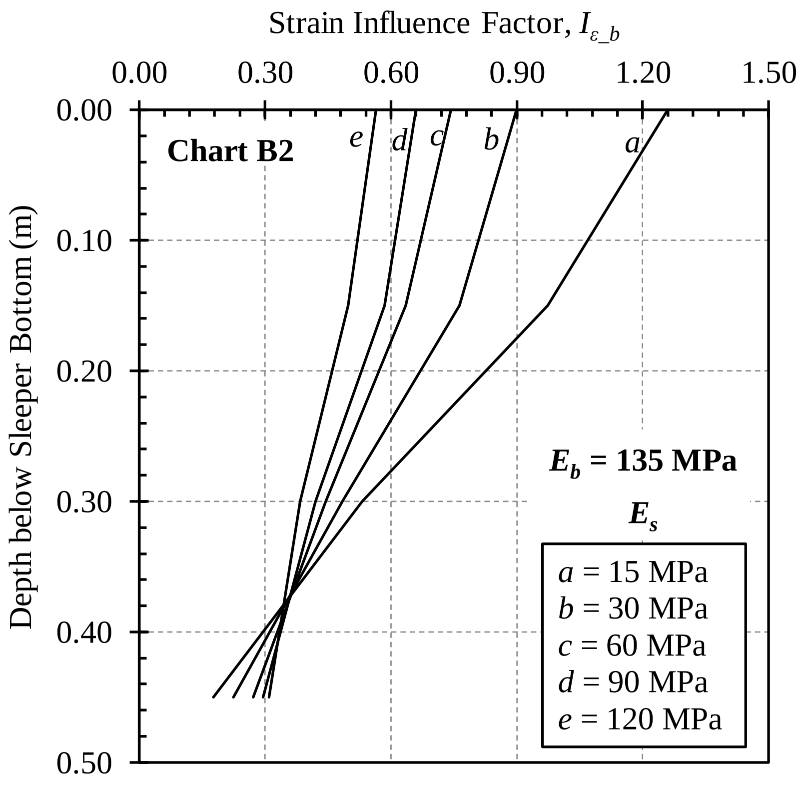

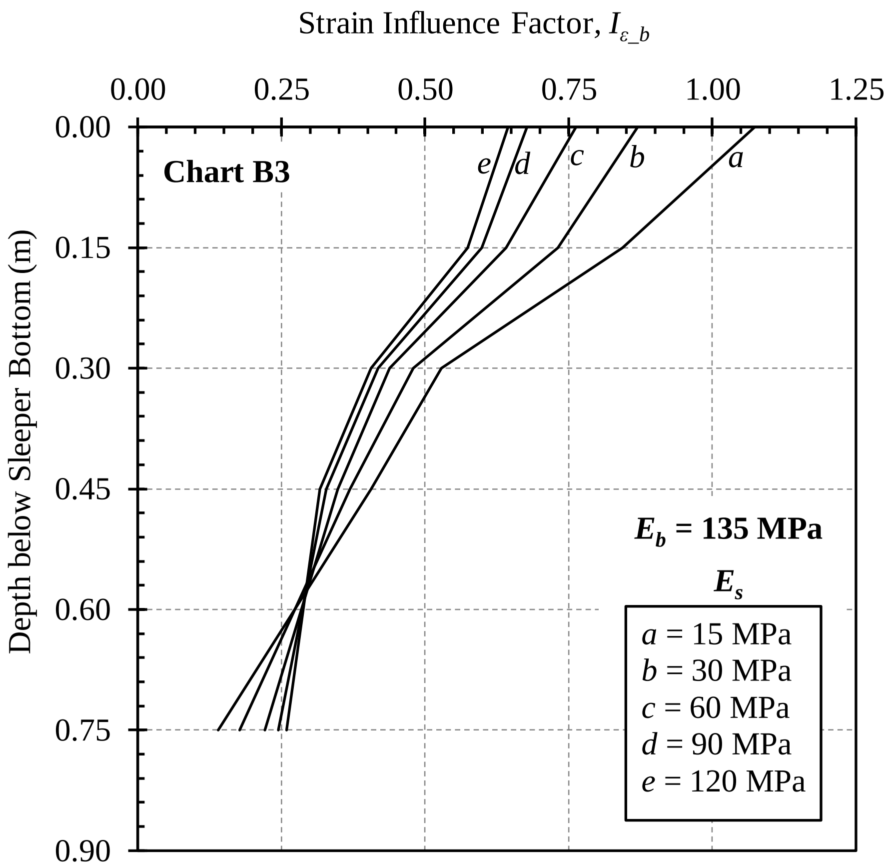
Strain Influence Factor, I_{ε_b}
0.00
0.25
0.50
0.75
1.00
1.25
Chart B3
Depth below Sleeper Bottom (m)
0.00
0.15
0.30
0.45
0.60
0.75
0.90
a
b
c
d
e
E_b = 135 MPa
E_s
a = 15 MPa
b = 30 MPa
c = 60 MPa
d = 90 MPa
e = 120 MPa

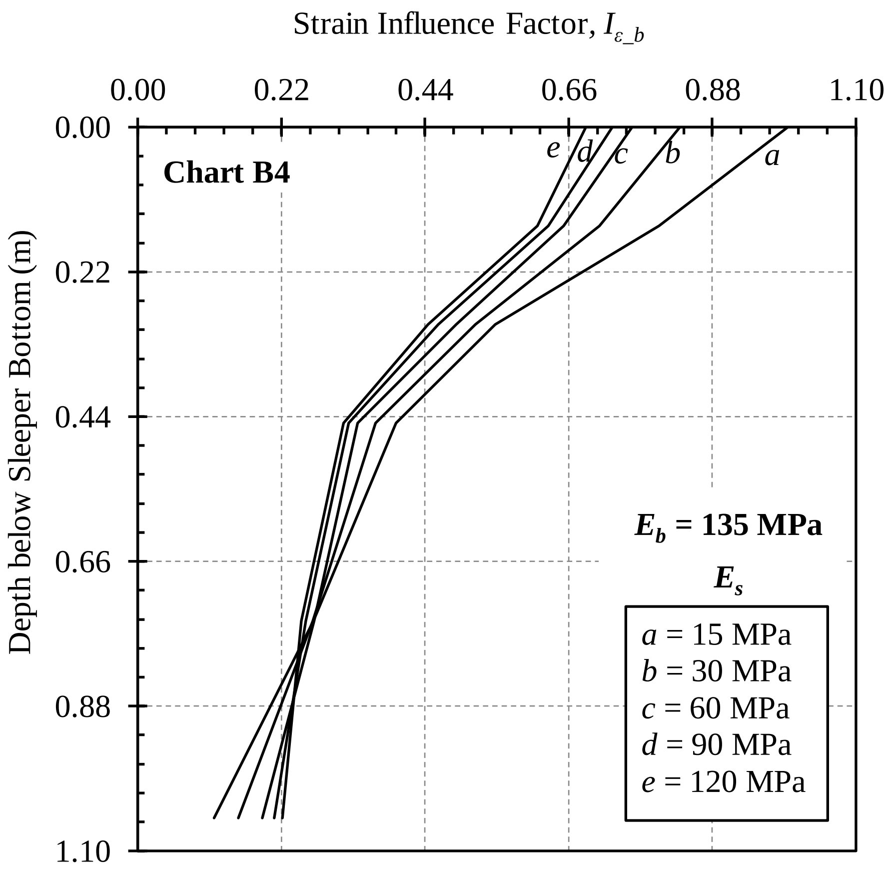
Strain Influence Factor, I_{ε_b}
0.00
0.22
0.44
0.66
0.88
1.10
Chart B4
Depth below Sleeper Bottom (m)
0.00
0.22
0.44
0.66
0.88
1.10
a
b
c
d
e
E_b = 135 MPa
E_s
a = 15 MPa
b = 30 MPa
c = 60 MPa
d = 90 MPa
e = 120 MPa

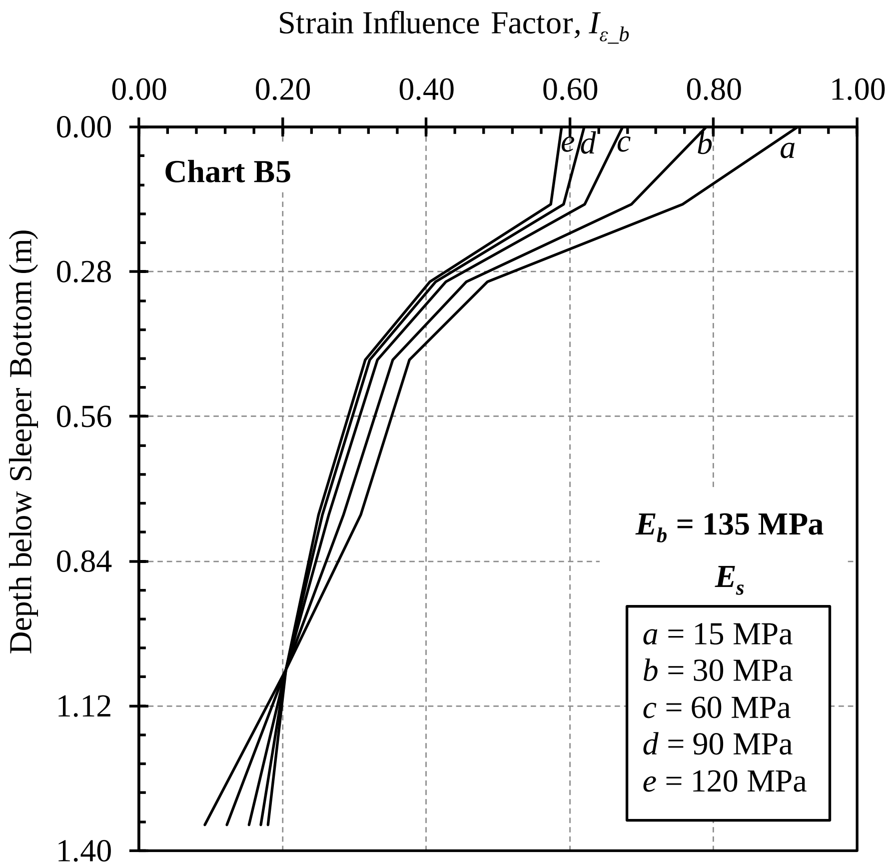
Strain Influence Factor, I_{ε_b}
0.00
0.20
0.40
0.60
0.80
1.00
Depth below Sleeper Bottom (m)
0.00
0.28
0.56
0.84
1.12
1.40
Chart B5
e
d
c
b
a
E_b = 135 MPa
E_s
a = 15 MPa
b = 30 MPa
c = 60 MPa
d = 90 MPa
e = 120 MPa

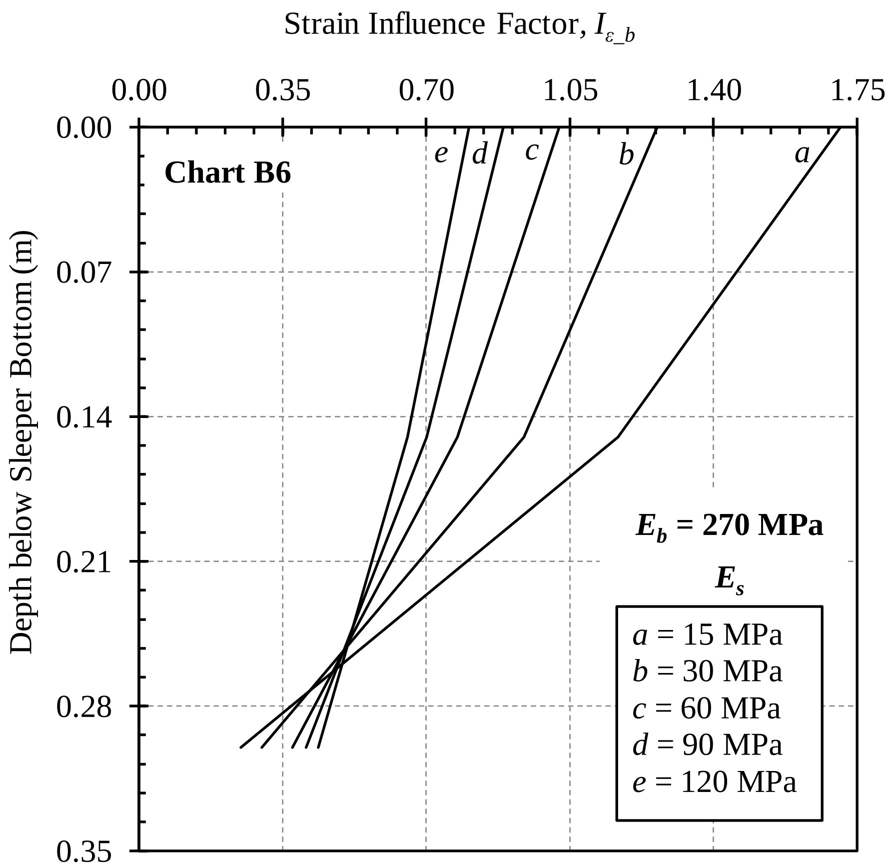
Strain Influence Factor, I_{ε_b}
0.00
0.35
0.70
1.05
1.40
1.75
Depth below Sleeper Bottom (m)
0.00
0.07
0.14
0.21
0.28
0.35
Chart B6
e
d
c
b
a
E_b = 270 MPa
E_s
a = 15 MPa
b = 30 MPa
c = 60 MPa
d = 90 MPa
e = 120 MPa

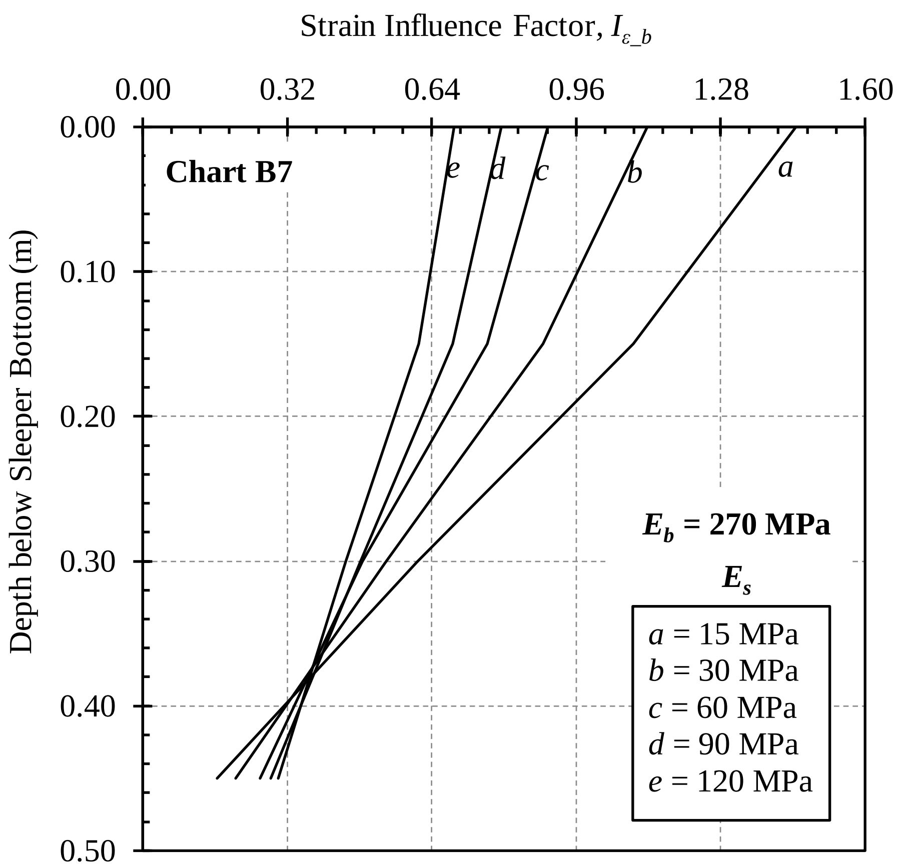
Strain Influence Factor, I_{ε_b}
0.00
0.32
0.64
0.96
1.28
1.60
Depth below Sleeper Bottom (m)
0.00
0.10
0.20
0.30
0.40
0.50
Chart B7
e
d
c
b
a
E_b = 270 MPa
E_s
a = 15 MPa
b = 30 MPa
c = 60 MPa
d = 90 MPa
e = 120 MPa

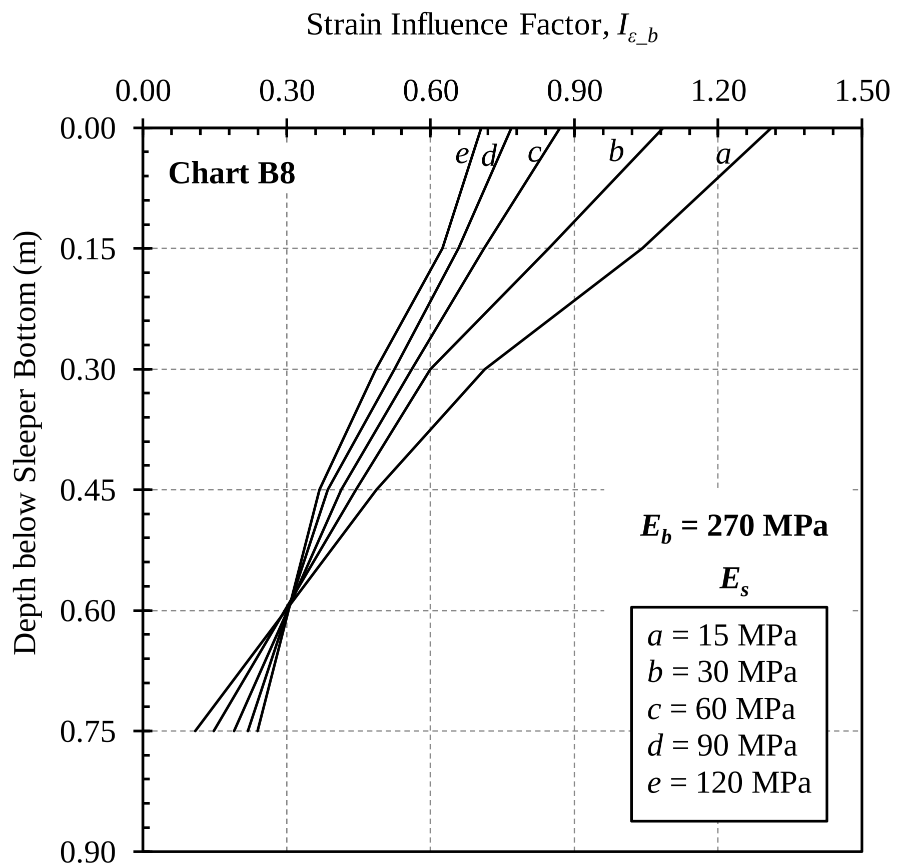
Strain Influence Factor, I_{ε_b}
0.00
0.30
0.60
0.90
1.20
1.50
Depth below Sleeper Bottom (m)
0.00
0.15
0.30
0.45
0.60
0.75
0.90
Chart B8
e
d
c
b
a
E_b = 270 MPa
E_s
a = 15 MPa
b = 30 MPa
c = 60 MPa
d = 90 MPa
e = 120 MPa

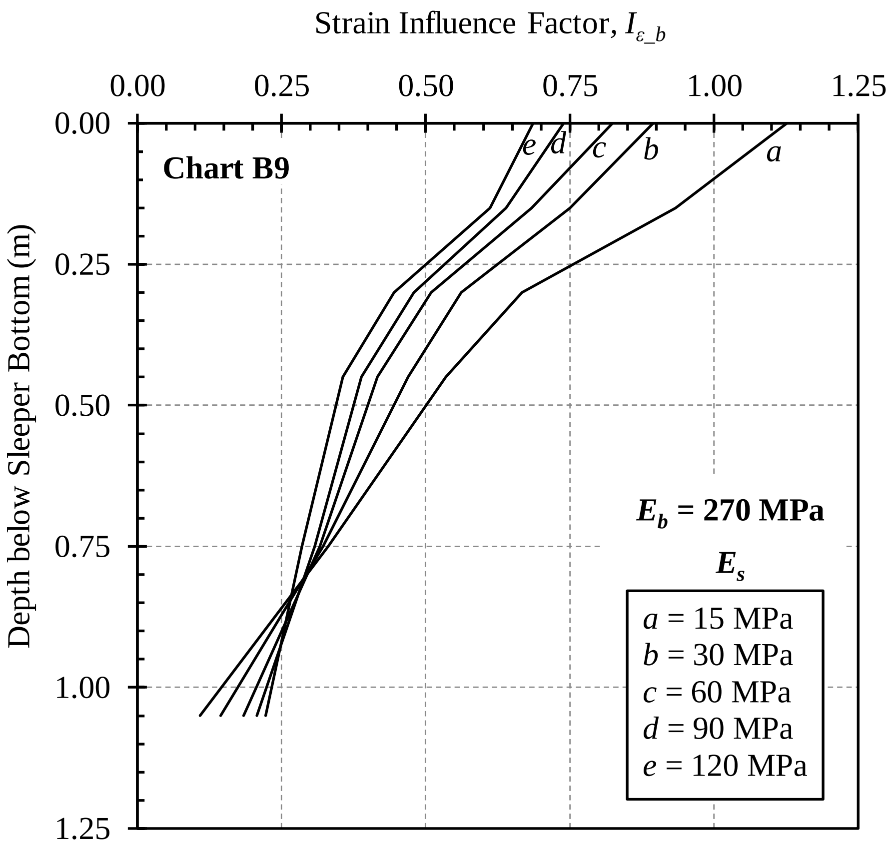

Strain Influence Factor, I_{ε_b}
0.00
0.25
0.50
0.75
1.00
1.25
Depth below Sleeper Bottom (m)
0.00
0.25
0.50
0.75
1.00
1.25
Chart B9
e
d
c
b
a
E_b = 270 MPa
E_s
a = 15 MPa
b = 30 MPa
c = 60 MPa
d = 90 MPa
e = 120 MPa

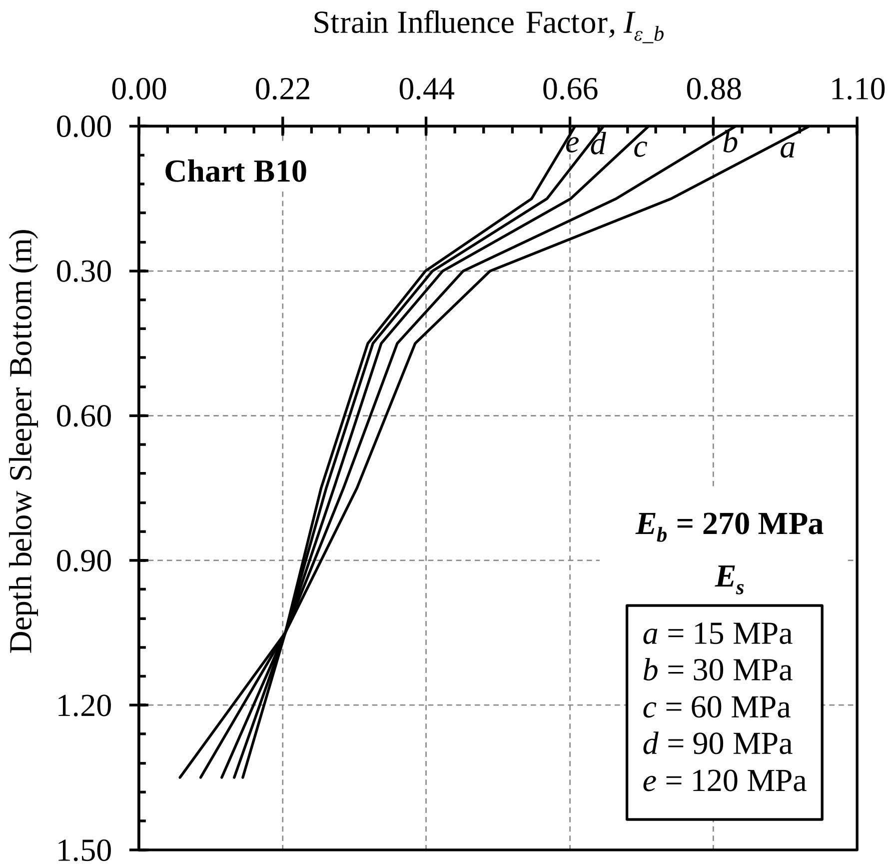

Strain Influence Factor, I_{ε_b}
0.00
0.22
0.44
0.66
0.88
1.10
Depth below Sleeper Bottom (m)
0.00
0.30
0.60
0.90
1.20
1.50
Chart B10
e
d
c
b
a
E_b = 270 MPa
E_s
a = 15 MPa
b = 30 MPa
c = 60 MPa
d = 90 MPa
e = 120 MPa

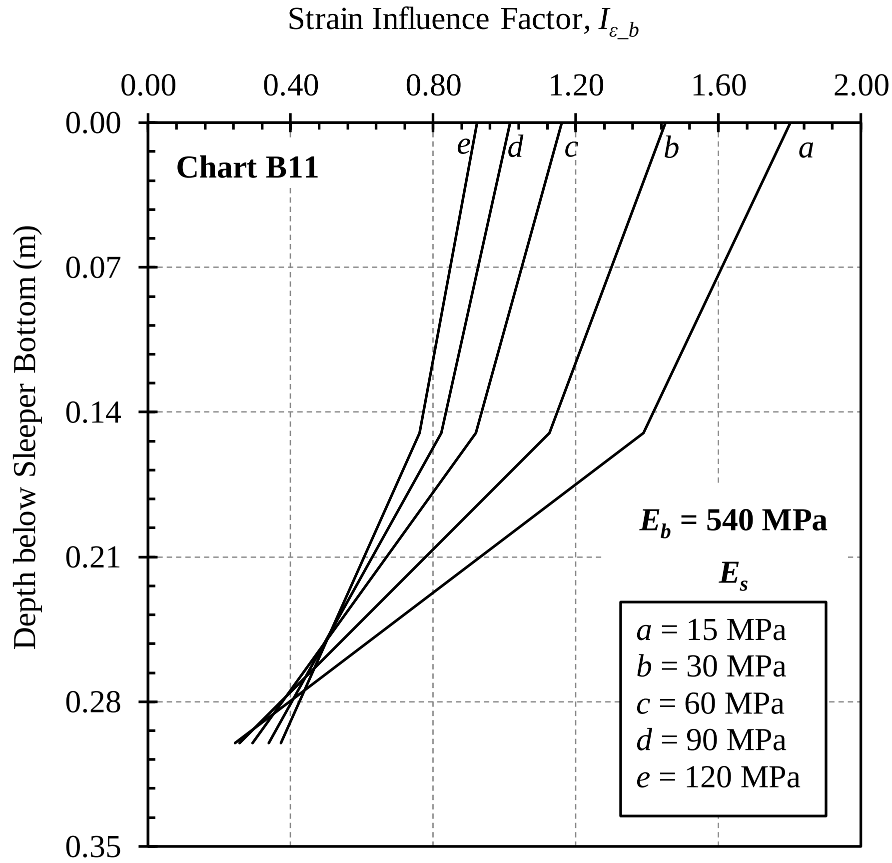
Strain Influence Factor, I_{ε_b}
0.00
0.40
0.80
1.20
1.60
2.00
Depth below Sleeper Bottom (m)
0.00
0.07
0.14
0.21
0.28
0.35
Chart B11
e
d
c
b
a
E_b = 540 MPa
E_s
a = 15 MPa
b = 30 MPa
c = 60 MPa
d = 90 MPa
e = 120 MPa

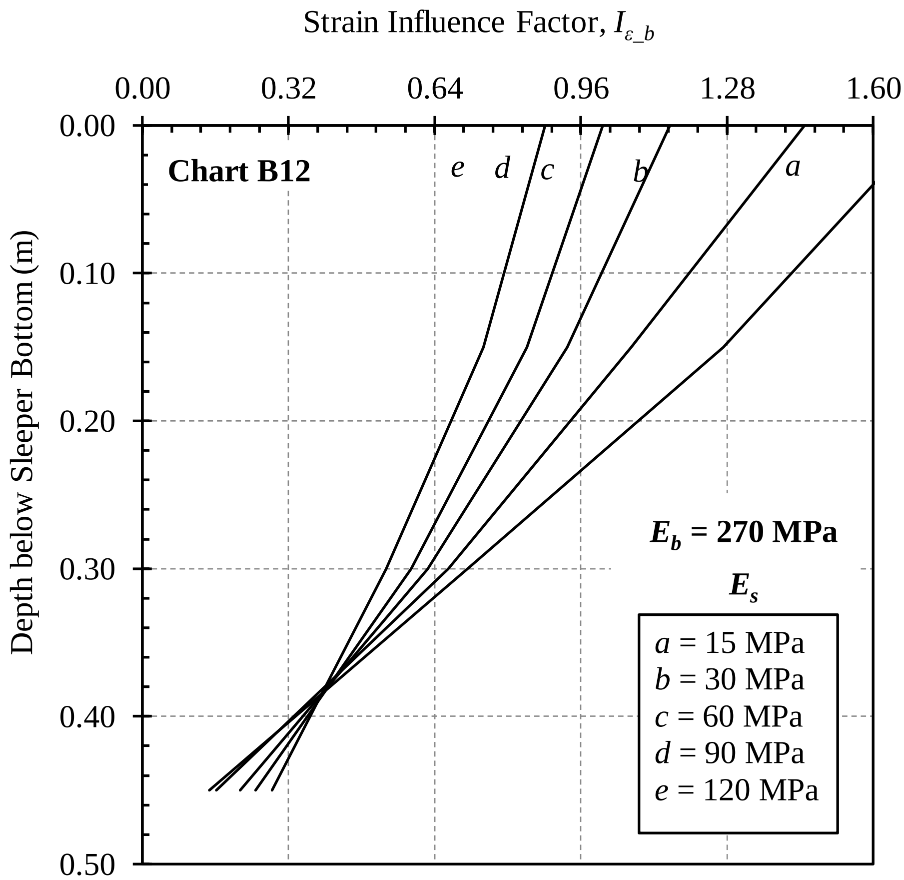
Strain Influence Factor, I_{ε_b}
0.00
0.32
0.64
0.96
1.28
1.60
Depth below Sleeper Bottom (m)
0.00
0.10
0.20
0.30
0.40
0.50
Chart B12
e
d
c
b
a
E_b = 270 MPa
E_s
a = 15 MPa
b = 30 MPa
c = 60 MPa
d = 90 MPa
e = 120 MPa

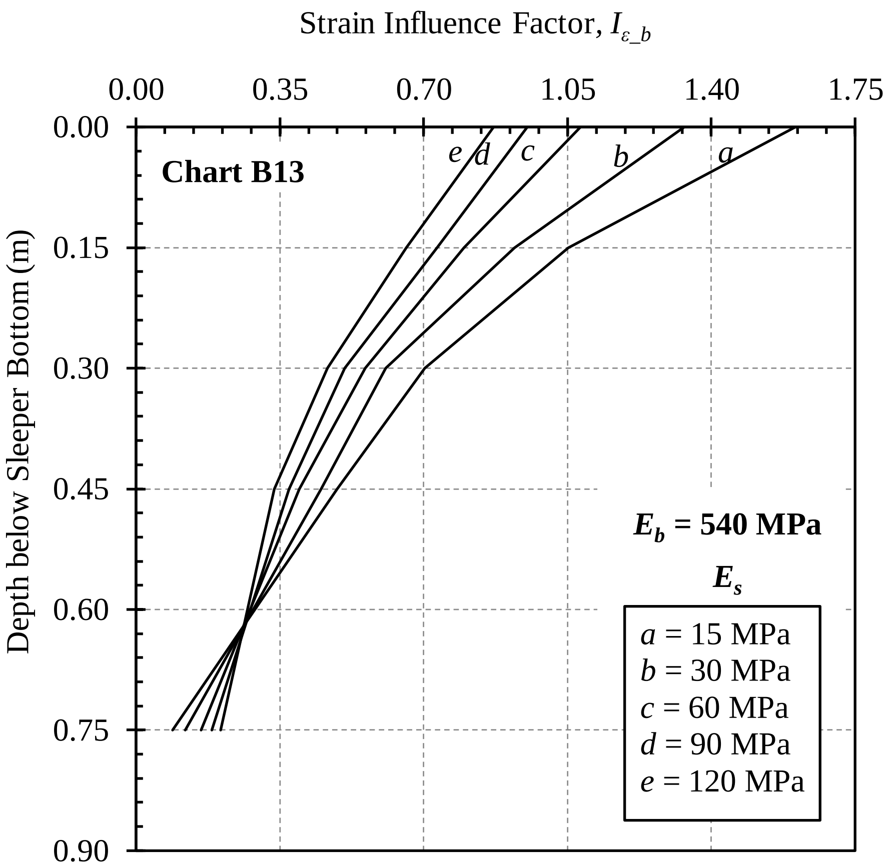

Strain Influence Factor, I_{ε_b}
0.00
0.35
0.70
1.05
1.40
1.75
Chart B13
e
d
c
b
a
Depth below Sleeper Bottom (m)
0.00
0.15
0.30
0.45
0.60
0.75
0.90
E_b = 540 MPa
E_s
a = 15 MPa
b = 30 MPa
c = 60 MPa
d = 90 MPa
e = 120 MPa

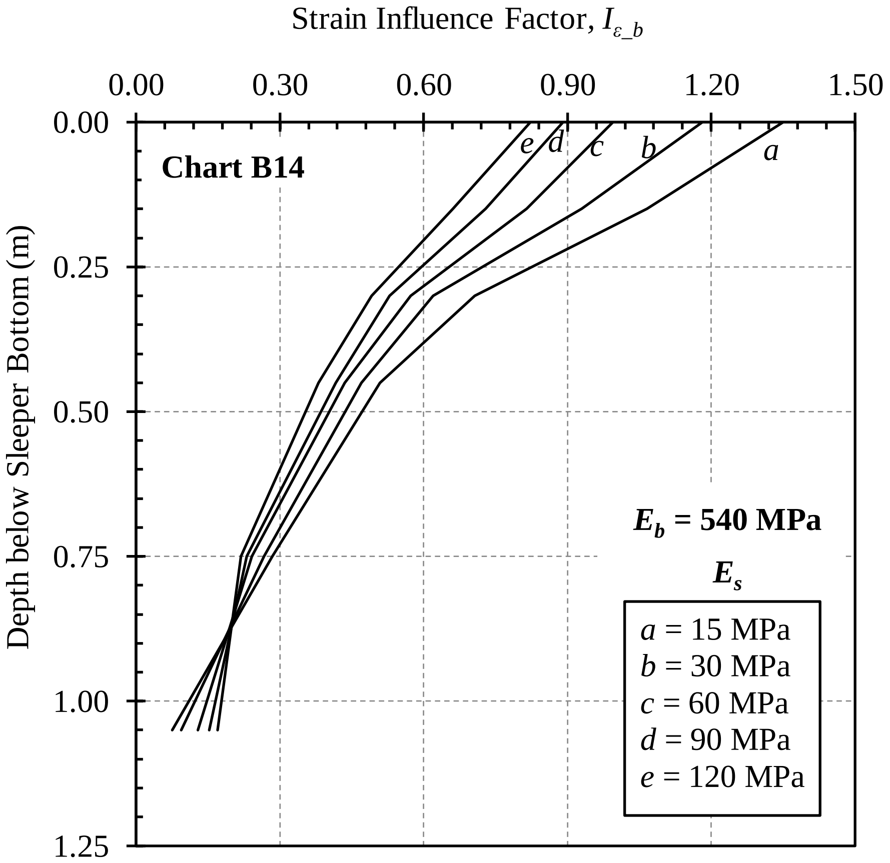

Strain Influence Factor, I_{ε_b}
0.00
0.30
0.60
0.90
1.20
1.50
Chart B14
e
d
c
b
a
Depth below Sleeper Bottom (m)
0.00
0.25
0.50
0.75
1.00
1.25
E_b = 540 MPa
E_s
a = 15 MPa
b = 30 MPa
c = 60 MPa
d = 90 MPa
e = 120 MPa

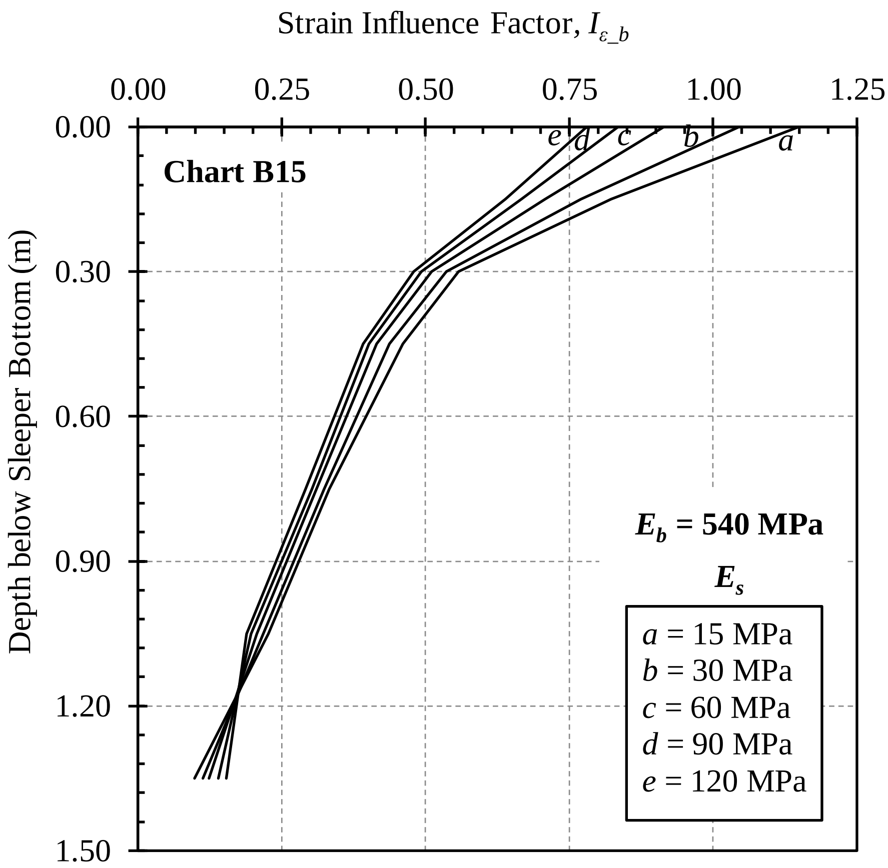
Strain Influence Factor, I_{ε_b}
0.00
0.25
0.50
0.75
1.00
1.25
0.00
0.30
0.60
0.90
1.20
1.50
Depth below Sleeper Bottom (m)
Chart B15
e
d
c
b
a
E_b = 540 MPa
E_s
a = 15 MPa
b = 30 MPa
c = 60 MPa
d = 90 MPa
e = 120 MPa

Appendix C: Design Charts to Calculate the Granular Layer Thickness for Preventing the Excessive Plastic Deformation.

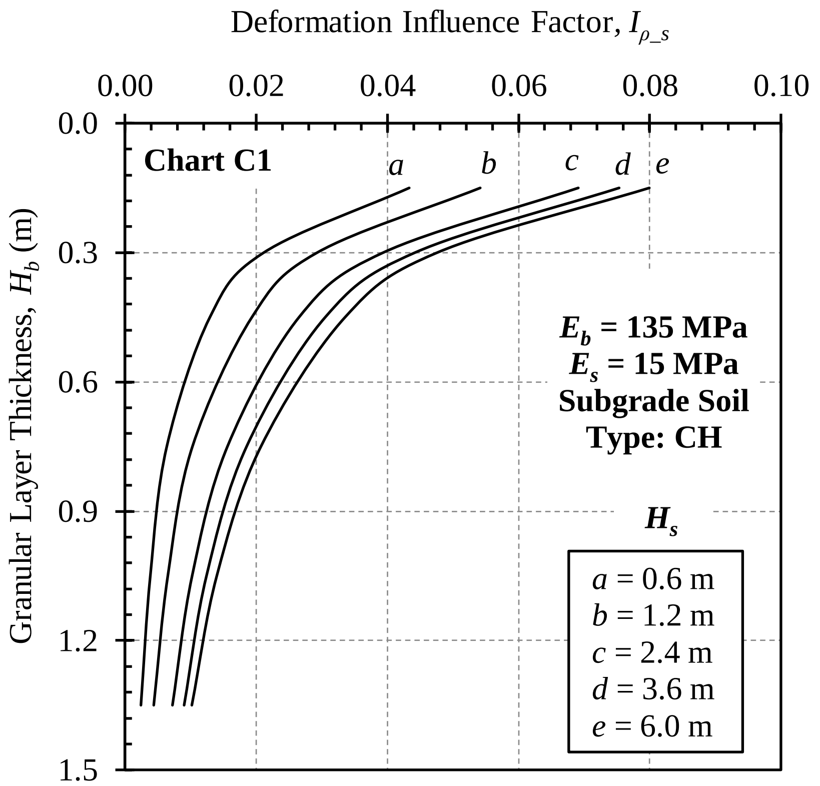

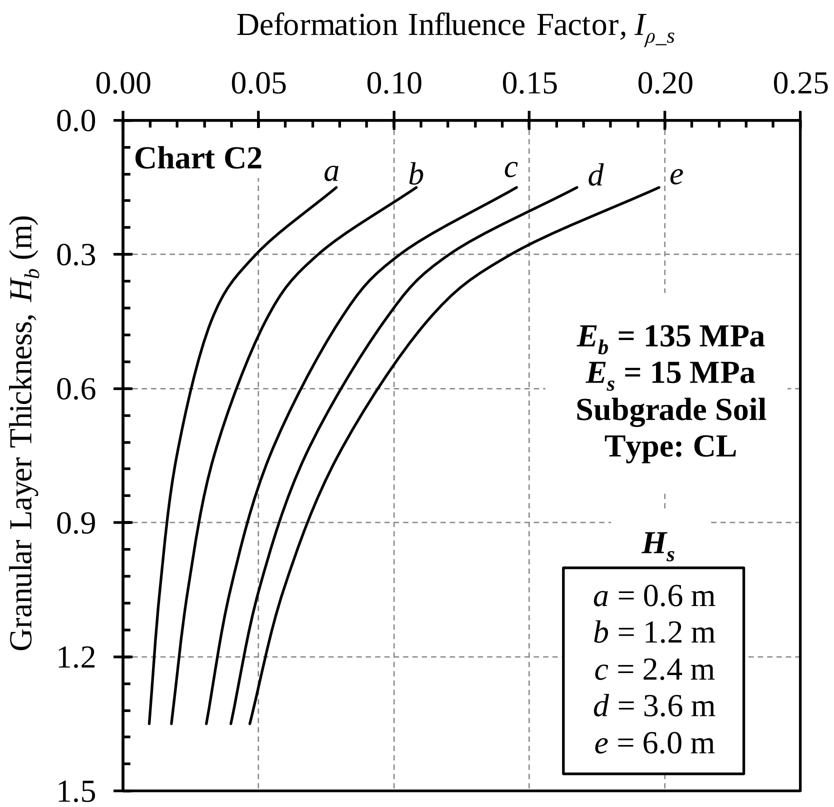

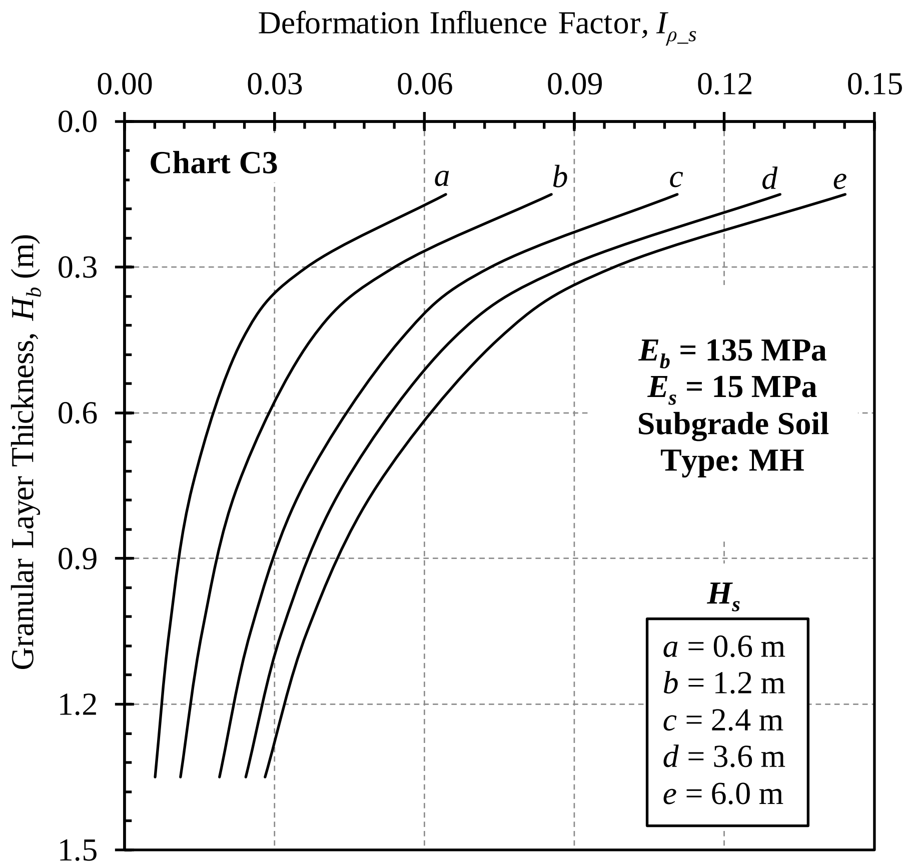
Deformation Influence Factor, I_{ρ_s}
0.00
0.03
0.06
0.09
0.12
0.15
0.0
0.3
0.6
0.9
1.2
1.5
Granular Layer Thickness, H_b (m)
Chart C3
a
b
c
d
e
E_b = 135 MPa
E_s = 15 MPa
Subgrade Soil
Type: MH
H_s
a = 0.6 m
b = 1.2 m
c = 2.4 m
d = 3.6 m
e = 6.0 m

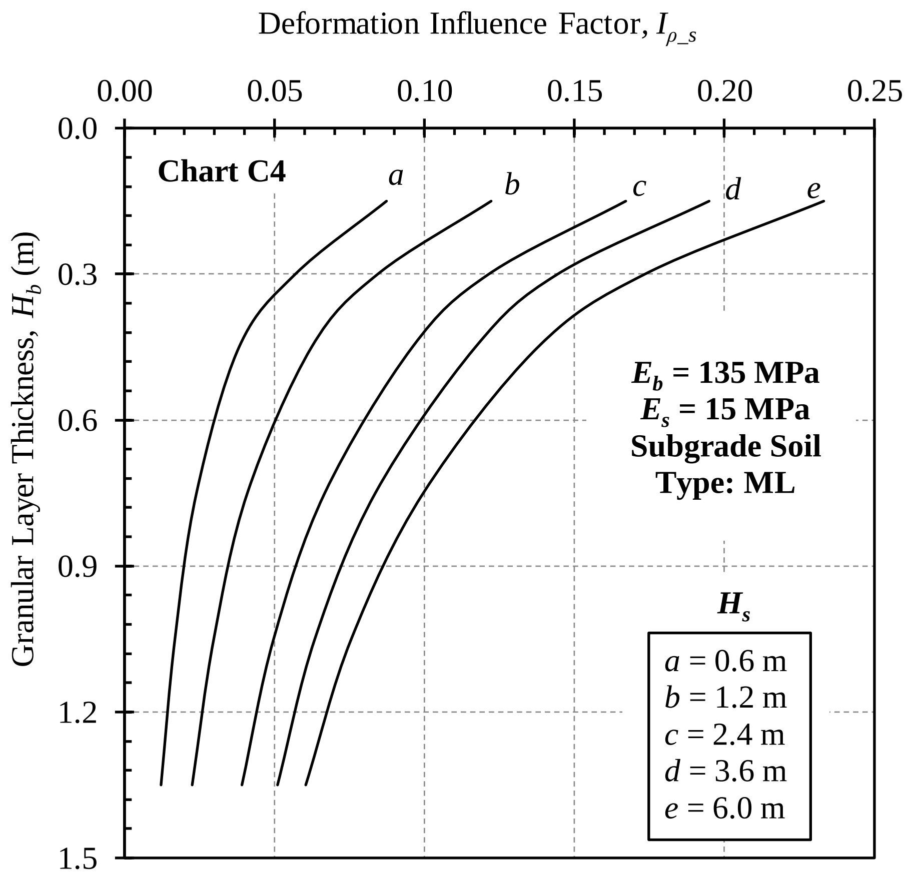
Deformation Influence Factor, I_{ρ_s}
0.00
0.05
0.10
0.15
0.20
0.25
0.0
0.3
0.6
0.9
1.2
1.5
Granular Layer Thickness, H_b (m)
Chart C4
a
b
c
d
e
E_b = 135 MPa
E_s = 15 MPa
Subgrade Soil
Type: ML
H_s
a = 0.6 m
b = 1.2 m
c = 2.4 m
d = 3.6 m
e = 6.0 m

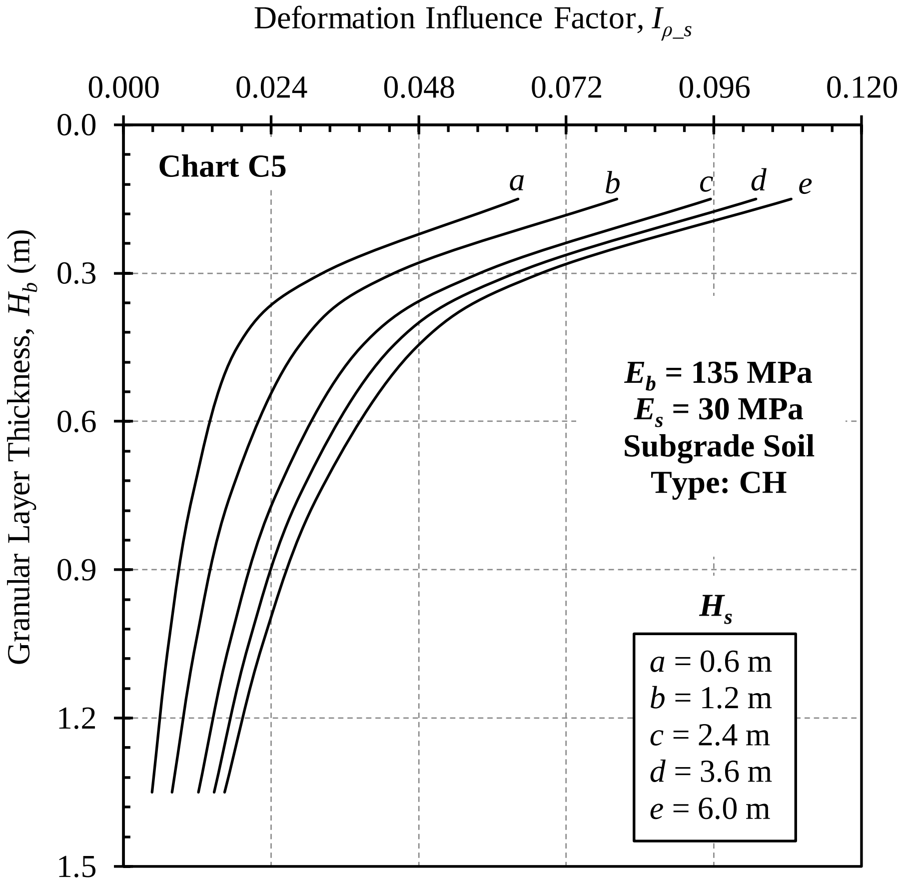
Deformation Influence Factor, I_{ρ_s}
0.000
0.024
0.048
0.072
0.096
0.120
0.0
0.3
0.6
0.9
1.2
1.5
Granular Layer Thickness, H_b (m)
Chart C5
a
b
c
d
e
E_b = 135 MPa
E_s = 30 MPa
Subgrade Soil
Type: CH
H_s
a = 0.6 m
b = 1.2 m
c = 2.4 m
d = 3.6 m
e = 6.0 m

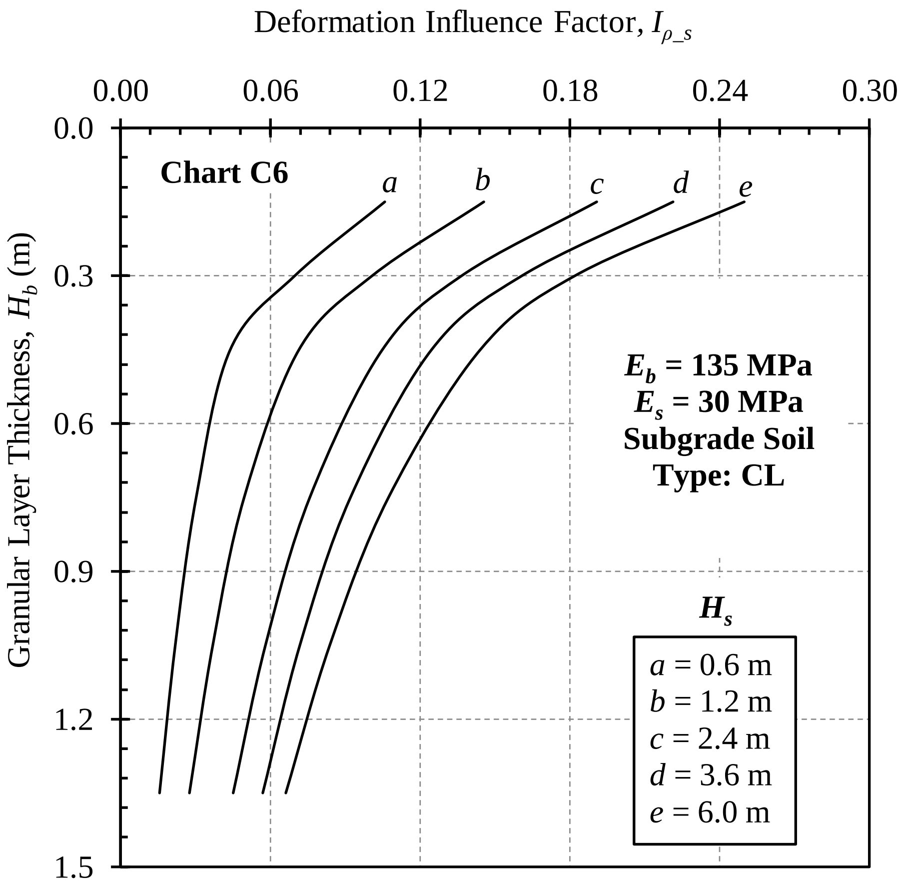
Deformation Influence Factor, I_{ρ_s}
0.00
0.06
0.12
0.18
0.24
0.30
0.0
0.3
0.6
0.9
1.2
1.5
Granular Layer Thickness, H_b (m)
Chart C6
a
b
c
d
e
E_b = 135 MPa
E_s = 30 MPa
Subgrade Soil
Type: CL
H_s
a = 0.6 m
b = 1.2 m
c = 2.4 m
d = 3.6 m
e = 6.0 m

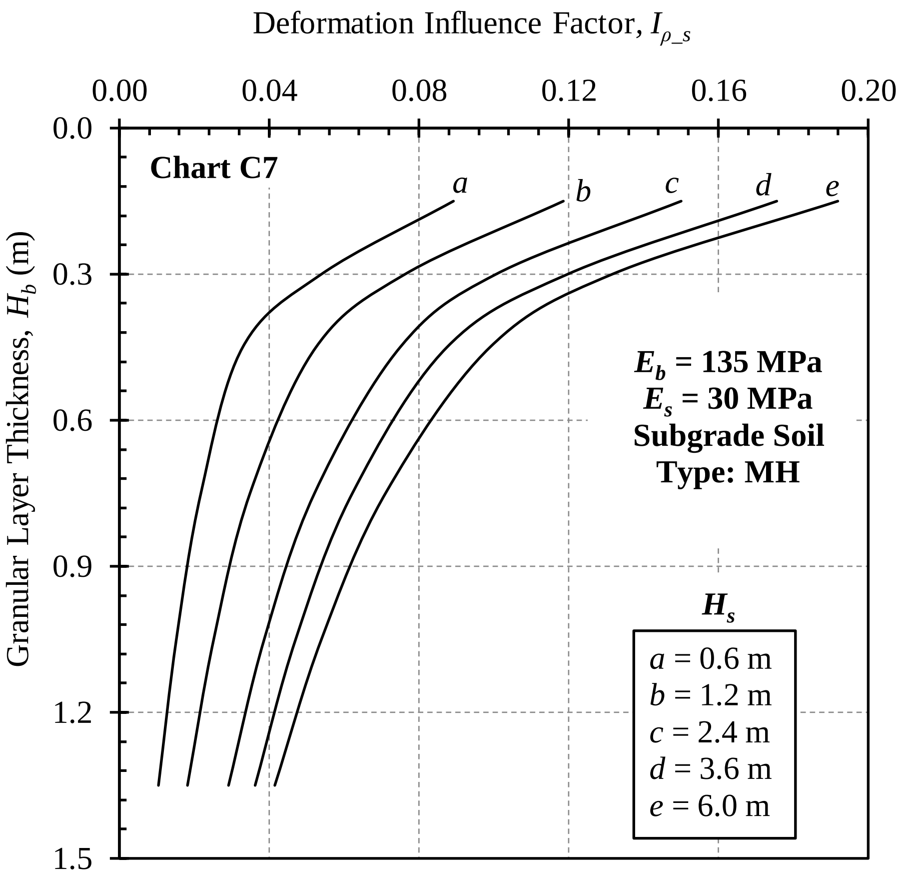
Deformation Influence Factor, I_{ρ_s}
0.00
0.04
0.08
0.12
0.16
0.20
0.0
0.3
0.6
0.9
1.2
1.5
Granular Layer Thickness, H_b (m)
Chart C7
a
b
c
d
e
E_b = 135 MPa
E_s = 30 MPa
Subgrade Soil
Type: MH
H_s
a = 0.6 m
b = 1.2 m
c = 2.4 m
d = 3.6 m
e = 6.0 m

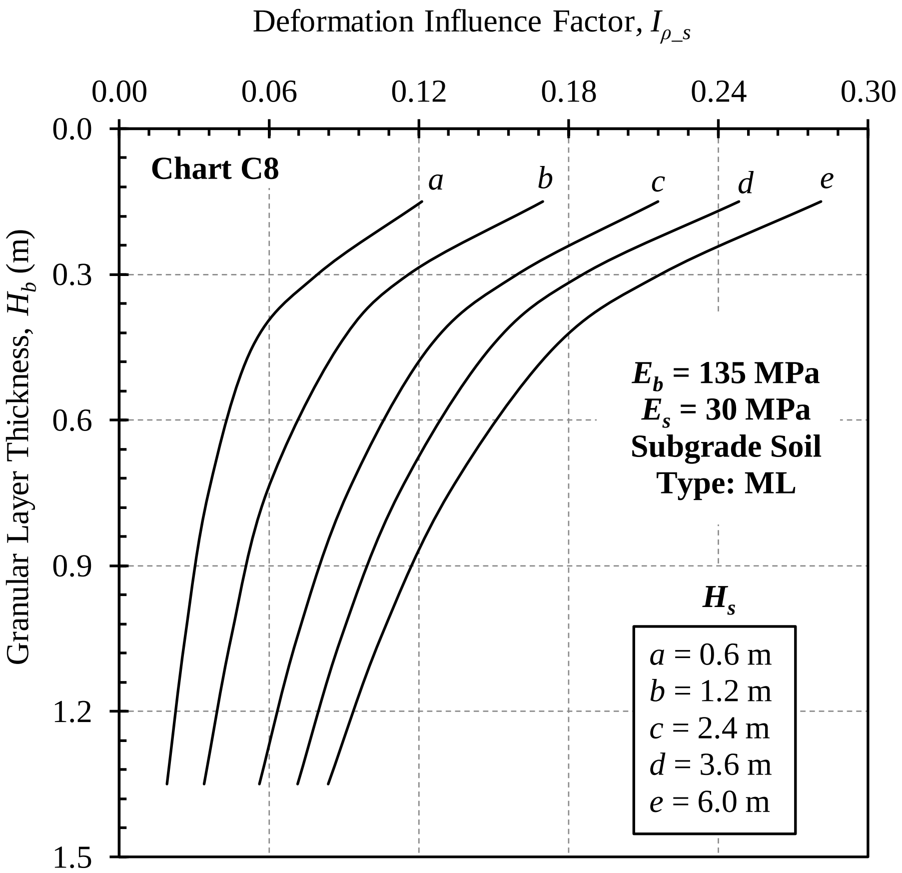
Deformation Influence Factor, I_{ρ_s}
0.00
0.06
0.12
0.18
0.24
0.30
0.0
0.3
0.6
0.9
1.2
1.5
Granular Layer Thickness, H_b (m)
Chart C8
a
b
c
d
e
E_b = 135 MPa
E_s = 30 MPa
Subgrade Soil
Type: ML
H_s
a = 0.6 m
b = 1.2 m
c = 2.4 m
d = 3.6 m
e = 6.0 m

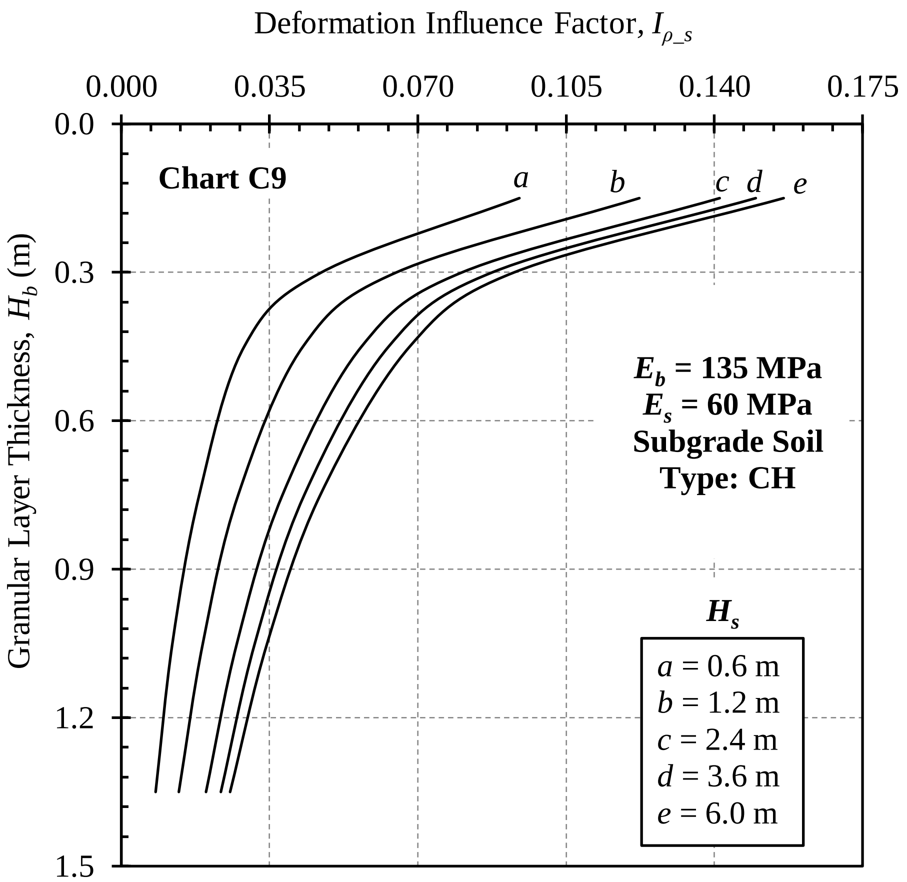
Deformation Influence Factor, I_{ρ_s}
0.000
0.035
0.070
0.105
0.140
0.175
0.0
0.3
0.6
0.9
1.2
1.5
Granular Layer Thickness, H_b (m)
Chart C9
a
b
c
d
e
E_b = 135 MPa
E_s = 60 MPa
Subgrade Soil
Type: CH
H_s
a = 0.6 m
b = 1.2 m
c = 2.4 m
d = 3.6 m
e = 6.0 m

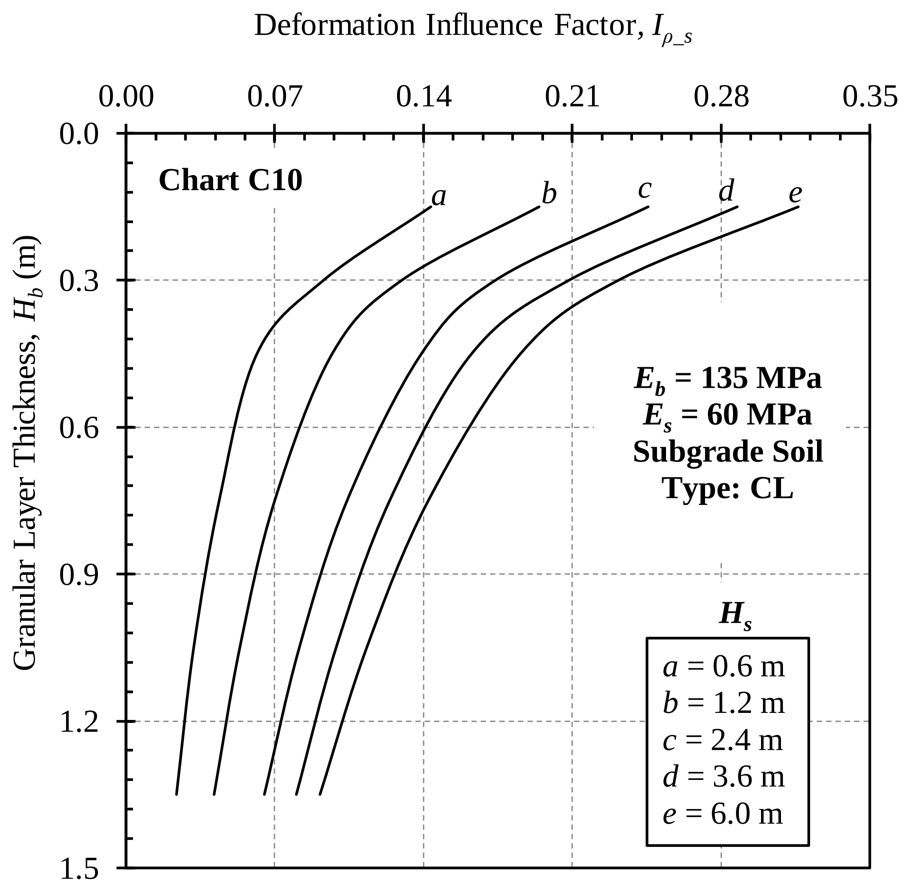
Deformation Influence Factor, I_{ρ_s}
0.00
0.07
0.14
0.21
0.28
0.35
0.0
0.3
0.6
0.9
1.2
1.5
Granular Layer Thickness, H_b (m)
Chart C10
a
b
c
d
e
E_b = 135 MPa
E_s = 60 MPa
Subgrade Soil
Type: CL
H_s
a = 0.6 m
b = 1.2 m
c = 2.4 m
d = 3.6 m
e = 6.0 m

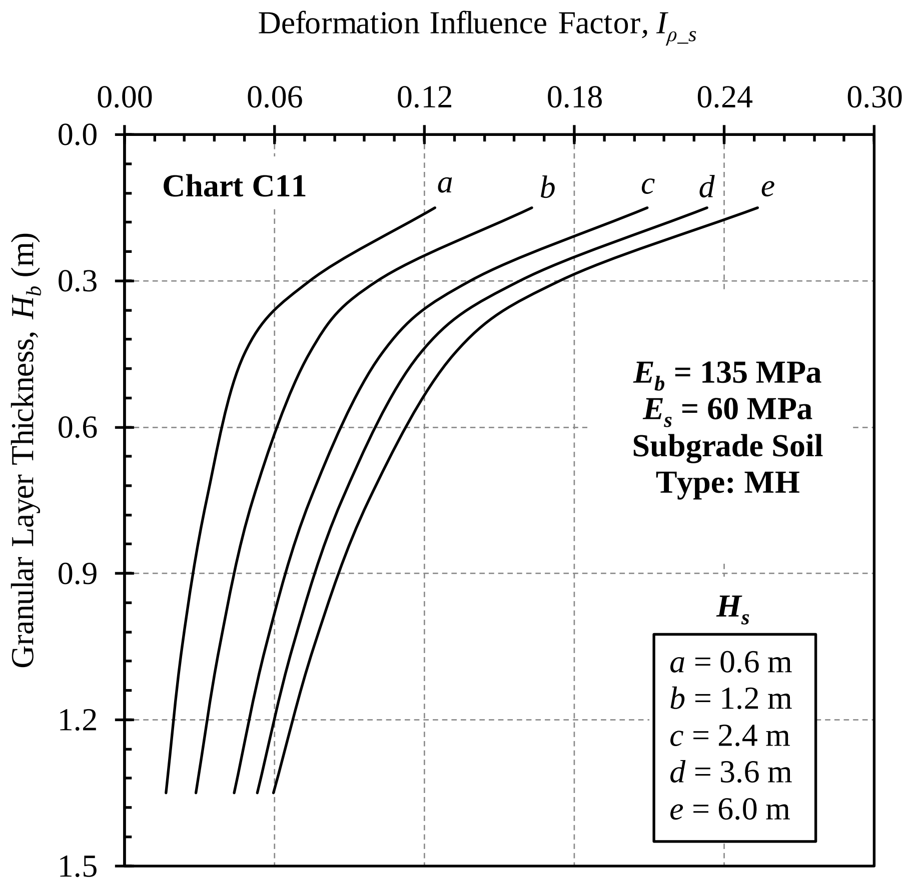
Deformation Influence Factor, I_{ρ_s}
0.00
0.06
0.12
0.18
0.24
0.30
0.0
0.3
0.6
0.9
1.2
1.5
Granular Layer Thickness, H_b (m)
Chart C11
a
b
c
d
e
E_b = 135 MPa
E_s = 60 MPa
Subgrade Soil
Type: MH
H_s
a = 0.6 m
b = 1.2 m
c = 2.4 m
d = 3.6 m
e = 6.0 m

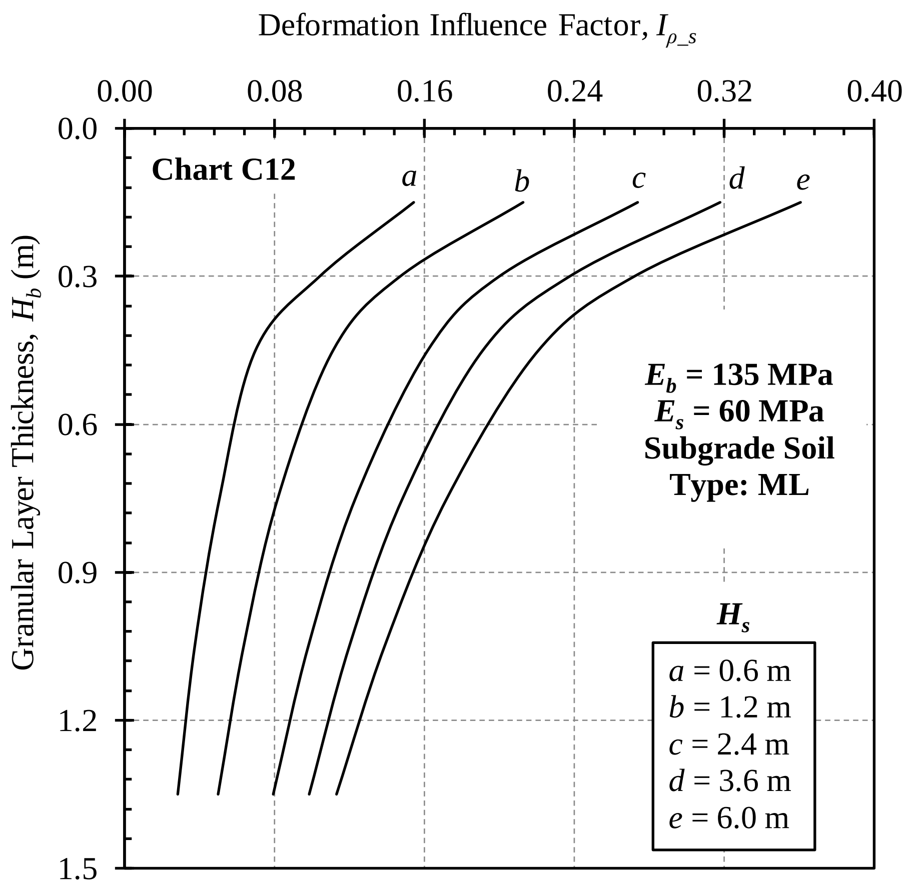
Deformation Influence Factor, I_{ρ_s}
0.00
0.08
0.16
0.24
0.32
0.40
0.0
0.3
0.6
0.9
1.2
1.5
Granular Layer Thickness, H_b (m)
Chart C12
a
b
c
d
e
E_b = 135 MPa
E_s = 60 MPa
Subgrade Soil
Type: ML
H_s
a = 0.6 m
b = 1.2 m
c = 2.4 m
d = 3.6 m
e = 6.0 m

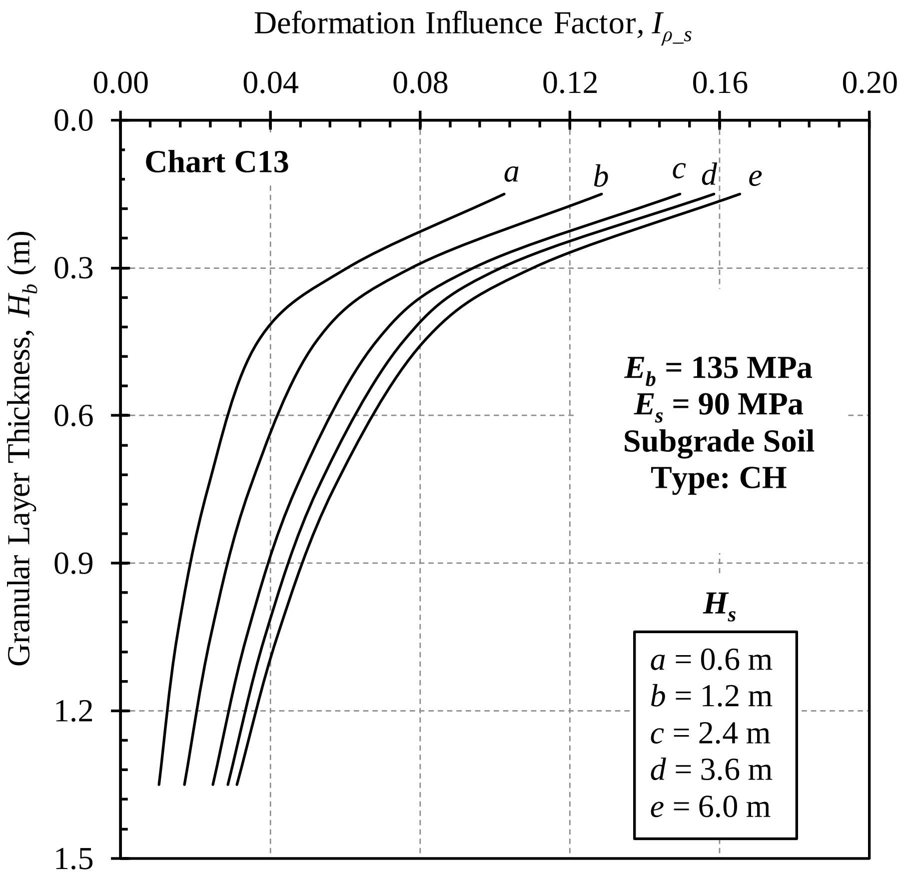

Deformation Influence Factor, I_{ρ_s}
0.00
0.04
0.08
0.12
0.16
0.20
0.0
0.3
0.6
0.9
1.2
1.5
Granular Layer Thickness, H_b (m)
Chart C13
a
b
c
d
e
E_b = 135 MPa
E_s = 90 MPa
Subgrade Soil
Type: CH
H_s
a = 0.6 m
b = 1.2 m
c = 2.4 m
d = 3.6 m
e = 6.0 m

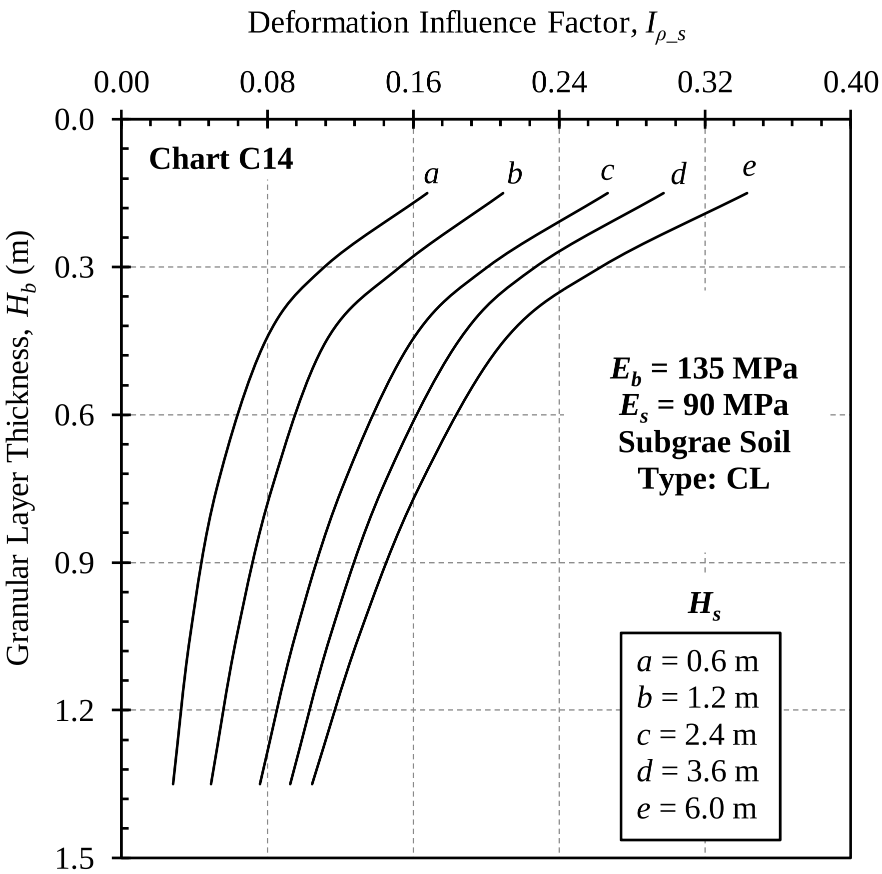

Deformation Influence Factor, I_{ρ_s}
0.00
0.08
0.16
0.24
0.32
0.40
0.0
0.3
0.6
0.9
1.2
1.5
Granular Layer Thickness, H_b (m)
Chart C14
a
b
c
d
e
E_b = 135 MPa
E_s = 90 MPa
Subgrae Soil
Type: CL
H_s
a = 0.6 m
b = 1.2 m
c = 2.4 m
d = 3.6 m
e = 6.0 m

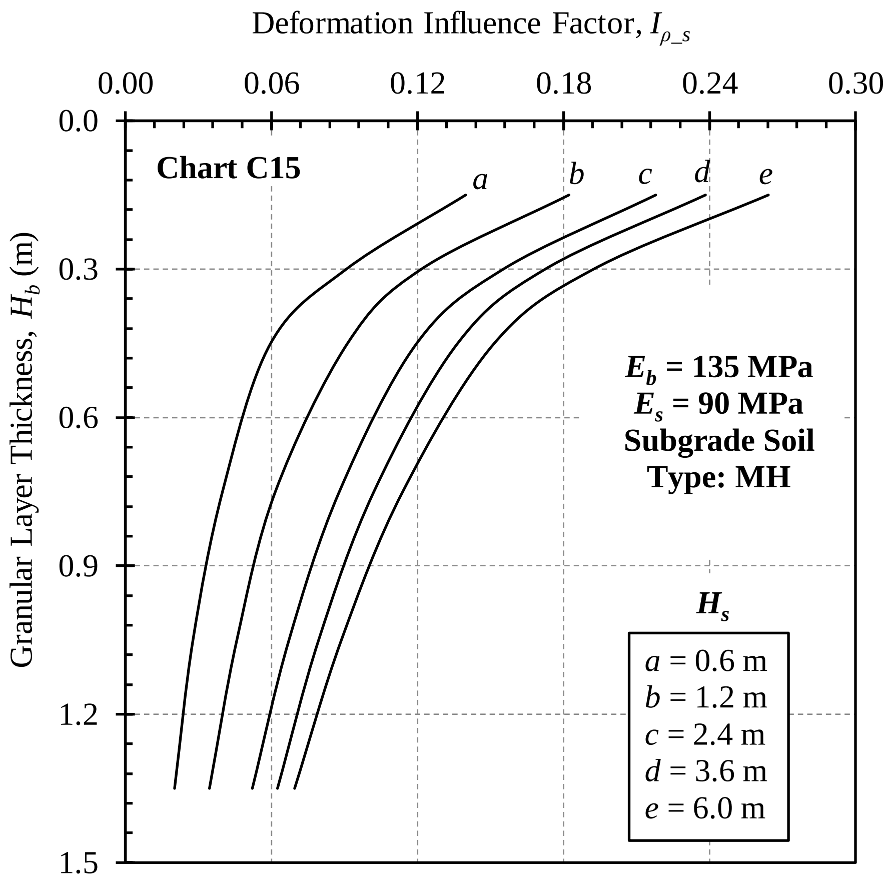

Deformation Influence Factor, I_{ρ_s}
0.00
0.06
0.12
0.18
0.24
0.30
Granular Layer Thickness, H_b (m)
0.0
0.3
0.6
0.9
1.2
1.5
Chart C15
a
b
c
d
e
E_b = 135 MPa
E_s = 90 MPa
Subgrade Soil
Type: MH
H_s
a = 0.6 m
b = 1.2 m
c = 2.4 m
d = 3.6 m
e = 6.0 m

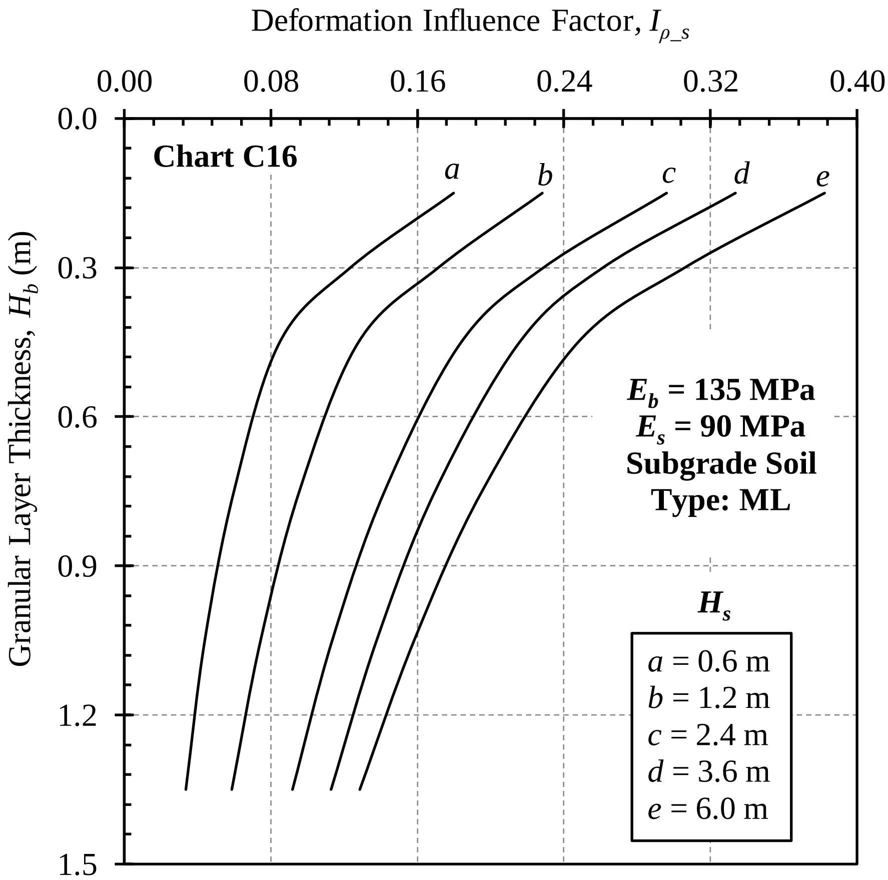

Deformation Influence Factor, I_{ρ_s}
0.00
0.08
0.16
0.24
0.32
0.40
Granular Layer Thickness, H_b (m)
0.0
0.3
0.6
0.9
1.2
1.5
Chart C16
a
b
c
d
e
E_b = 135 MPa
E_s = 90 MPa
Subgrade Soil
Type: ML
H_s
a = 0.6 m
b = 1.2 m
c = 2.4 m
d = 3.6 m
e = 6.0 m

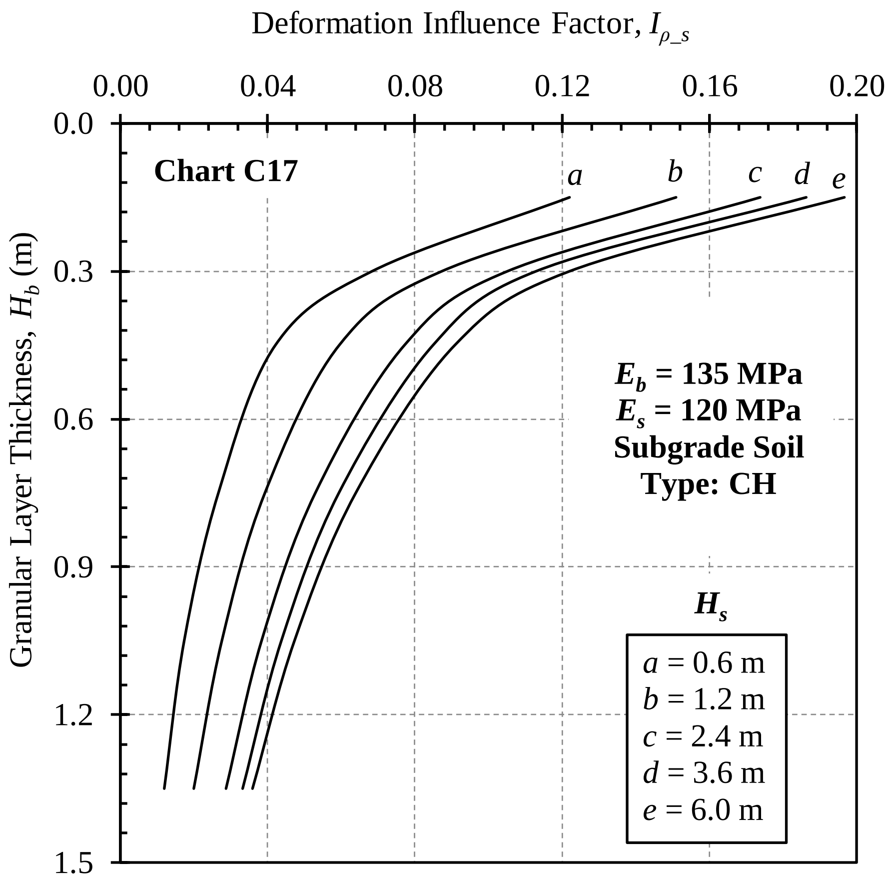
Deformation Influence Factor, I_{ρ_s}
0.00
0.04
0.08
0.12
0.16
0.20
0.0
0.3
0.6
0.9
1.2
1.5
Granular Layer Thickness, H_b (m)
Chart C17
a
b
c
d
e
E_b = 135 MPa
E_s = 120 MPa
Subgrade Soil
Type: CH
H_s
a = 0.6 m
b = 1.2 m
c = 2.4 m
d = 3.6 m
e = 6.0 m

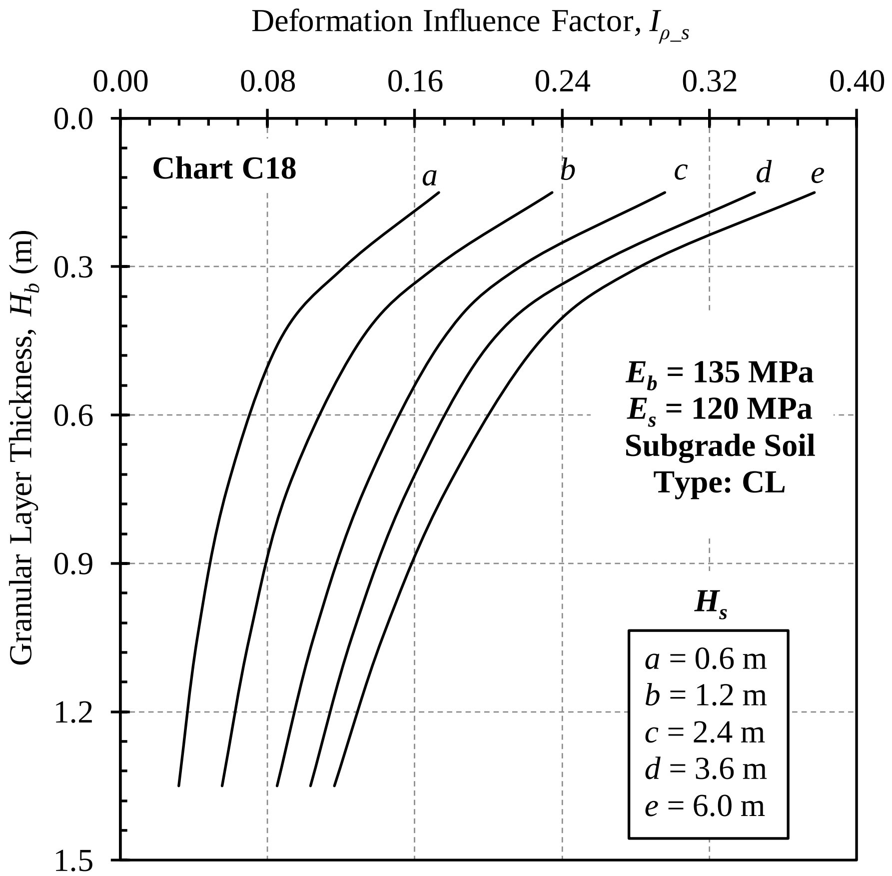
Deformation Influence Factor, I_{ρ_s}
0.00
0.08
0.16
0.24
0.32
0.40
0.0
0.3
0.6
0.9
1.2
1.5
Granular Layer Thickness, H_b (m)
Chart C18
a
b
c
d
e
E_b = 135 MPa
E_s = 120 MPa
Subgrade Soil
Type: CL
H_s
a = 0.6 m
b = 1.2 m
c = 2.4 m
d = 3.6 m
e = 6.0 m

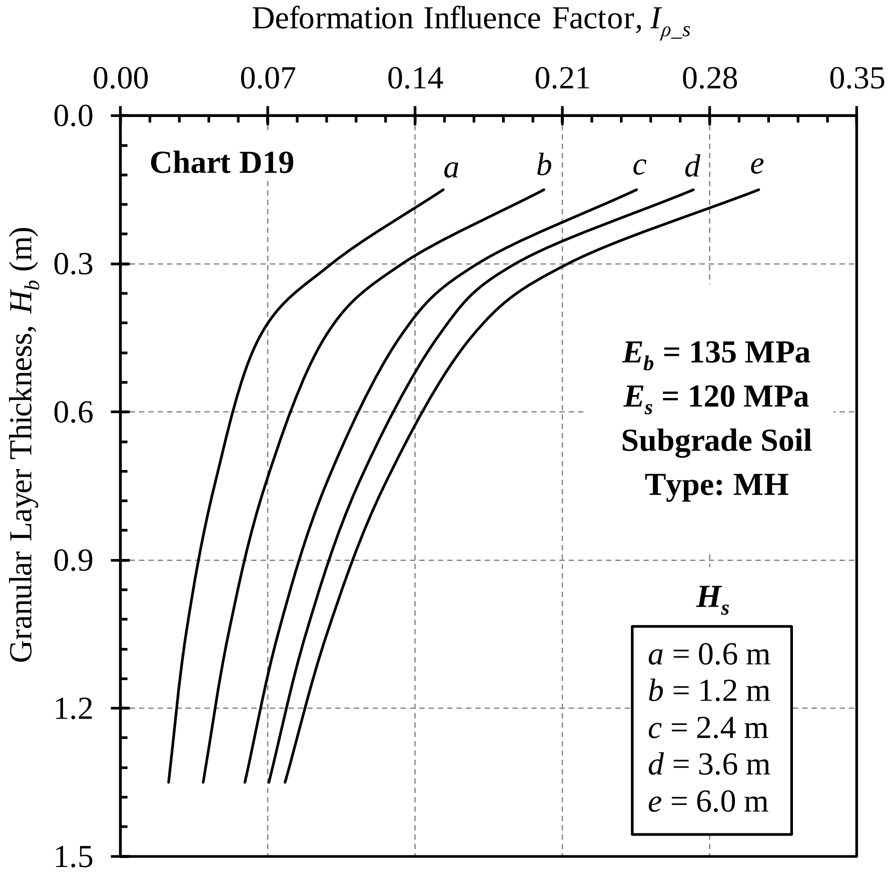
Deformation Influence Factor, I_{ρ_s}
0.00
0.07
0.14
0.21
0.28
0.35
Granular Layer Thickness, H_b (m)
0.0
0.3
0.6
0.9
1.2
1.5
Chart D19
a
b
c
d
e
E_b = 135 MPa
E_s = 120 MPa
Subgrade Soil
Type: MH
H_s
a = 0.6 m
b = 1.2 m
c = 2.4 m
d = 3.6 m
e = 6.0 m

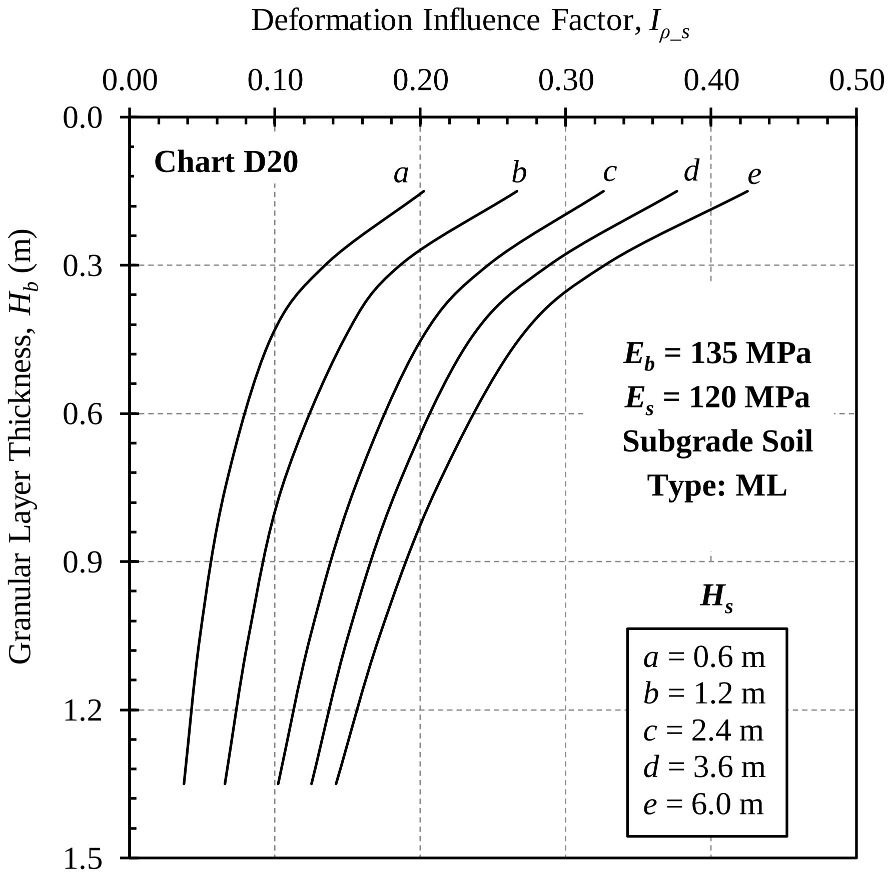
Deformation Influence Factor, I_{ρ_s}
0.00
0.10
0.20
0.30
0.40
0.50
Granular Layer Thickness, H_b (m)
0.0
0.3
0.6
0.9
1.2
1.5
Chart D20
a
b
c
d
e
E_b = 135 MPa
E_s = 120 MPa
Subgrade Soil
Type: ML
H_s
a = 0.6 m
b = 1.2 m
c = 2.4 m
d = 3.6 m
e = 6.0 m

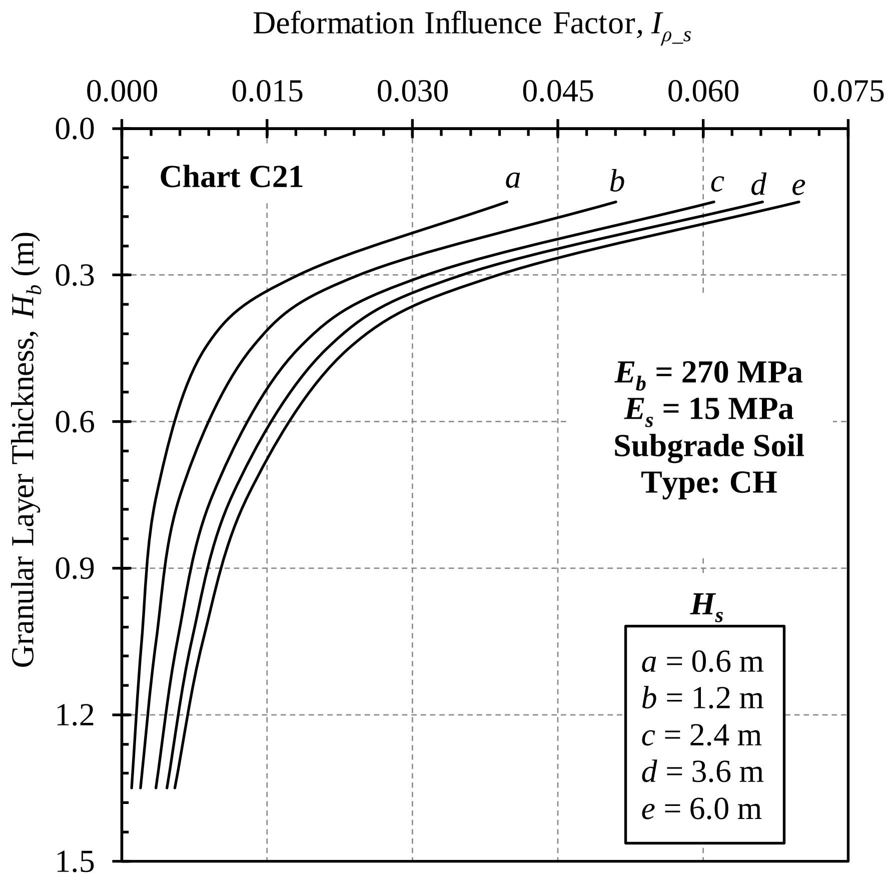
Deformation Influence Factor, I_{ρ_s}
0.000
0.015
0.030
0.045
0.060
0.075
0.0
0.3
0.6
0.9
1.2
1.5
Granular Layer Thickness, H_b (m)
Chart C21
a
b
c
d
e
E_b = 270 MPa
E_s = 15 MPa
Subgrade Soil
Type: CH
H_s
a = 0.6 m
b = 1.2 m
c = 2.4 m
d = 3.6 m
e = 6.0 m

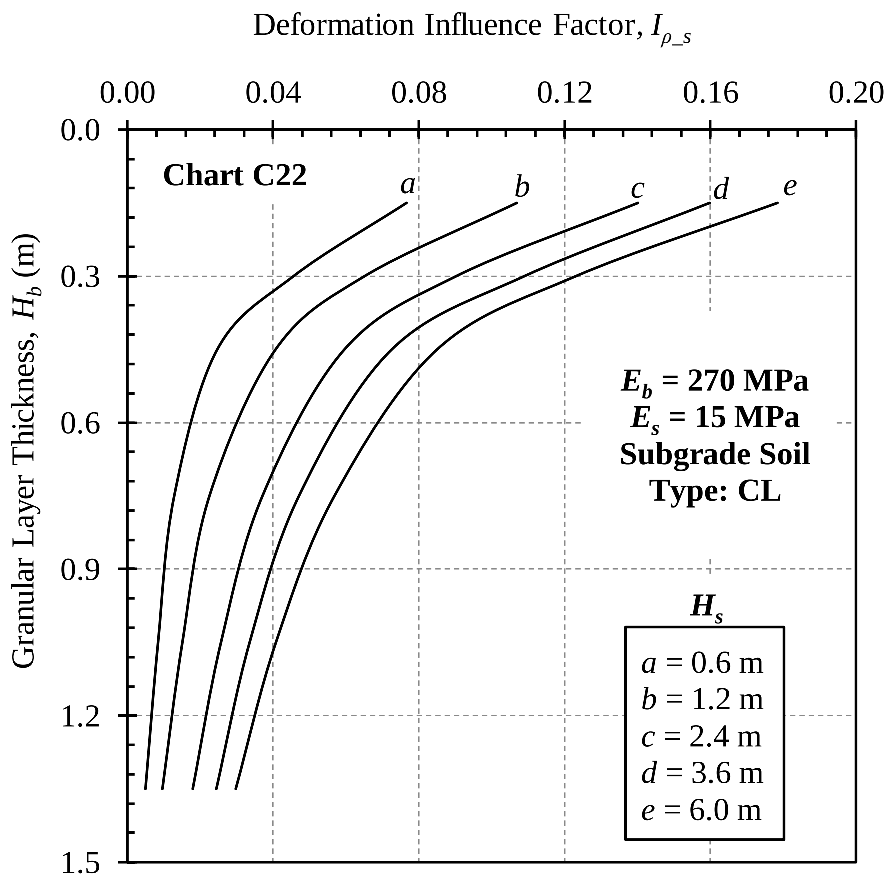
Deformation Influence Factor, I_{ρ_s}
0.00
0.04
0.08
0.12
0.16
0.20
0.0
0.3
0.6
0.9
1.2
1.5
Granular Layer Thickness, H_b (m)
Chart C22
a
b
c
d
e
E_b = 270 MPa
E_s = 15 MPa
Subgrade Soil
Type: CL
H_s
a = 0.6 m
b = 1.2 m
c = 2.4 m
d = 3.6 m
e = 6.0 m

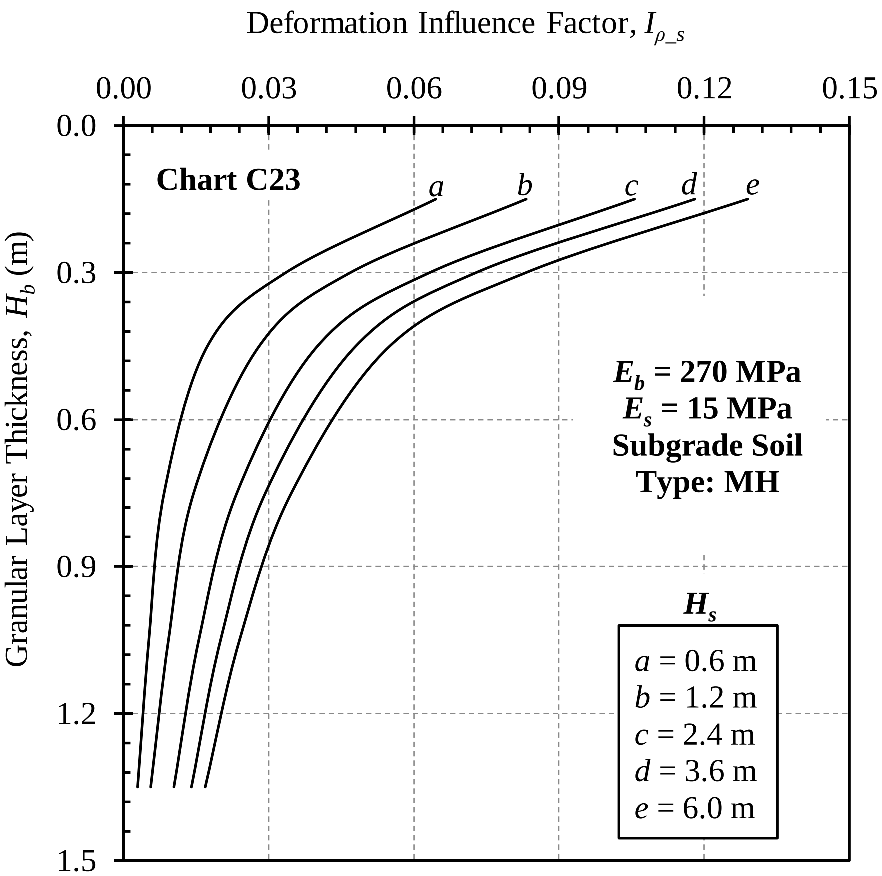

Deformation Influence Factor, I_{ρ_s}
0.00
0.03
0.06
0.09
0.12
0.15
0.0
0.3
0.6
0.9
1.2
1.5
Granular Layer Thickness, H_b (m)
Chart C23
a
b
c
d
e
E_b = 270 MPa
E_s = 15 MPa
Subgrade Soil
Type: MH
H_s
a = 0.6 m
b = 1.2 m
c = 2.4 m
d = 3.6 m
e = 6.0 m

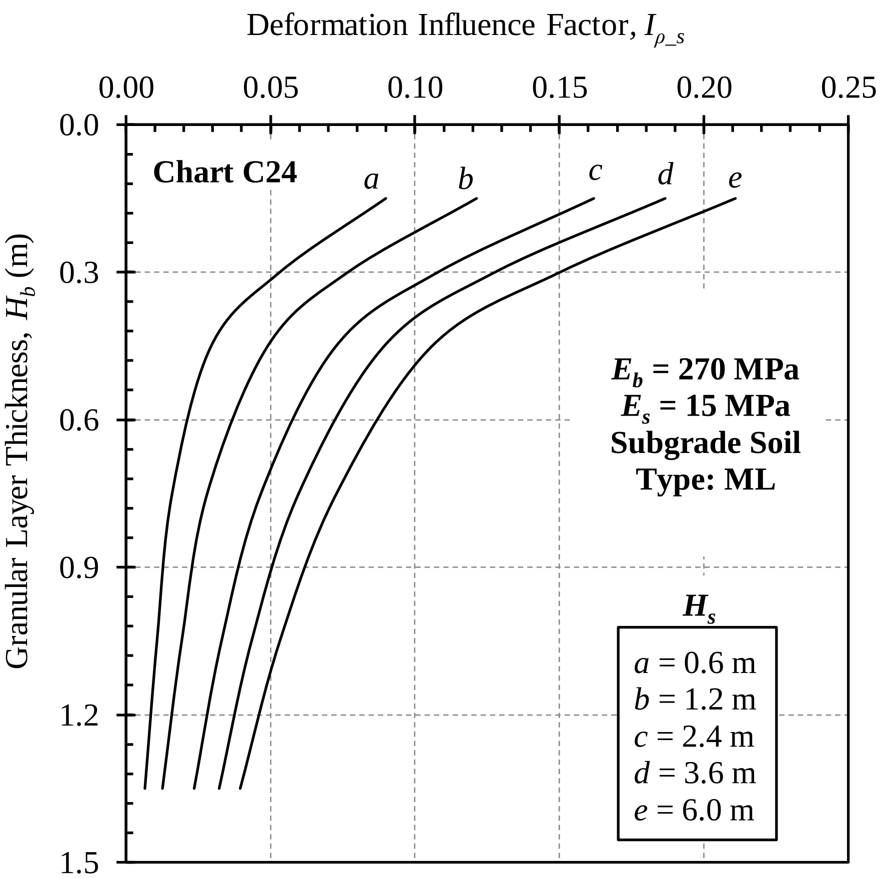

Deformation Influence Factor, I_{ρ_s}
0.00
0.05
0.10
0.15
0.20
0.25
0.0
0.3
0.6
0.9
1.2
1.5
Granular Layer Thickness, H_b (m)
Chart C24
a
b
c
d
e
E_b = 270 MPa
E_s = 15 MPa
Subgrade Soil
Type: ML
H_s
a = 0.6 m
b = 1.2 m
c = 2.4 m
d = 3.6 m
e = 6.0 m

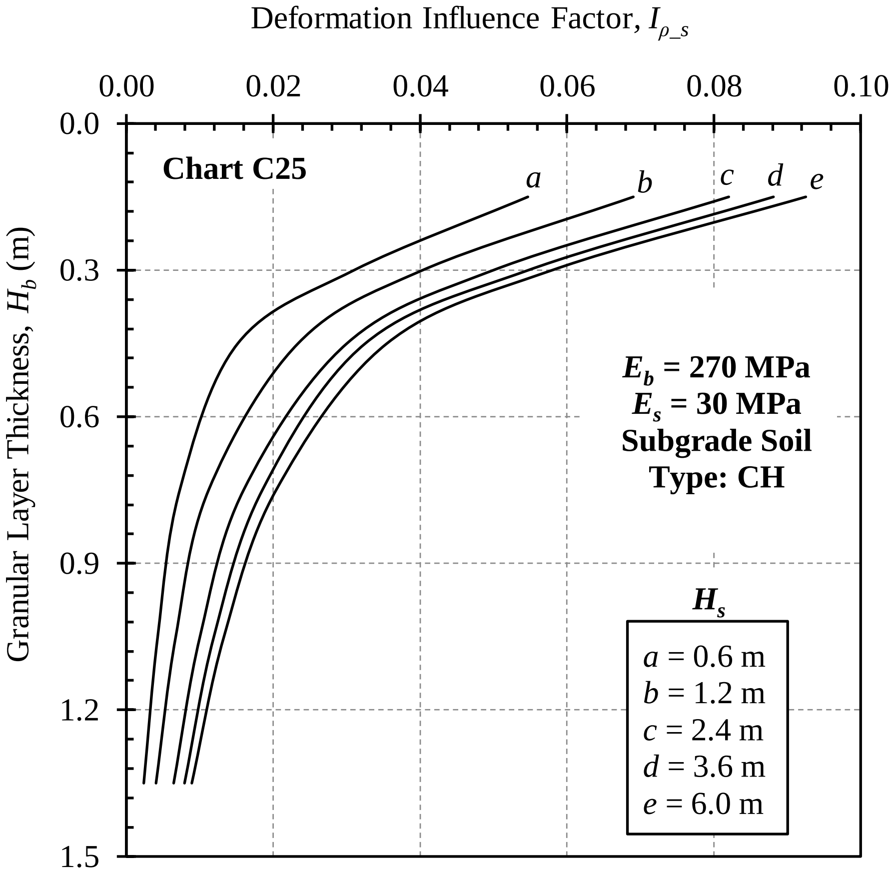
Deformation Influence Factor, I_{ρ_s}
0.00
0.02
0.04
0.06
0.08
0.10
Granular Layer Thickness, H_b (m)
0.0
0.3
0.6
0.9
1.2
1.5
Chart C25
a
b
c
d
e
E_b = 270 MPa
E_s = 30 MPa
Subgrade Soil
Type: CH
H_s
a = 0.6 m
b = 1.2 m
c = 2.4 m
d = 3.6 m
e = 6.0 m

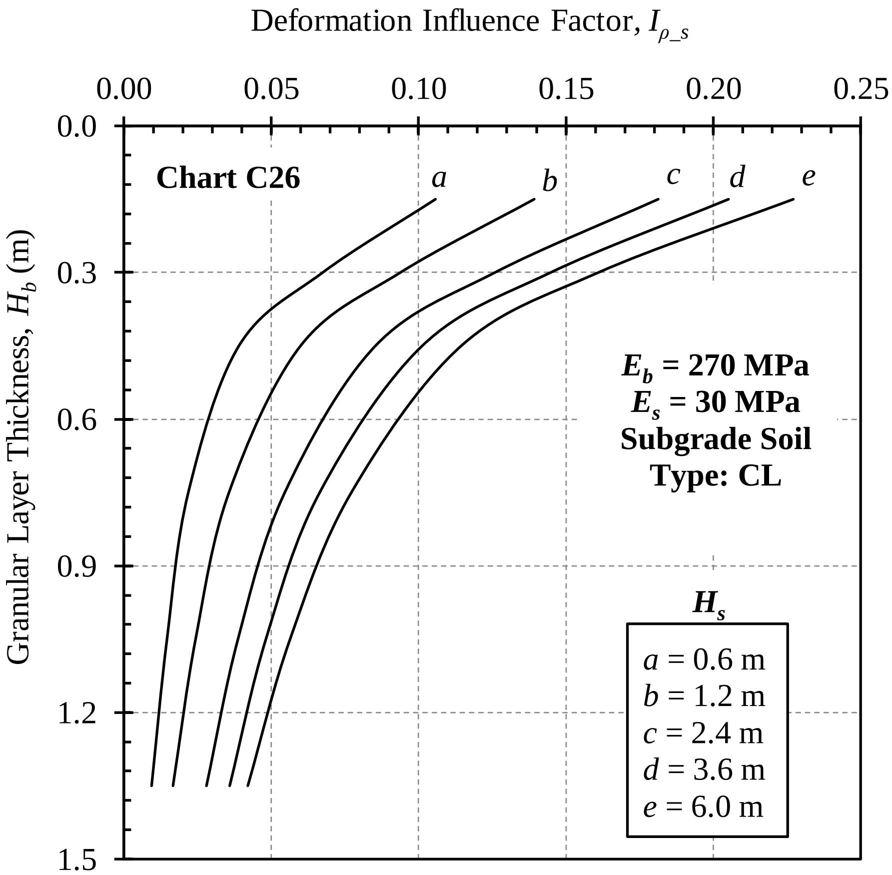
Deformation Influence Factor, I_{ρ_s}
0.00
0.05
0.10
0.15
0.20
0.25
Granular Layer Thickness, H_b (m)
0.0
0.3
0.6
0.9
1.2
1.5
Chart C26
a
b
c
d
e
E_b = 270 MPa
E_s = 30 MPa
Subgrade Soil
Type: CL
H_s
a = 0.6 m
b = 1.2 m
c = 2.4 m
d = 3.6 m
e = 6.0 m

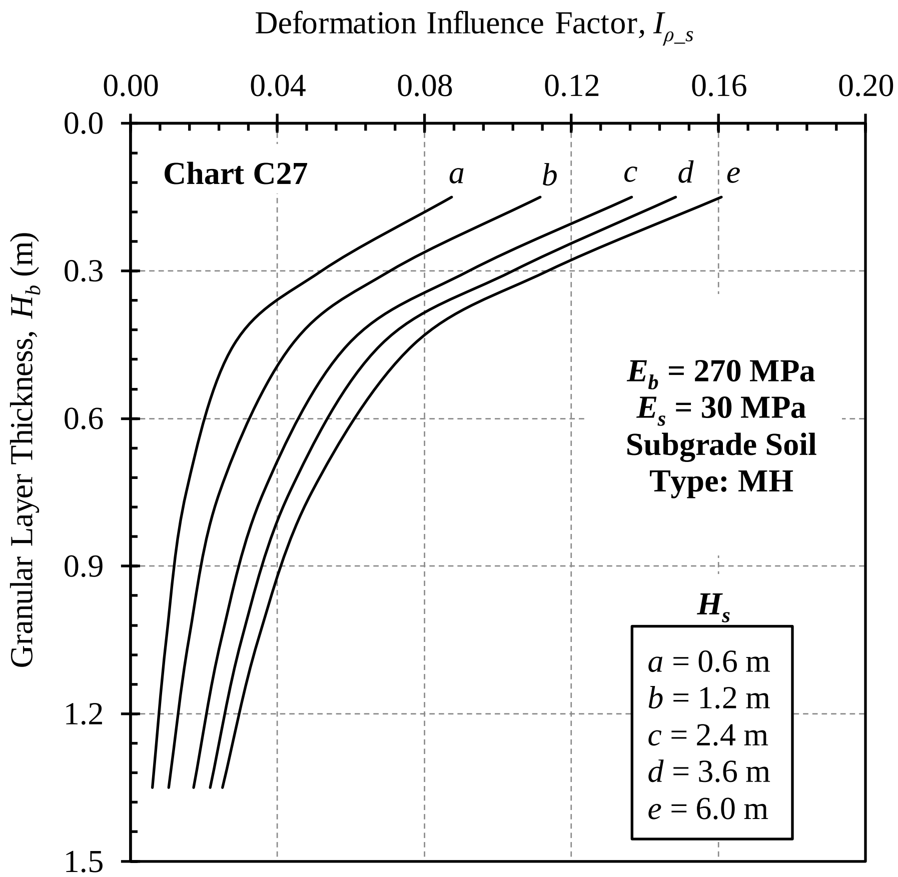
Deformation Influence Factor, I_{ρ_s}
0.00
0.04
0.08
0.12
0.16
0.20
0.0
0.3
0.6
0.9
1.2
1.5
Granular Layer Thickness, H_b (m)
Chart C27
a
b
c
d
e
E_b = 270 MPa
E_s = 30 MPa
Subgrade Soil
Type: MH
H_s
a = 0.6 m
b = 1.2 m
c = 2.4 m
d = 3.6 m
e = 6.0 m

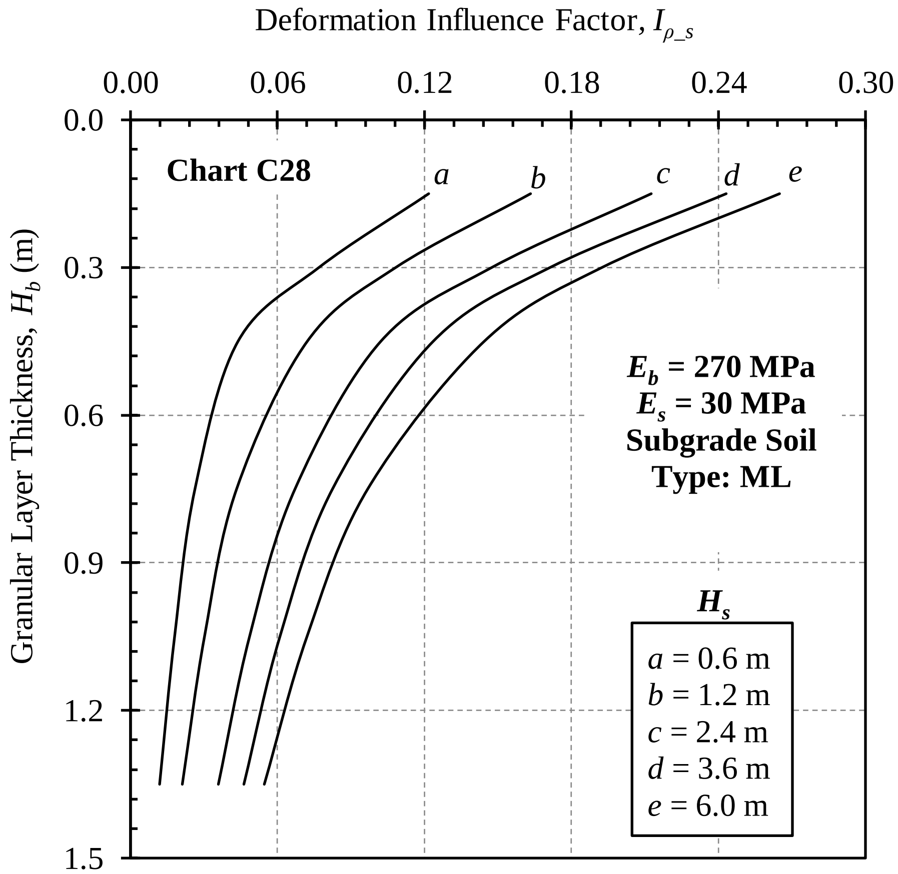
Deformation Influence Factor, I_{ρ_s}
0.00
0.06
0.12
0.18
0.24
0.30
0.0
0.3
0.6
0.9
1.2
1.5
Granular Layer Thickness, H_b (m)
Chart C28
a
b
c
d
e
E_b = 270 MPa
E_s = 30 MPa
Subgrade Soil
Type: ML
H_s
a = 0.6 m
b = 1.2 m
c = 2.4 m
d = 3.6 m
e = 6.0 m

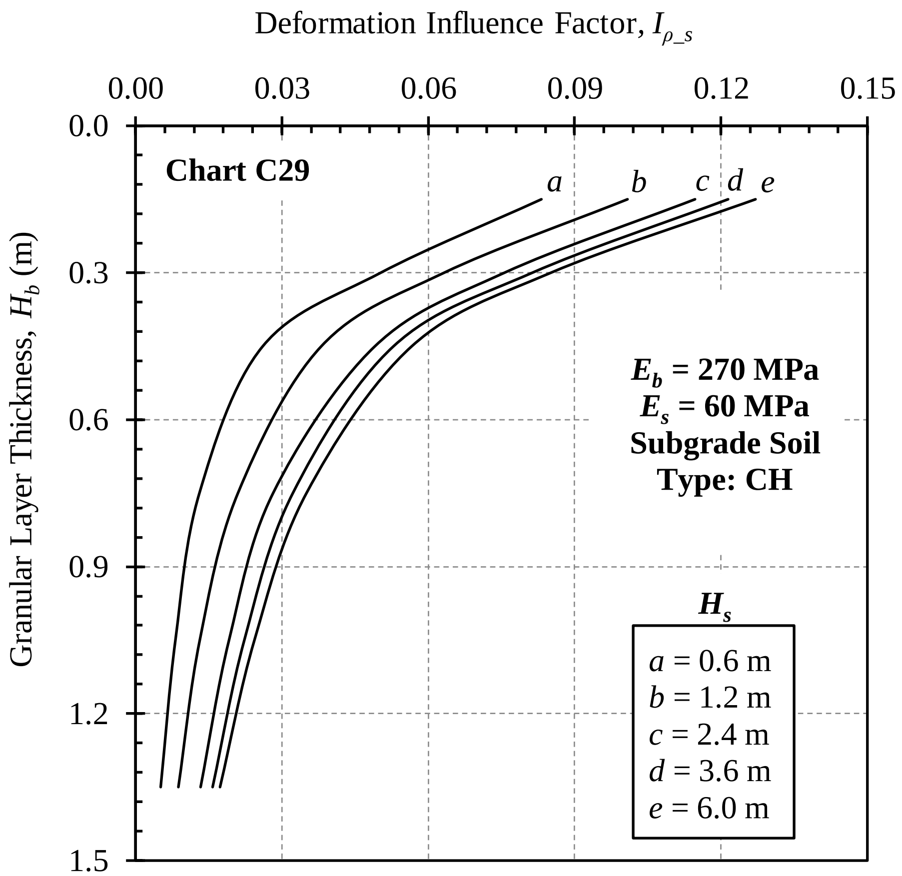
Deformation Influence Factor, I_{ρ_s}
0.00
0.03
0.06
0.09
0.12
0.15
0.0
0.3
0.6
0.9
1.2
1.5
Granular Layer Thickness, H_b (m)
Chart C29
a
b
c
d
e
E_b = 270 MPa
E_s = 60 MPa
Subgrade Soil
Type: CH
H_s
a = 0.6 m
b = 1.2 m
c = 2.4 m
d = 3.6 m
e = 6.0 m

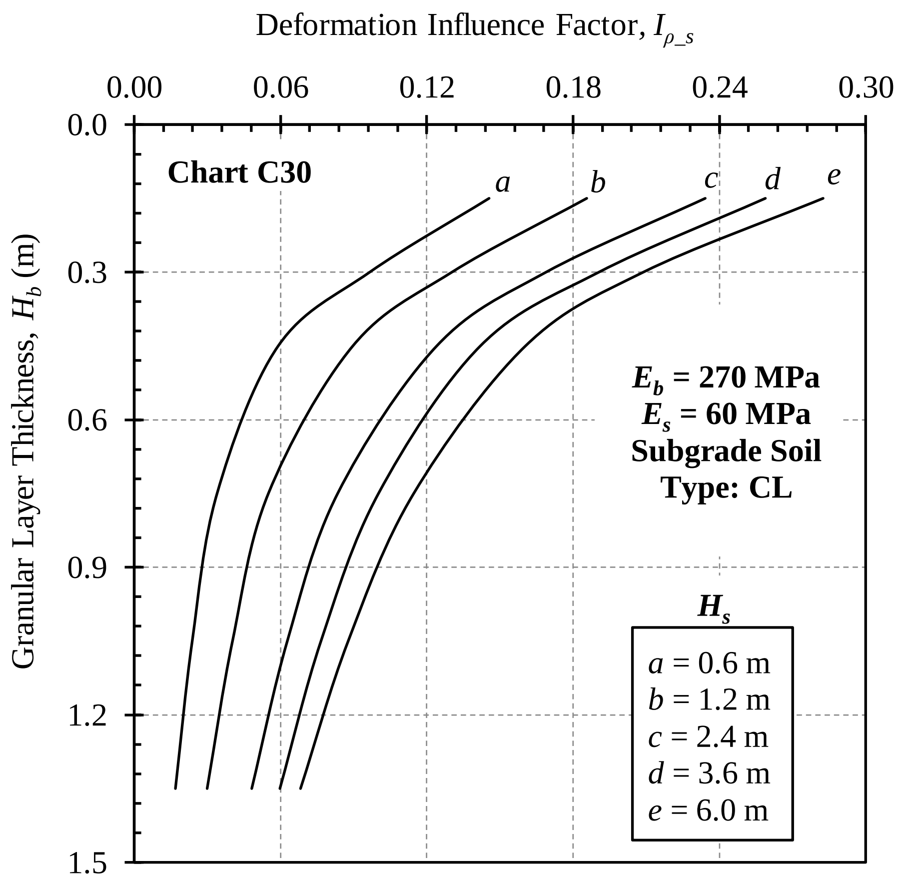
Deformation Influence Factor, I_{ρ_s}
0.00
0.06
0.12
0.18
0.24
0.30
0.0
0.3
0.6
0.9
1.2
1.5
Granular Layer Thickness, H_b (m)
Chart C30
a
b
c
d
e
E_b = 270 MPa
E_s = 60 MPa
Subgrade Soil
Type: CL
H_s
a = 0.6 m
b = 1.2 m
c = 2.4 m
d = 3.6 m
e = 6.0 m

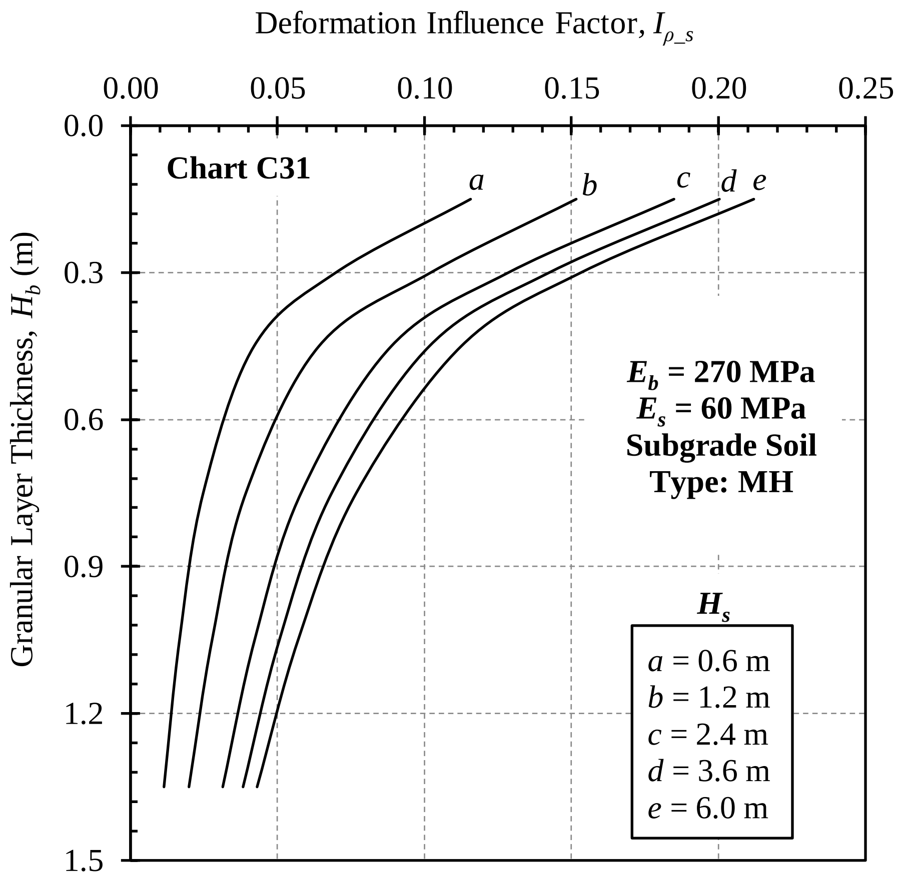
Deformation Influence Factor, I_{ρ_s}
0.00
0.05
0.10
0.15
0.20
0.25
0.0
0.3
0.6
0.9
1.2
1.5
Granular Layer Thickness, H_b (m)
Chart C31
a
b
c
d
e
E_b = 270 MPa
E_s = 60 MPa
Subgrade Soil
Type: MH
H_s
a = 0.6 m
b = 1.2 m
c = 2.4 m
d = 3.6 m
e = 6.0 m

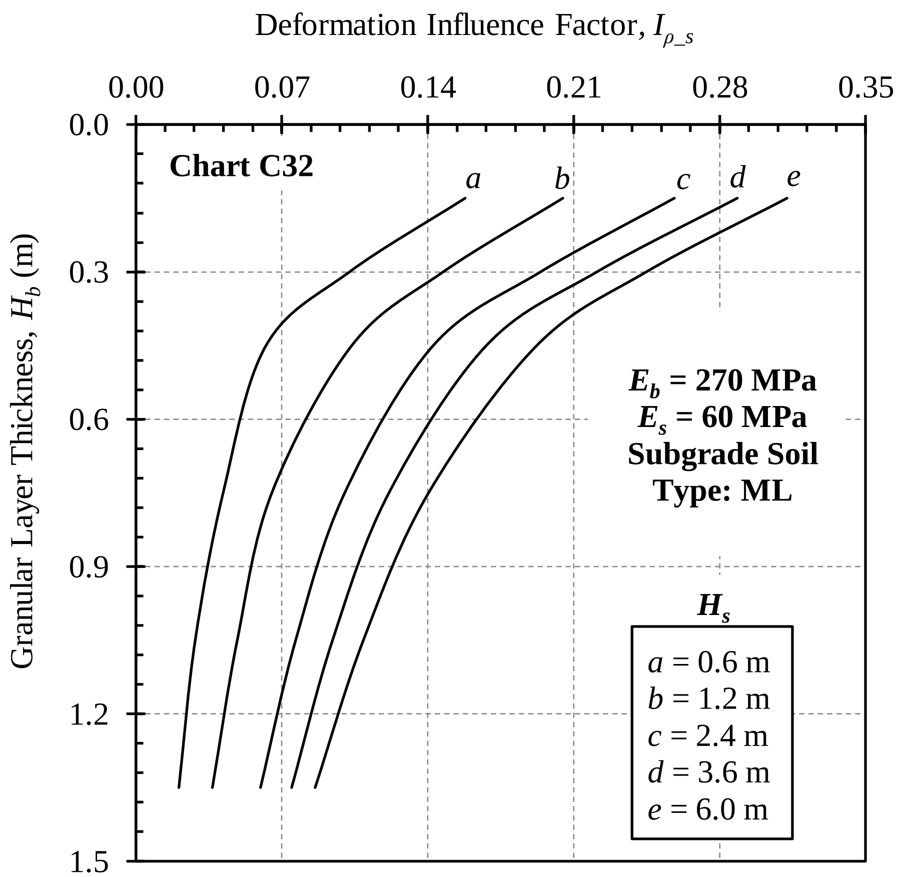
Deformation Influence Factor, I_{ρ_s}
0.00
0.07
0.14
0.21
0.28
0.35
0.0
0.3
0.6
0.9
1.2
1.5
Granular Layer Thickness, H_b (m)
Chart C32
a
b
c
d
e
E_b = 270 MPa
E_s = 60 MPa
Subgrade Soil
Type: ML
H_s
a = 0.6 m
b = 1.2 m
c = 2.4 m
d = 3.6 m
e = 6.0 m

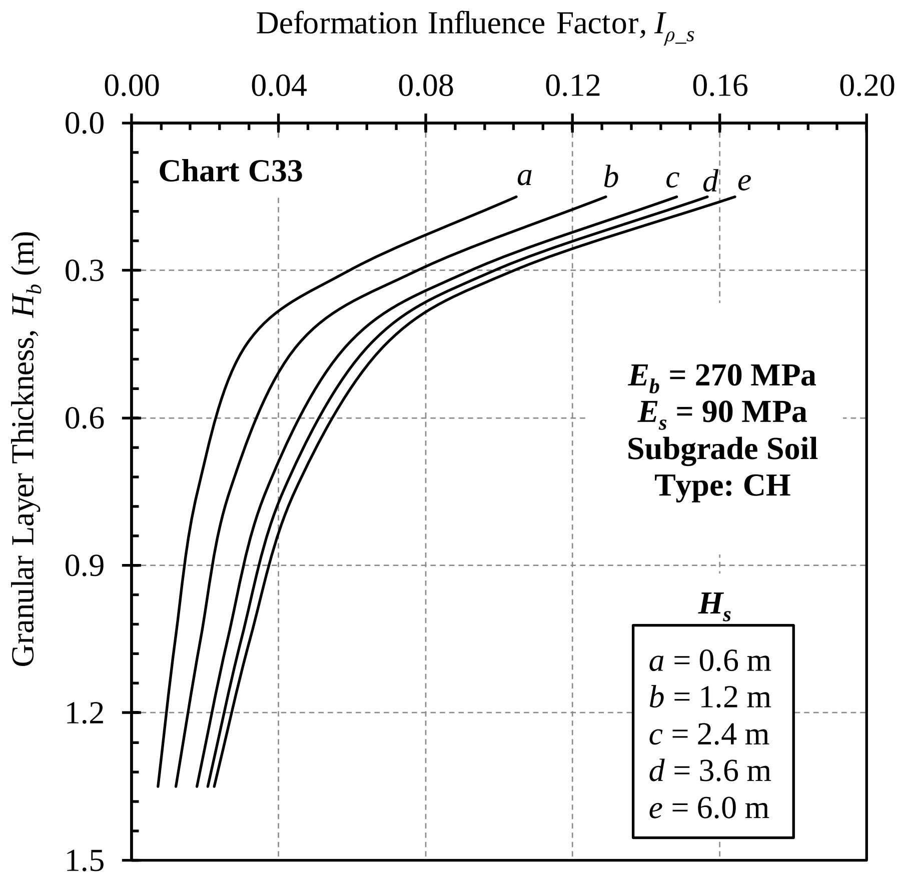

Deformation Influence Factor, I_{ρ_s}
0.00
0.04
0.08
0.12
0.16
0.20
0.0
0.3
0.6
0.9
1.2
1.5
Granular Layer Thickness, H_b (m)
Chart C33
a
b
c
d
e
E_b = 270 MPa
E_s = 90 MPa
Subgrade Soil
Type: CH
H_s
a = 0.6 m
b = 1.2 m
c = 2.4 m
d = 3.6 m
e = 6.0 m

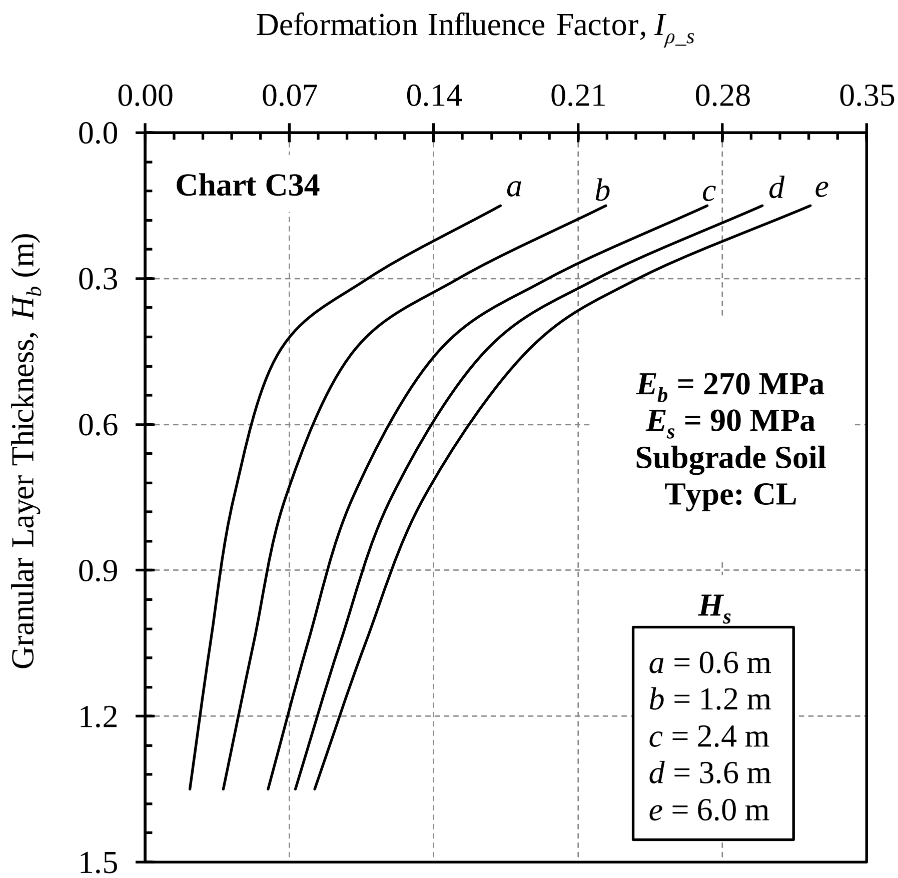

Deformation Influence Factor, I_{ρ_s}
0.00
0.07
0.14
0.21
0.28
0.35
0.0
0.3
0.6
0.9
1.2
1.5
Granular Layer Thickness, H_b (m)
Chart C34
a
b
c
d
e
E_b = 270 MPa
E_s = 90 MPa
Subgrade Soil
Type: CL
H_s
a = 0.6 m
b = 1.2 m
c = 2.4 m
d = 3.6 m
e = 6.0 m

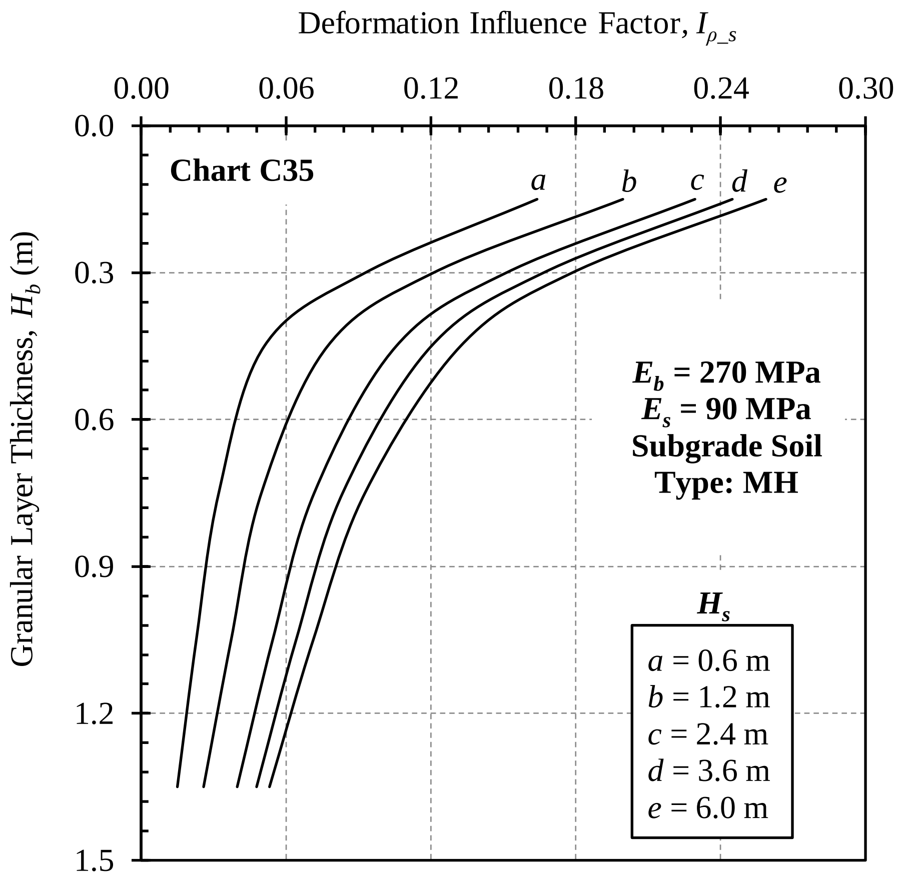
Deformation Influence Factor, I_{ρ_s}
0.00
0.06
0.12
0.18
0.24
0.30
0.0
0.3
0.6
0.9
1.2
1.5
Granular Layer Thickness, H_b (m)
Chart C35
a
b
c
d
e
E_b = 270 MPa
E_s = 90 MPa
Subgrade Soil
Type: MH
H_s
a = 0.6 m
b = 1.2 m
c = 2.4 m
d = 3.6 m
e = 6.0 m

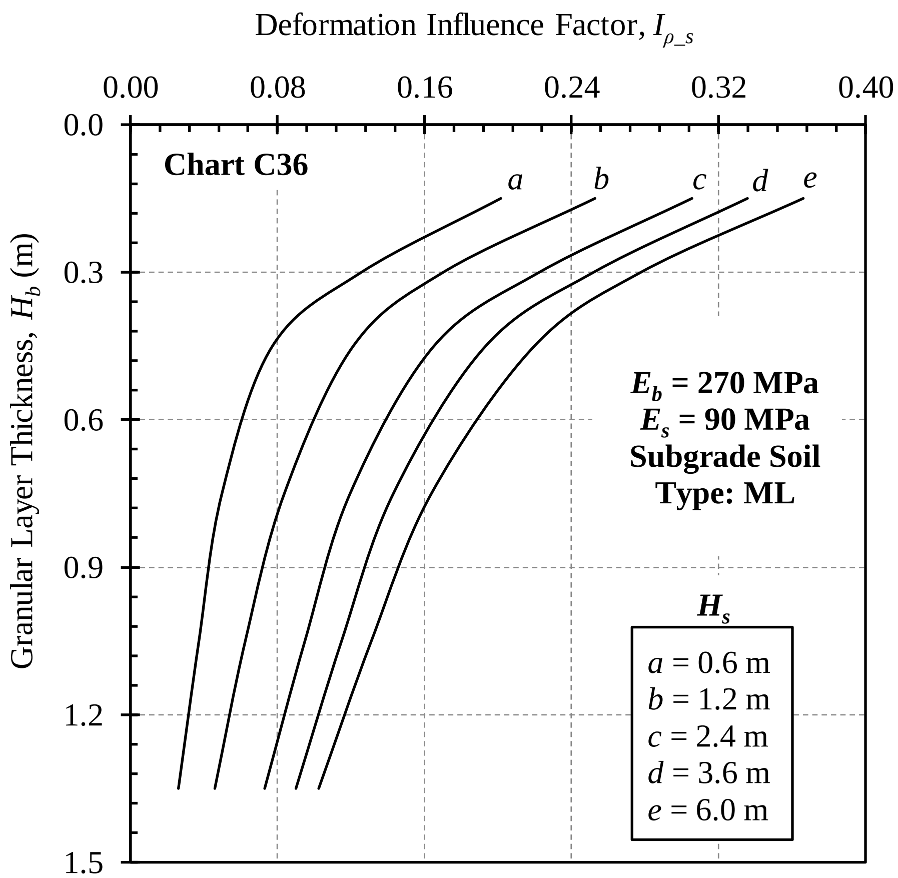
Deformation Influence Factor, I_{ρ_s}
0.00
0.08
0.16
0.24
0.32
0.40
0.0
0.3
0.6
0.9
1.2
1.5
Granular Layer Thickness, H_b (m)
Chart C36
a
b
c
d
e
E_b = 270 MPa
E_s = 90 MPa
Subgrade Soil
Type: ML
H_s
a = 0.6 m
b = 1.2 m
c = 2.4 m
d = 3.6 m
e = 6.0 m

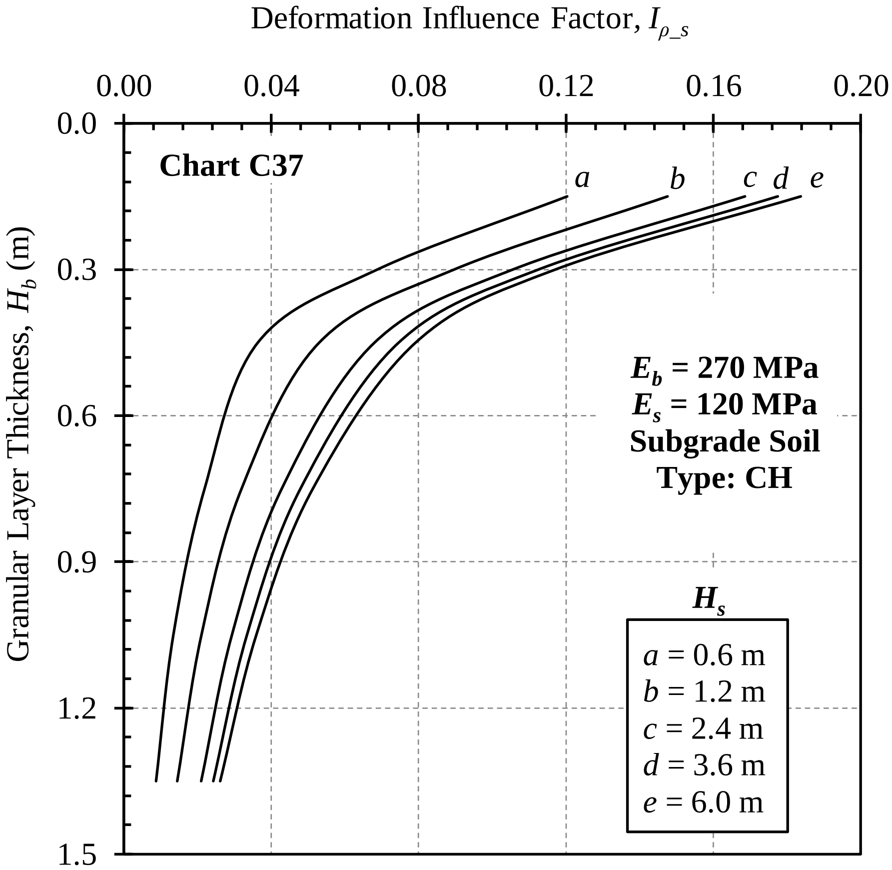
Deformation Influence Factor, I_{ρ_s}
0.00
0.04
0.08
0.12
0.16
0.20
0.0
0.3
0.6
0.9
1.2
1.5
Granular Layer Thickness, H_b (m)
Chart C37
a
b
c
d
e
E_b = 270 MPa
E_s = 120 MPa
Subgrade Soil
Type: CH
H_s
a = 0.6 m
b = 1.2 m
c = 2.4 m
d = 3.6 m
e = 6.0 m

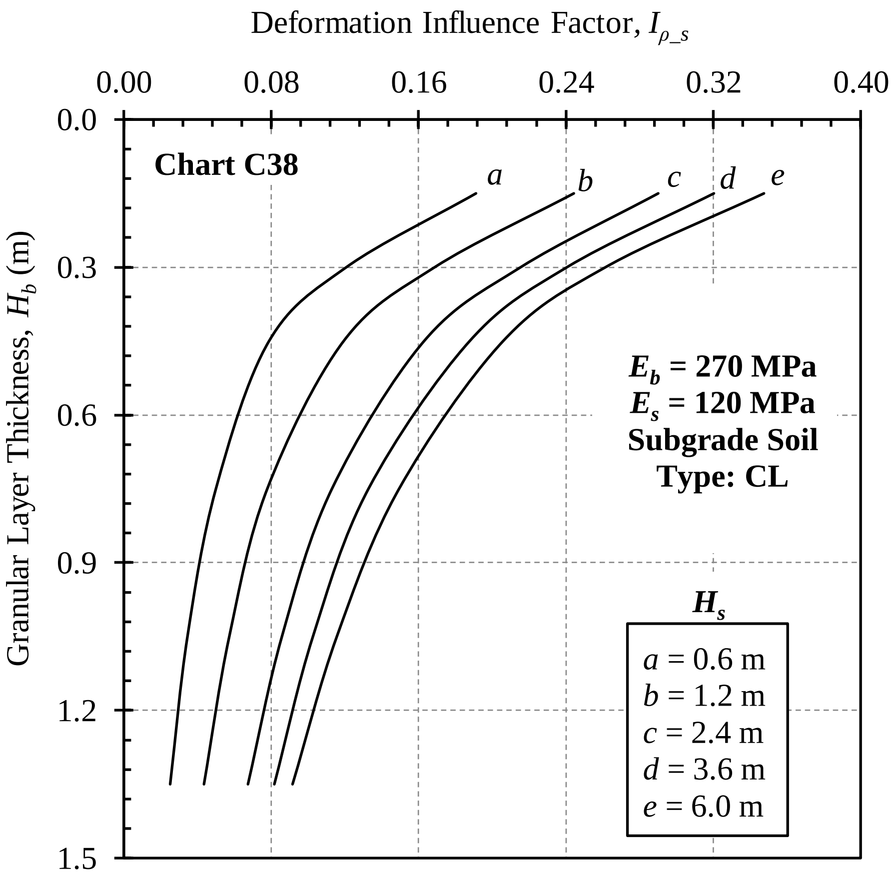
Deformation Influence Factor, I_{ρ_s}
0.00
0.08
0.16
0.24
0.32
0.40
0.0
0.3
0.6
0.9
1.2
1.5
Granular Layer Thickness, H_b (m)
Chart C38
a
b
c
d
e
E_b = 270 MPa
E_s = 120 MPa
Subgrade Soil
Type: CL
H_s
a = 0.6 m
b = 1.2 m
c = 2.4 m
d = 3.6 m
e = 6.0 m

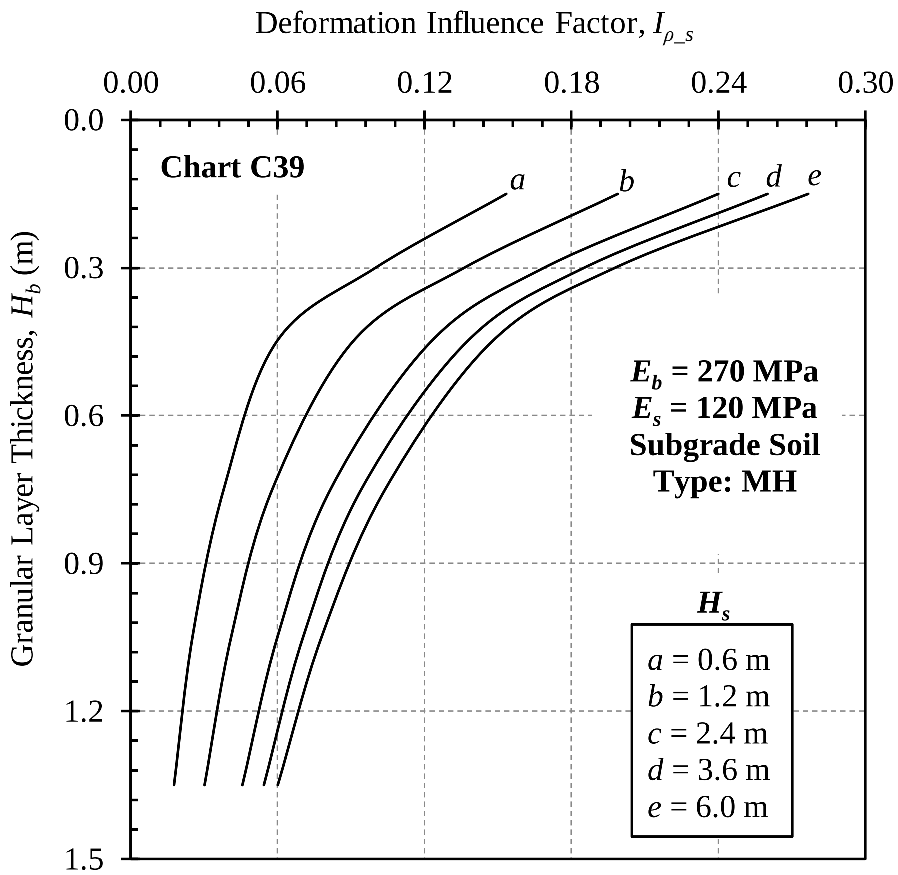
Deformation Influence Factor, I_{ρ_s}
0.00
0.06
0.12
0.18
0.24
0.30
0.0
0.3
0.6
0.9
1.2
1.5
Granular Layer Thickness, H_b (m)
Chart C39
a
b
c
d
e
E_b = 270 MPa
E_s = 120 MPa
Subgrade Soil
Type: MH
H_s
a = 0.6 m
b = 1.2 m
c = 2.4 m
d = 3.6 m
e = 6.0 m

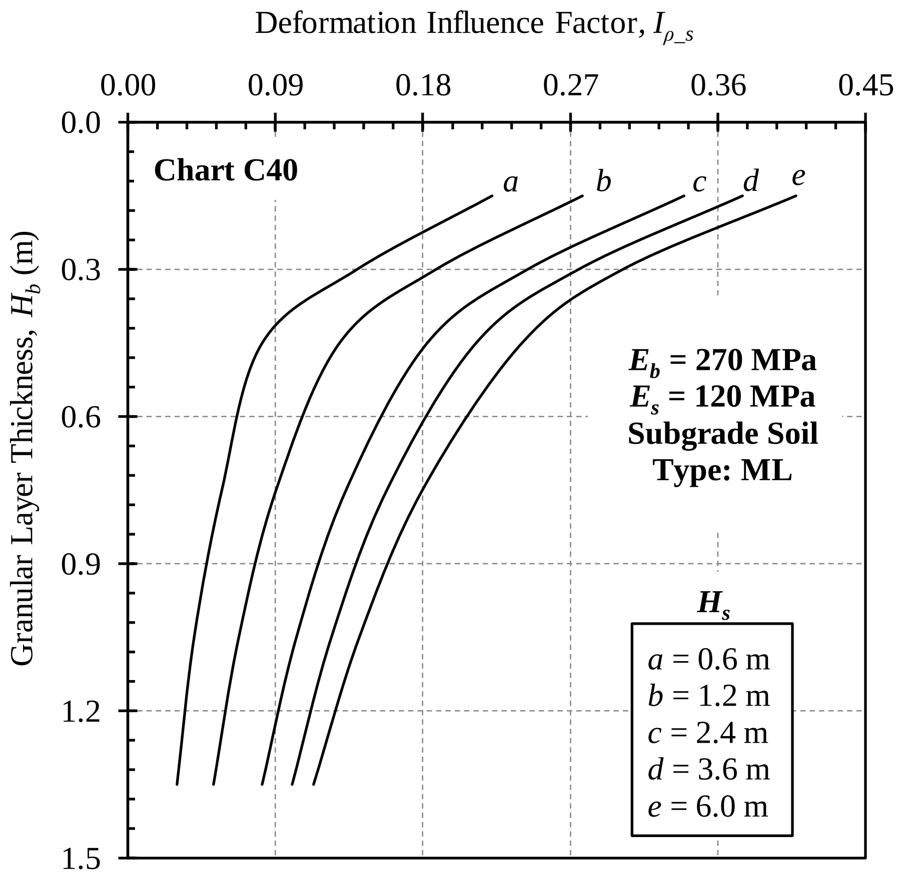
Deformation Influence Factor, I_{ρ_s}
0.00
0.09
0.18
0.27
0.36
0.45
0.0
0.3
0.6
0.9
1.2
1.5
Granular Layer Thickness, H_b (m)
Chart C40
a
b
c
d
e
E_b = 270 MPa
E_s = 120 MPa
Subgrade Soil
Type: ML
H_s
a = 0.6 m
b = 1.2 m
c = 2.4 m
d = 3.6 m
e = 6.0 m

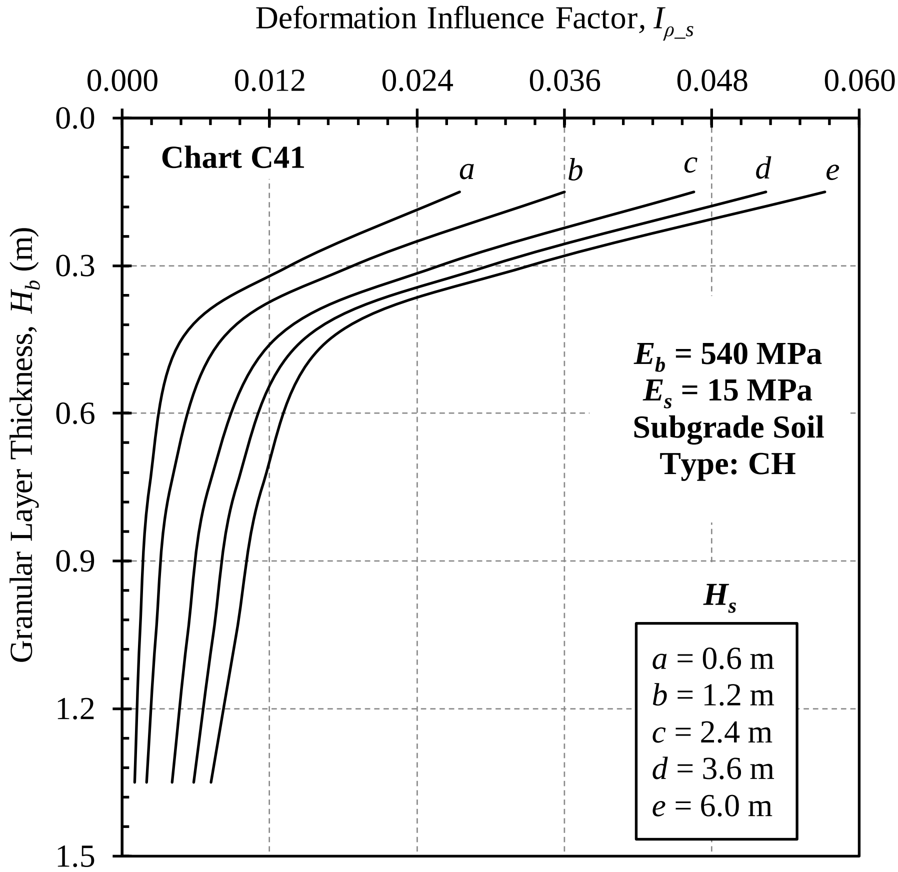
Deformation Influence Factor, I_{ρ_s}
0.000
0.012
0.024
0.036
0.048
0.060
0.0
0.3
0.6
0.9
1.2
1.5
Granular Layer Thickness, H_b (m)
Chart C41
a
b
c
d
e
E_b = 540 MPa
E_s = 15 MPa
Subgrade Soil
Type: CH
H_s
a = 0.6 m
b = 1.2 m
c = 2.4 m
d = 3.6 m
e = 6.0 m

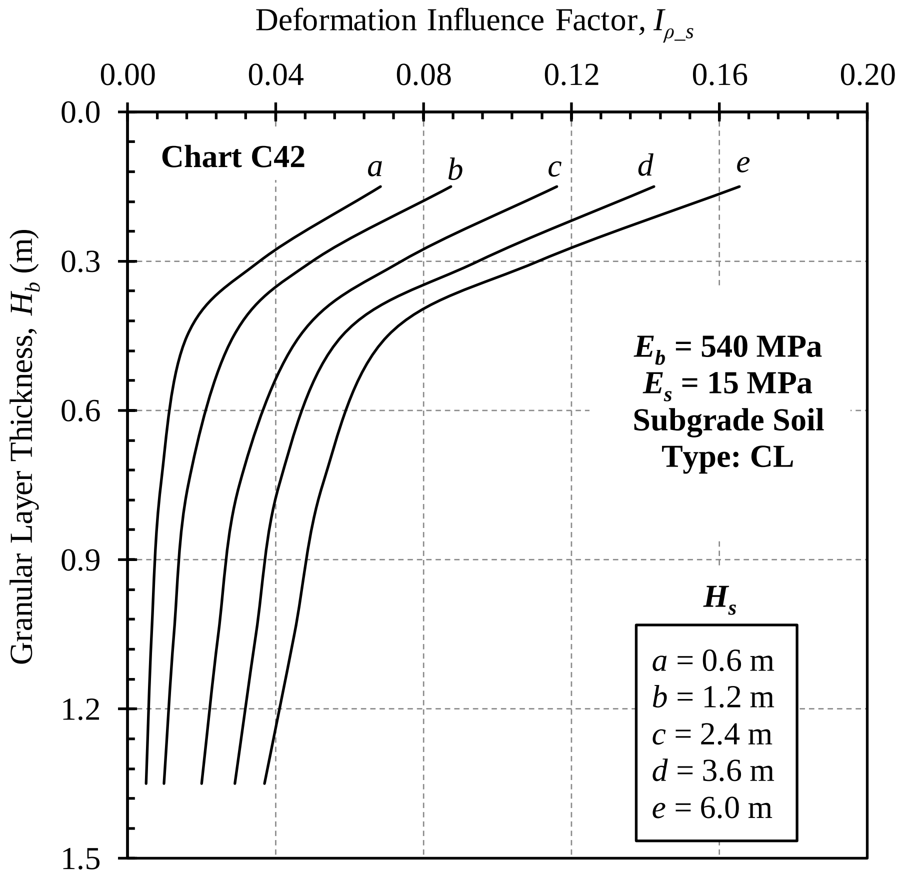
Deformation Influence Factor, I_{ρ_s}
0.00
0.04
0.08
0.12
0.16
0.20
0.0
0.3
0.6
0.9
1.2
1.5
Granular Layer Thickness, H_b (m)
Chart C42
a
b
c
d
e
E_b = 540 MPa
E_s = 15 MPa
Subgrade Soil
Type: CL
H_s
a = 0.6 m
b = 1.2 m
c = 2.4 m
d = 3.6 m
e = 6.0 m

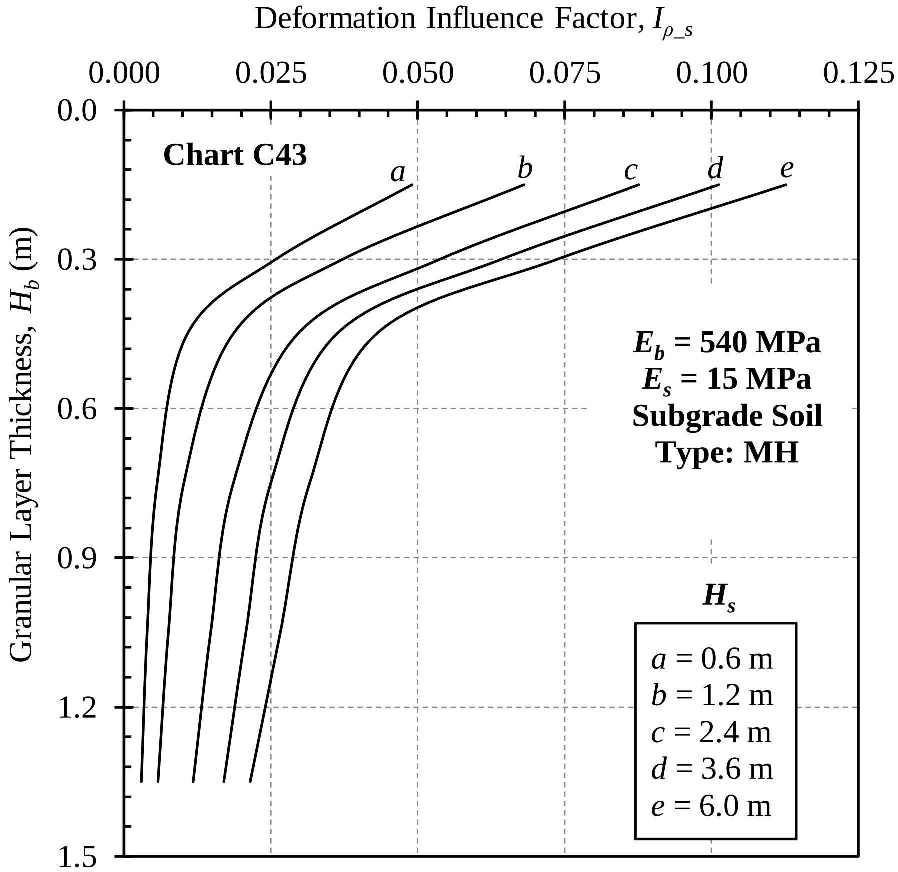
Deformation Influence Factor, I_{ρ_s}
0.000
0.025
0.050
0.075
0.100
0.125
0.0
0.3
0.6
0.9
1.2
1.5
Granular Layer Thickness, H_b (m)
Chart C43
a
b
c
d
e
E_b = 540 MPa
E_s = 15 MPa
Subgrade Soil
Type: MH
H_s
a = 0.6 m
b = 1.2 m
c = 2.4 m
d = 3.6 m
e = 6.0 m

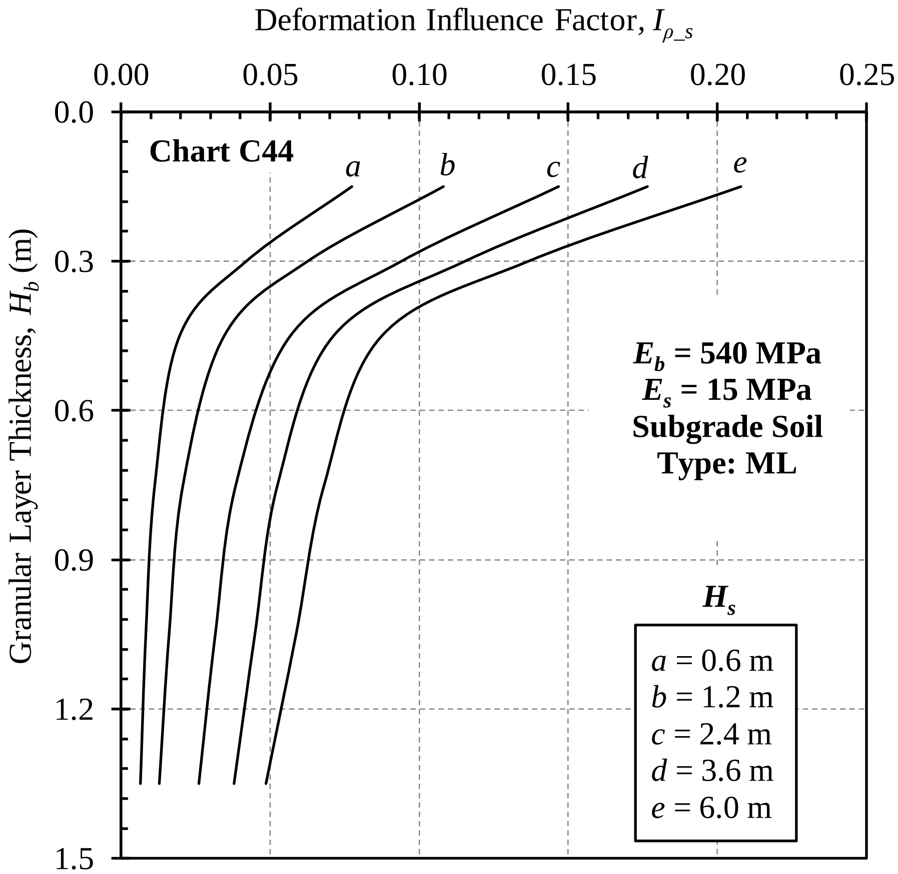
Deformation Influence Factor, I_{ρ_s}
0.00
0.05
0.10
0.15
0.20
0.25
0.0
0.3
0.6
0.9
1.2
1.5
Granular Layer Thickness, H_b (m)
Chart C44
a
b
c
d
e
E_b = 540 MPa
E_s = 15 MPa
Subgrade Soil
Type: ML
H_s
a = 0.6 m
b = 1.2 m
c = 2.4 m
d = 3.6 m
e = 6.0 m

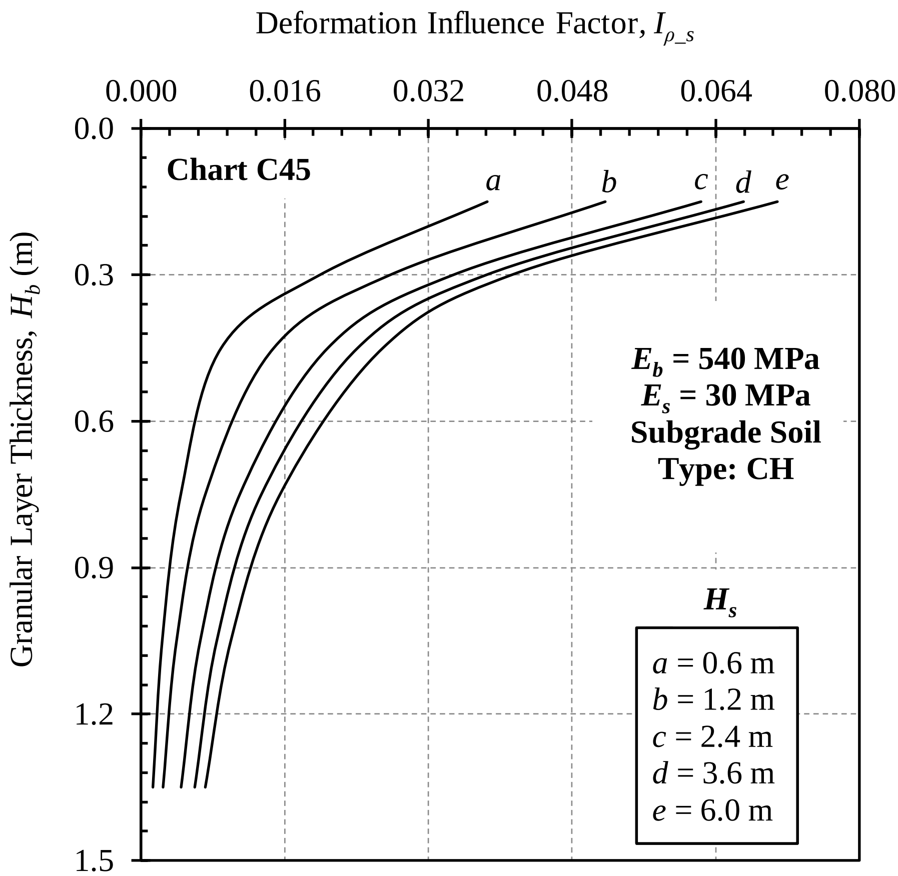
Deformation Influence Factor, I_{ρ_s}
0.000
0.016
0.032
0.048
0.064
0.080
0.0
0.3
0.6
0.9
1.2
1.5
Granular Layer Thickness, H_b (m)
Chart C45
a
b
c
d
e
E_b = 540 MPa
E_s = 30 MPa
Subgrade Soil
Type: CH
H_s
a = 0.6 m
b = 1.2 m
c = 2.4 m
d = 3.6 m
e = 6.0 m

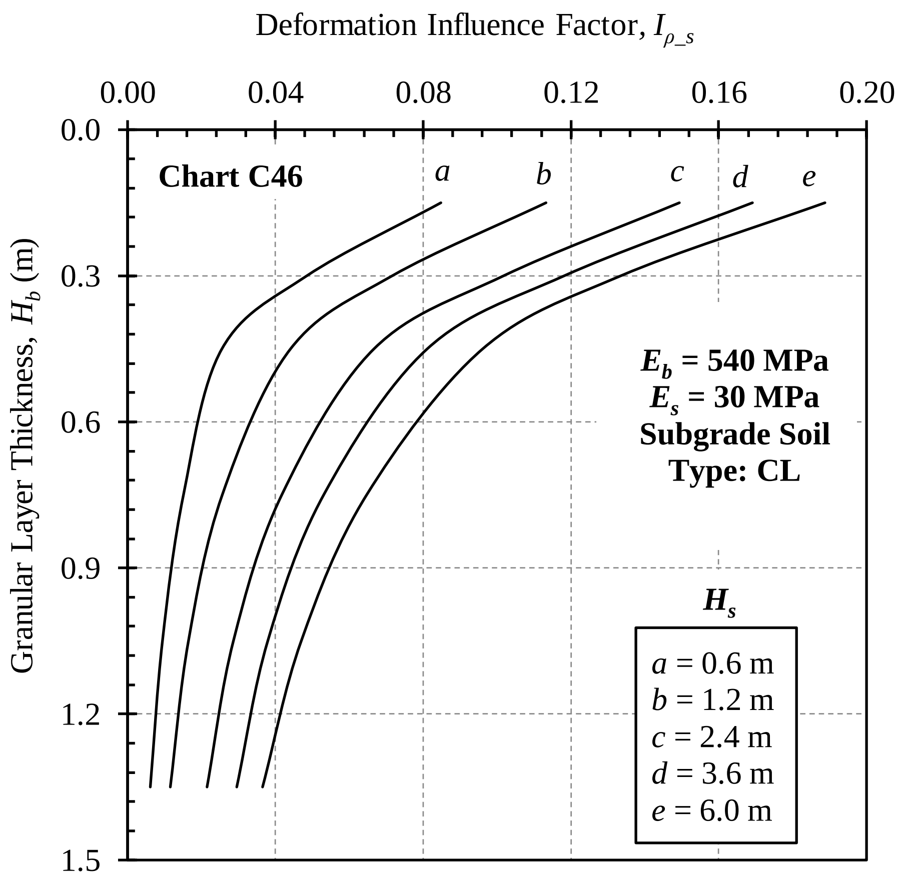
Deformation Influence Factor, I_{ρ_s}
0.00
0.04
0.08
0.12
0.16
0.20
0.0
0.3
0.6
0.9
1.2
1.5
Granular Layer Thickness, H_b (m)
Chart C46
a
b
c
d
e
E_b = 540 MPa
E_s = 30 MPa
Subgrade Soil
Type: CL
H_s
a = 0.6 m
b = 1.2 m
c = 2.4 m
d = 3.6 m
e = 6.0 m

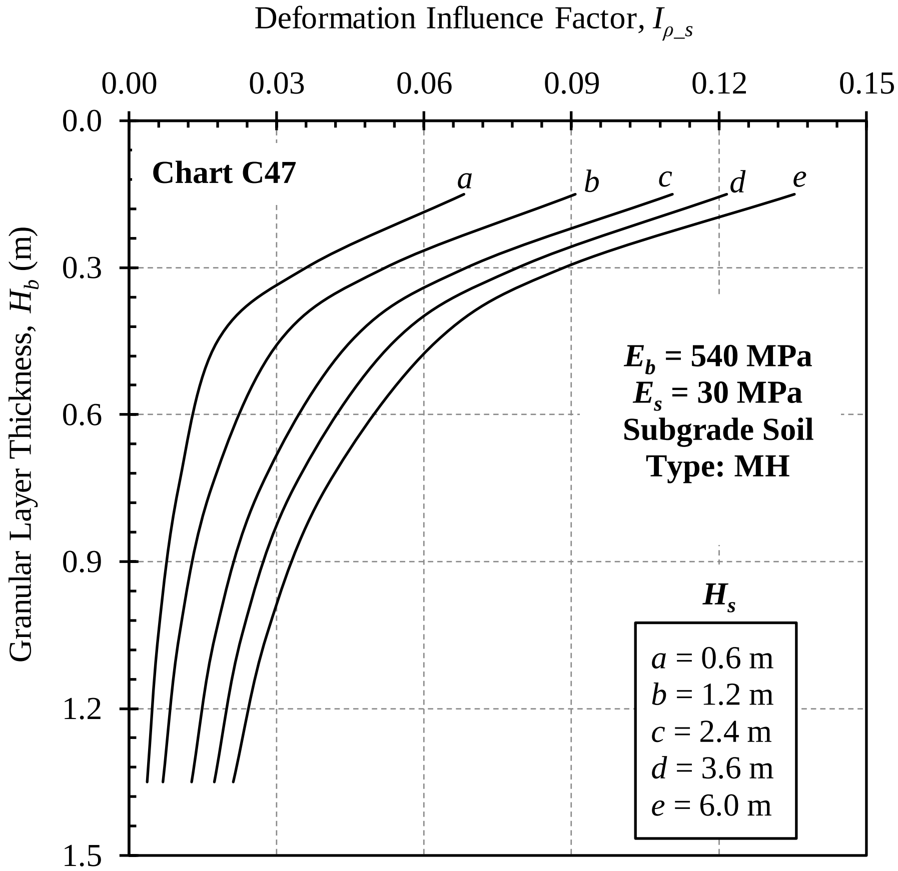

Deformation Influence Factor, I_{ρ_s}
0.00
0.03
0.06
0.09
0.12
0.15
0.0
0.3
0.6
0.9
1.2
1.5
Granular Layer Thickness, H_b (m)
Chart C47
a
b
c
d
e
E_b = 540 MPa
E_s = 30 MPa
Subgrade Soil
Type: MH
H_s
a = 0.6 m
b = 1.2 m
c = 2.4 m
d = 3.6 m
e = 6.0 m

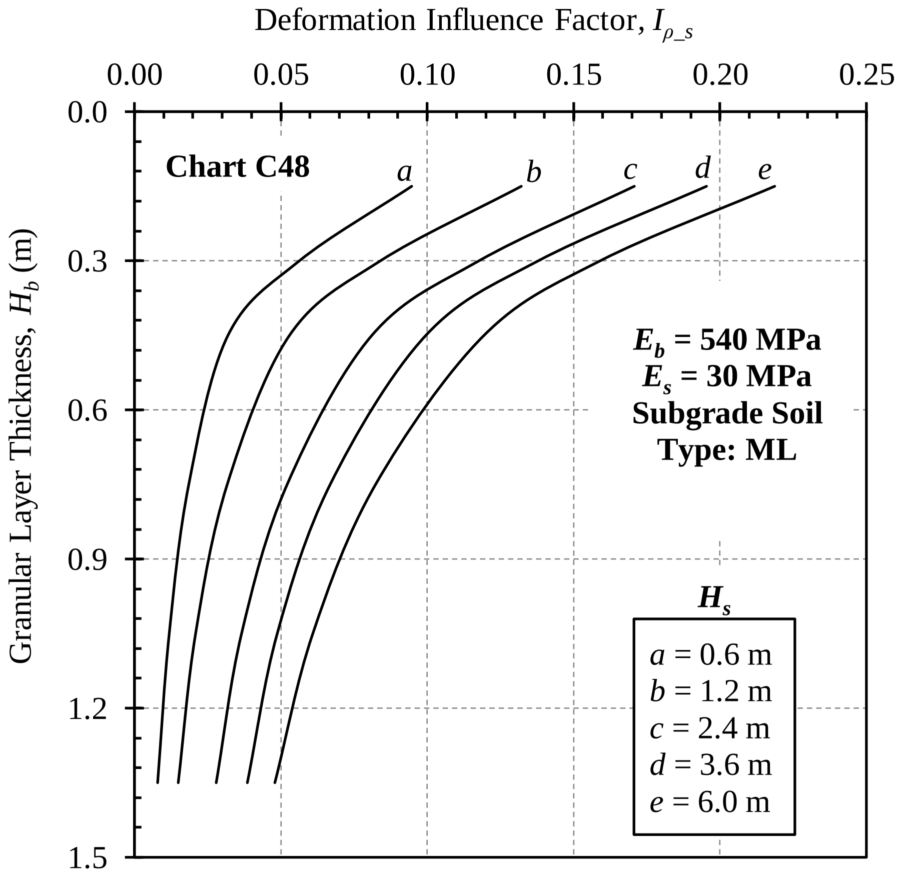

Deformation Influence Factor, I_{ρ_s}
0.00
0.05
0.10
0.15
0.20
0.25
0.0
0.3
0.6
0.9
1.2
1.5
Granular Layer Thickness, H_b (m)
Chart C48
a
b
c
d
e
E_b = 540 MPa
E_s = 30 MPa
Subgrade Soil
Type: ML
H_s
a = 0.6 m
b = 1.2 m
c = 2.4 m
d = 3.6 m
e = 6.0 m

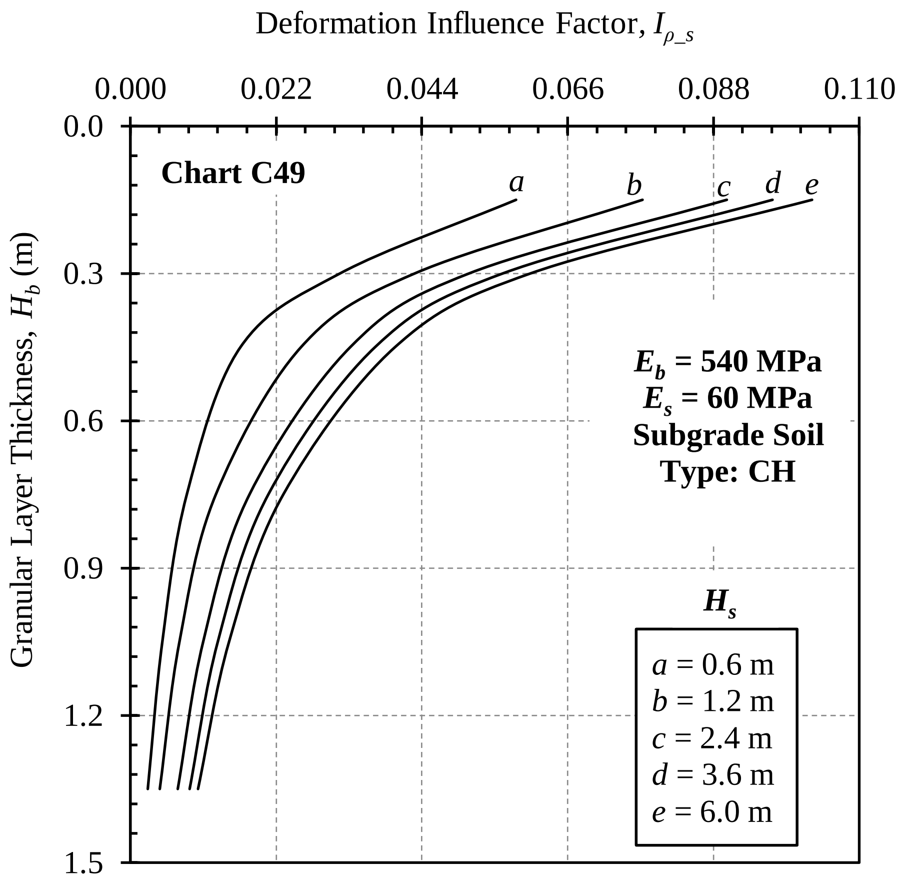

Deformation Influence Factor, I_{ρ_s}
0.000
0.022
0.044
0.066
0.088
0.110
0.0
0.3
0.6
0.9
1.2
1.5
Granular Layer Thickness, H_b (m)
Chart C49
a
b
c
d
e
E_b = 540 MPa
E_s = 60 MPa
Subgrade Soil
Type: CH
H_s
a = 0.6 m
b = 1.2 m
c = 2.4 m
d = 3.6 m
e = 6.0 m

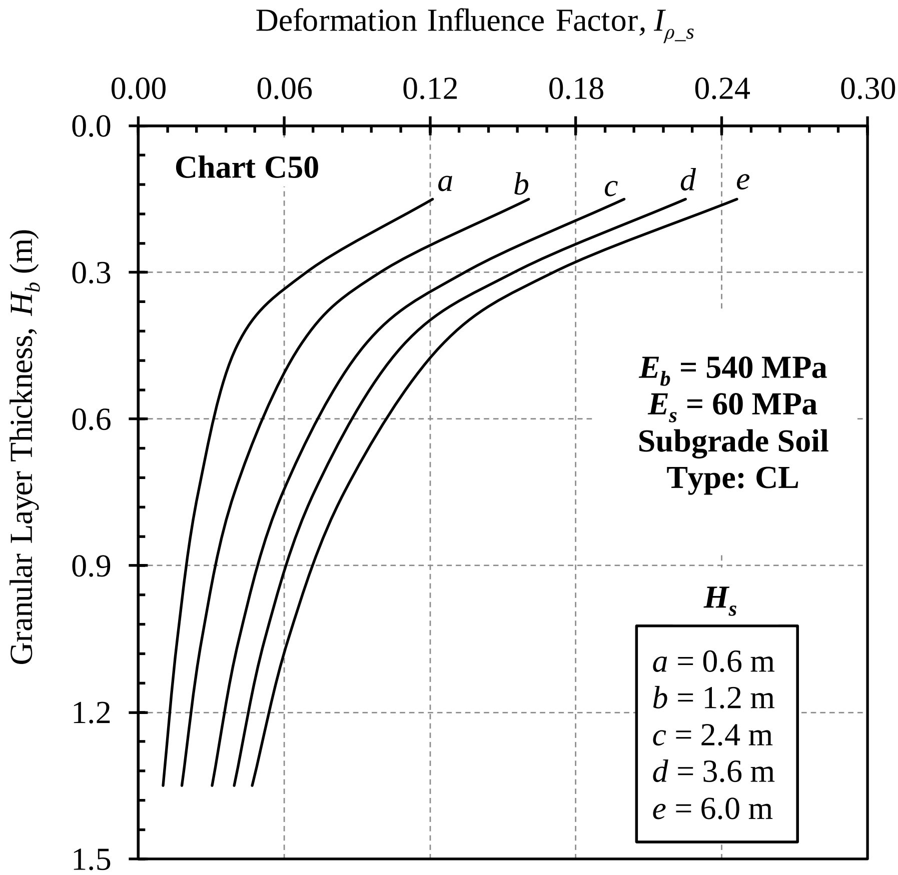

Deformation Influence Factor, I_{ρ_s}
0.00
0.06
0.12
0.18
0.24
0.30
0.0
0.3
0.6
0.9
1.2
1.5
Granular Layer Thickness, H_b (m)
Chart C50
a
b
c
d
e
E_b = 540 MPa
E_s = 60 MPa
Subgrade Soil
Type: CL
H_s
a = 0.6 m
b = 1.2 m
c = 2.4 m
d = 3.6 m
e = 6.0 m

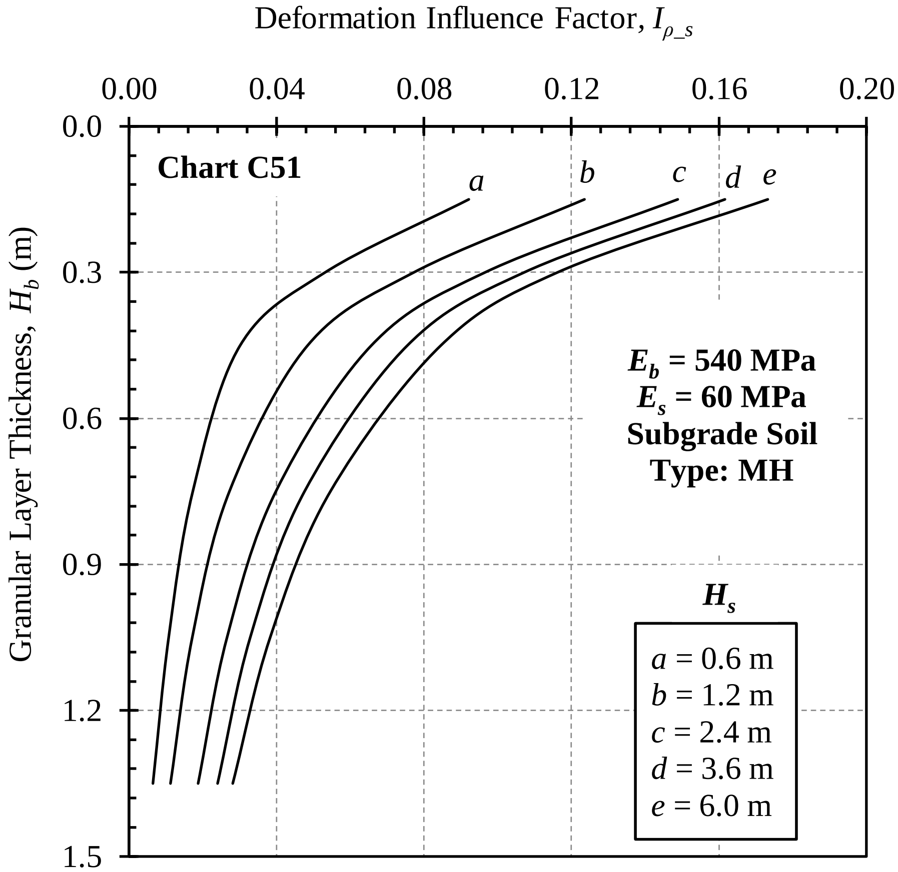
Deformation Influence Factor, I_{ρ_s}
0.00
0.04
0.08
0.12
0.16
0.20
0.0
0.3
0.6
0.9
1.2
1.5
Granular Layer Thickness, H_b (m)
Chart C51
a
b
c
d
e
E_b = 540 MPa
E_s = 60 MPa
Subgrade Soil
Type: MH
H_s
a = 0.6 m
b = 1.2 m
c = 2.4 m
d = 3.6 m
e = 6.0 m

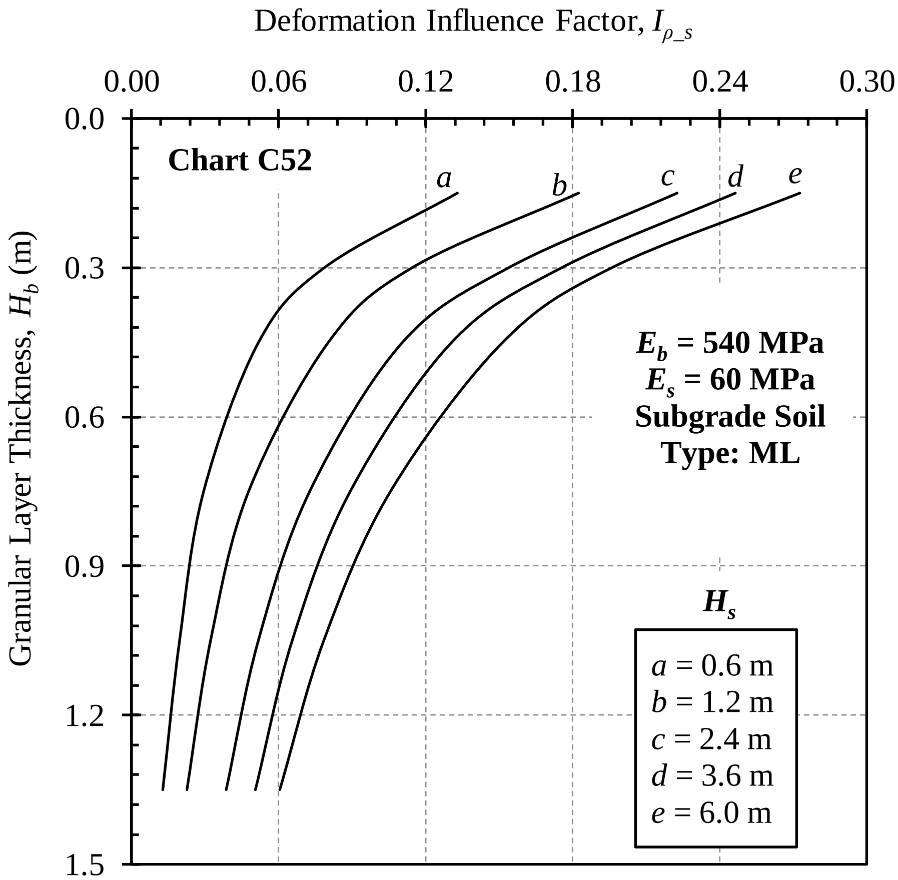
Deformation Influence Factor, I_{ρ_s}
0.00
0.06
0.12
0.18
0.24
0.30
0.0
0.3
0.6
0.9
1.2
1.5
Granular Layer Thickness, H_b (m)
Chart C52
a
b
c
d
e
E_b = 540 MPa
E_s = 60 MPa
Subgrade Soil
Type: ML
H_s
a = 0.6 m
b = 1.2 m
c = 2.4 m
d = 3.6 m
e = 6.0 m

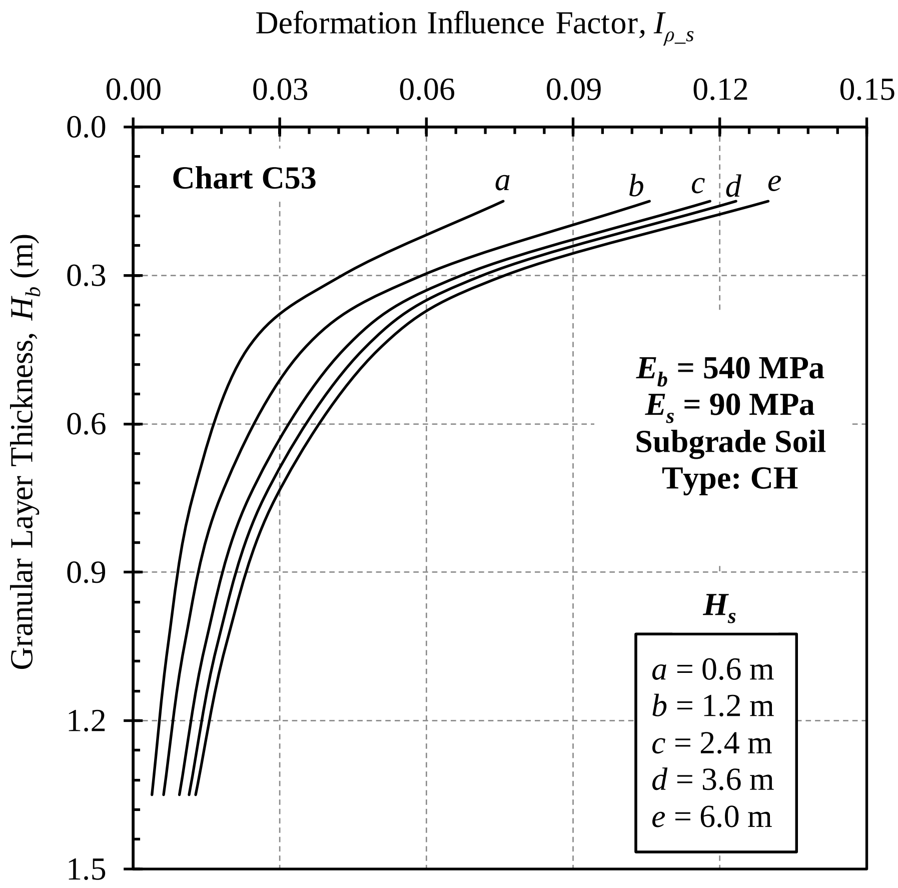
Deformation Influence Factor, I_{ρ_s}
0.00
0.03
0.06
0.09
0.12
0.15
0.0
0.3
0.6
0.9
1.2
1.5
Granular Layer Thickness, H_b (m)
Chart C53
a
b
c
d
e
E_b = 540 MPa
E_s = 90 MPa
Subgrade Soil
Type: CH
H_s
a = 0.6 m
b = 1.2 m
c = 2.4 m
d = 3.6 m
e = 6.0 m

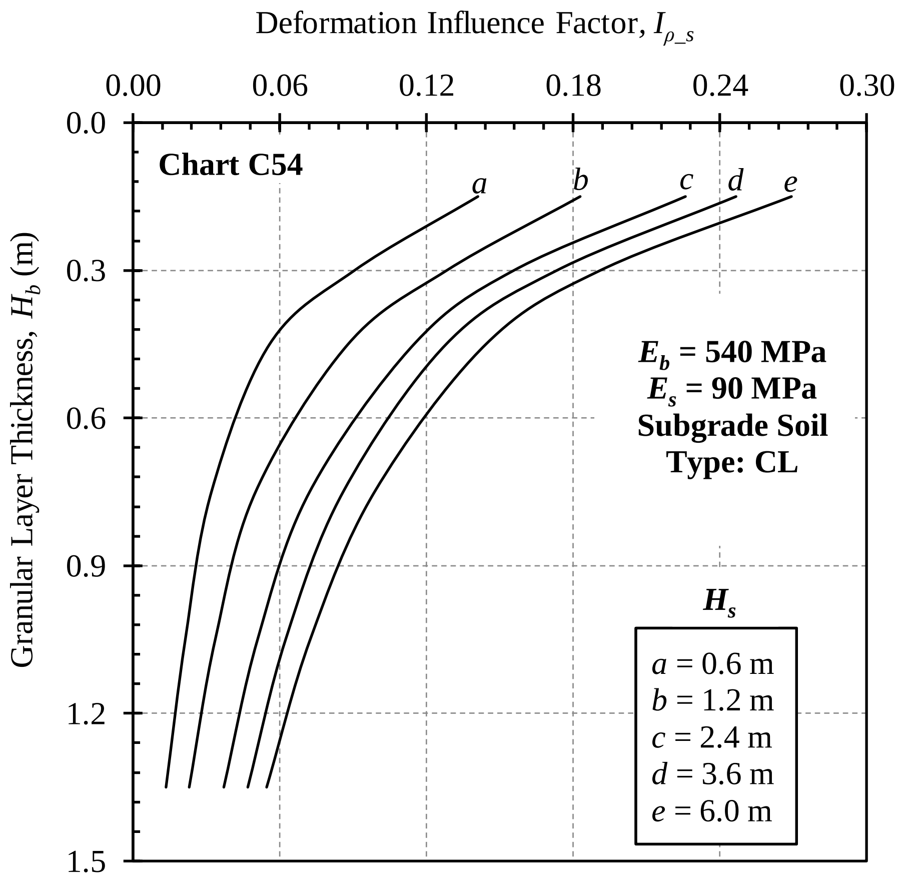
Deformation Influence Factor, I_{ρ_s}
0.00
0.06
0.12
0.18
0.24
0.30
0.0
0.3
0.6
0.9
1.2
1.5
Granular Layer Thickness, H_b (m)
Chart C54
a
b
c
d
e
E_b = 540 MPa
E_s = 90 MPa
Subgrade Soil
Type: CL
H_s
a = 0.6 m
b = 1.2 m
c = 2.4 m
d = 3.6 m
e = 6.0 m

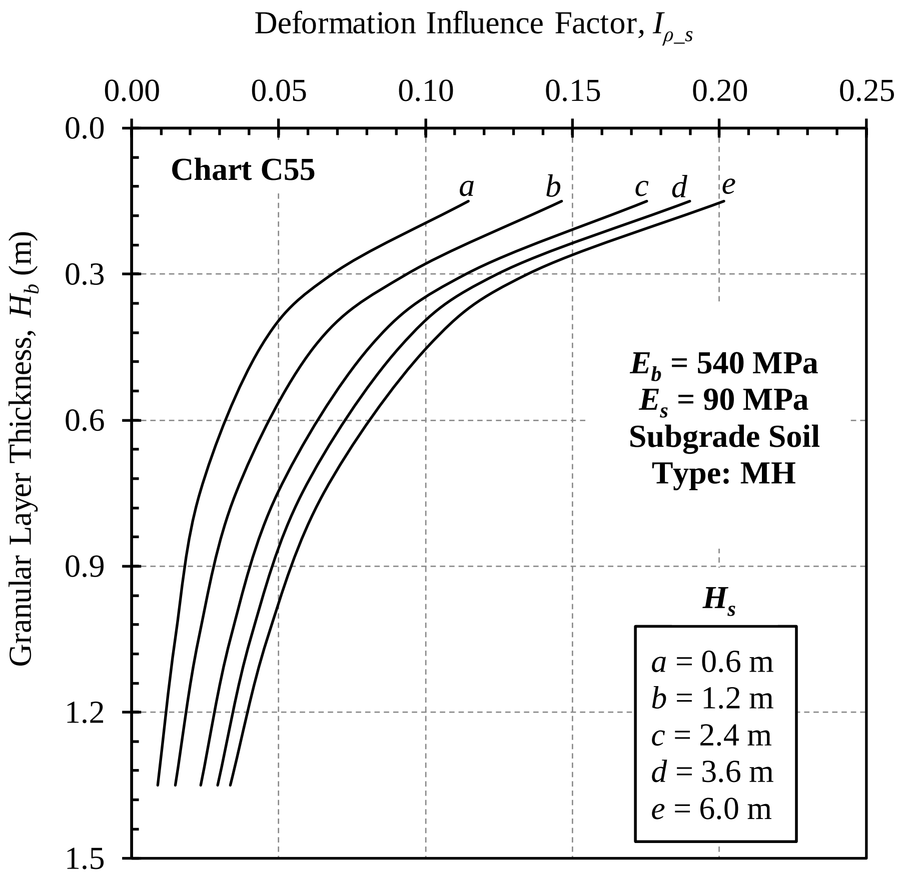
Deformation Influence Factor, I_{ρ_s}
0.00
0.05
0.10
0.15
0.20
0.25
0.0
0.3
0.6
0.9
1.2
1.5
Granular Layer Thickness, H_b (m)
Chart C55
a
b
c
d
e
E_b = 540 MPa
E_s = 90 MPa
Subgrade Soil
Type: MH
H_s
a = 0.6 m
b = 1.2 m
c = 2.4 m
d = 3.6 m
e = 6.0 m

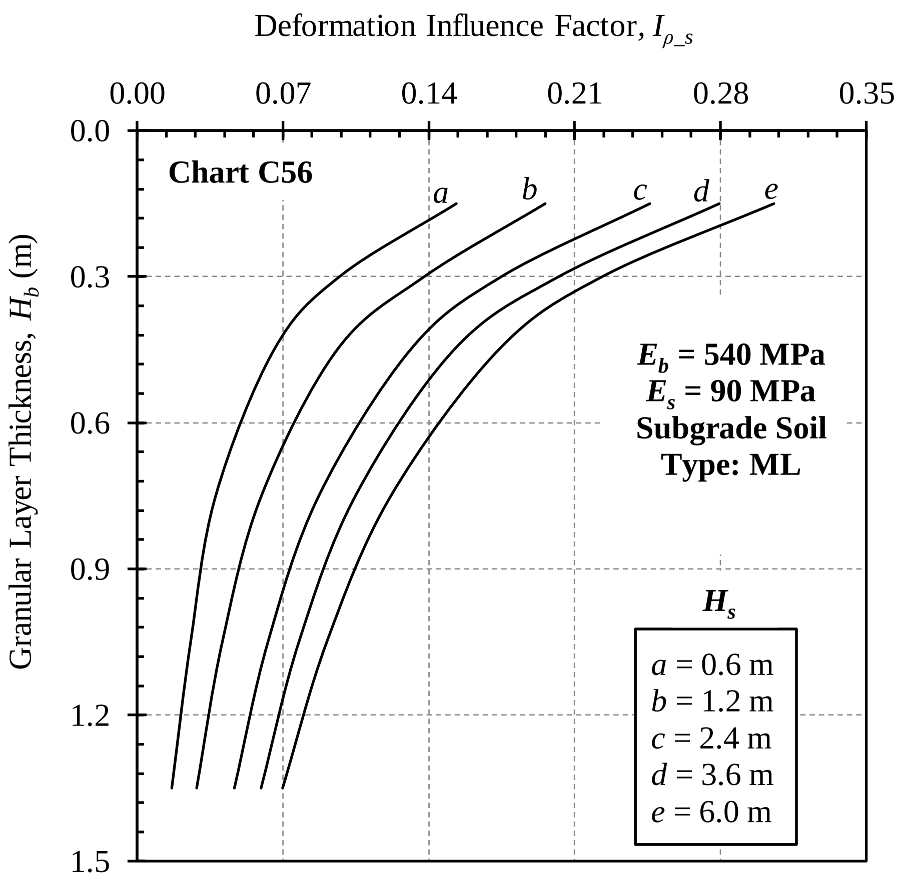
Deformation Influence Factor, I_{ρ_s}
0.00
0.07
0.14
0.21
0.28
0.35
0.0
0.3
0.6
0.9
1.2
1.5
Granular Layer Thickness, H_b (m)
Chart C56
a
b
c
d
e
E_b = 540 MPa
E_s = 90 MPa
Subgrade Soil
Type: ML
H_s
a = 0.6 m
b = 1.2 m
c = 2.4 m
d = 3.6 m
e = 6.0 m

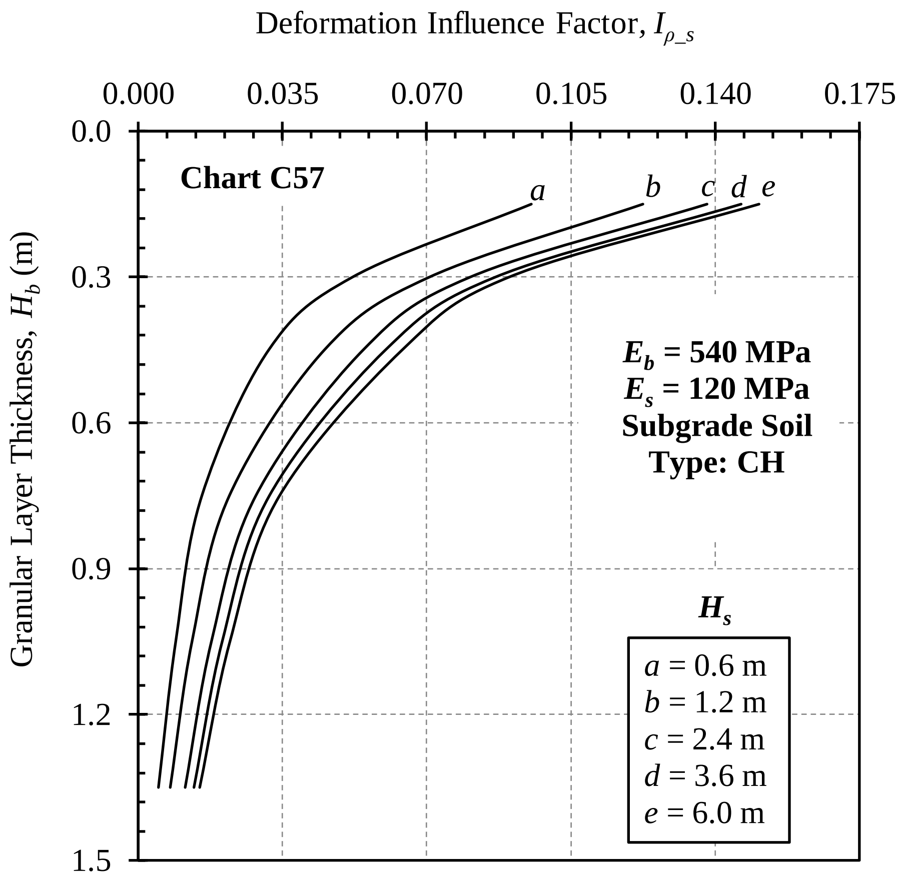
Deformation Influence Factor, I_{ρ_s}
0.000
0.035
0.070
0.105
0.140
0.175
0.0
0.3
0.6
0.9
1.2
1.5
Granular Layer Thickness, H_b (m)
Chart C57
a
b
c
d
e
E_b = 540 MPa
E_s = 120 MPa
Subgrade Soil
Type: CH
H_s
a = 0.6 m
b = 1.2 m
c = 2.4 m
d = 3.6 m
e = 6.0 m

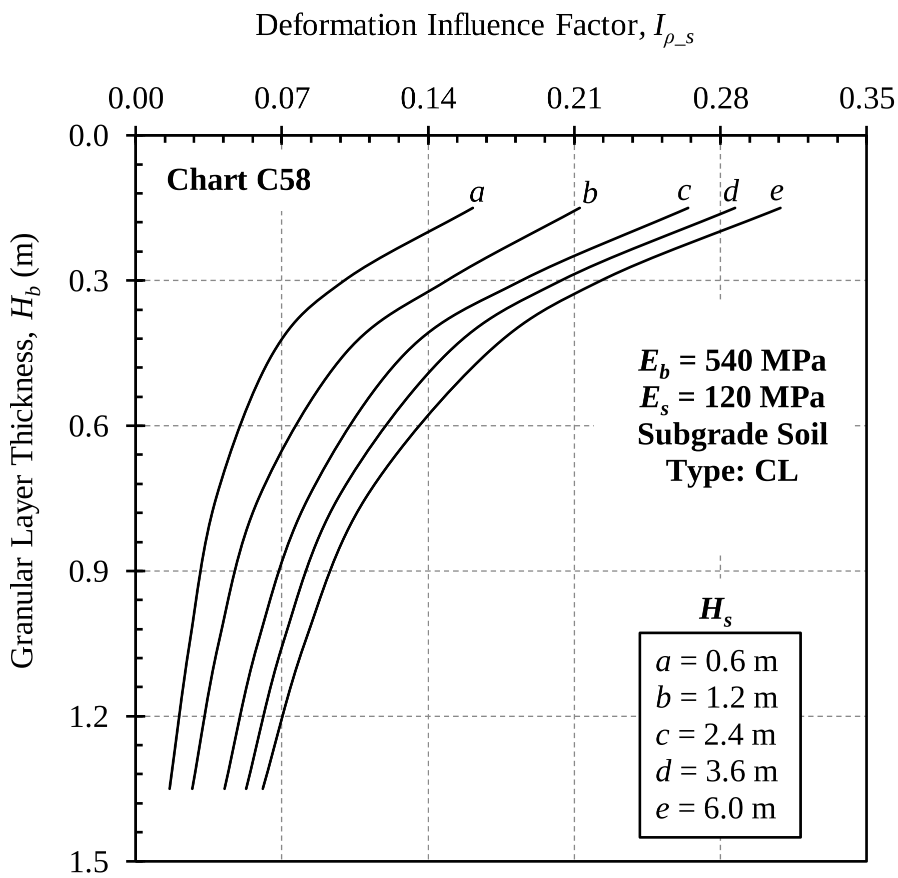
Deformation Influence Factor, I_{ρ_s}
0.00
0.07
0.14
0.21
0.28
0.35
0.0
0.3
0.6
0.9
1.2
1.5
Granular Layer Thickness, H_b (m)
Chart C58
a
b
c
d
e
E_b = 540 MPa
E_s = 120 MPa
Subgrade Soil
Type: CL
H_s
a = 0.6 m
b = 1.2 m
c = 2.4 m
d = 3.6 m
e = 6.0 m

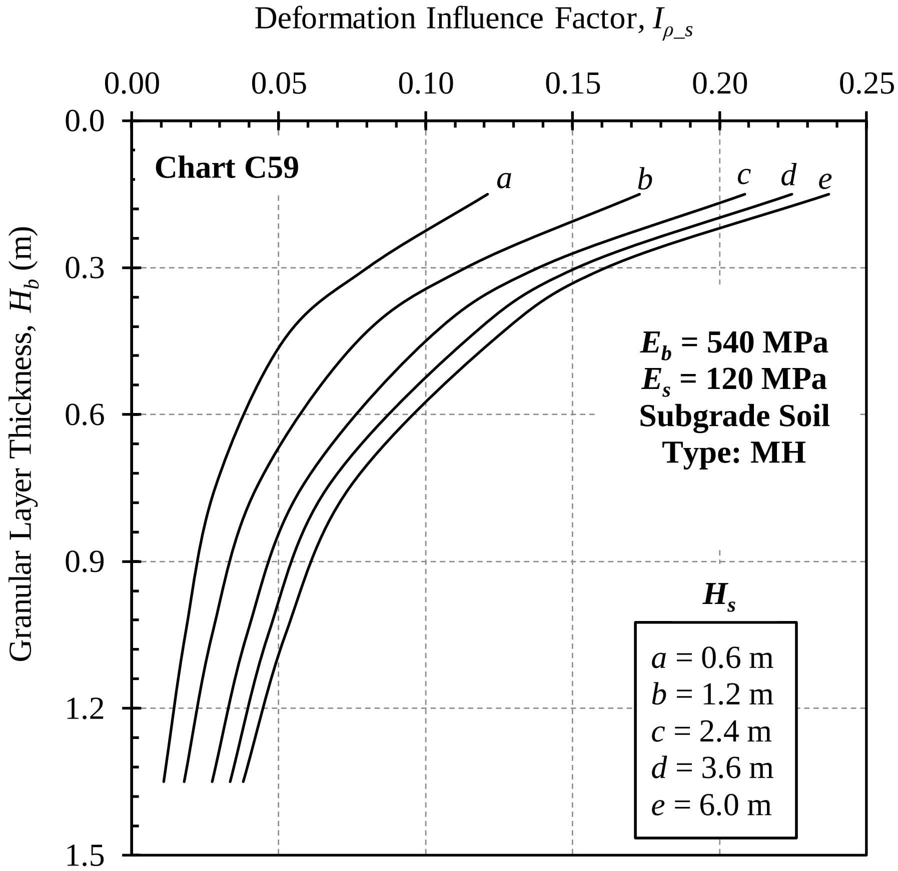

Deformation Influence Factor, I_{ρ_s}
0.00
0.05
0.10
0.15
0.20
0.25
0.0
0.3
0.6
0.9
1.2
1.5
Granular Layer Thickness, H_b (m)
Chart C59
a
b
c
d
e
E_b = 540 MPa
E_s = 120 MPa
Subgrade Soil
Type: MH
H_s
a = 0.6 m
b = 1.2 m
c = 2.4 m
d = 3.6 m
e = 6.0 m

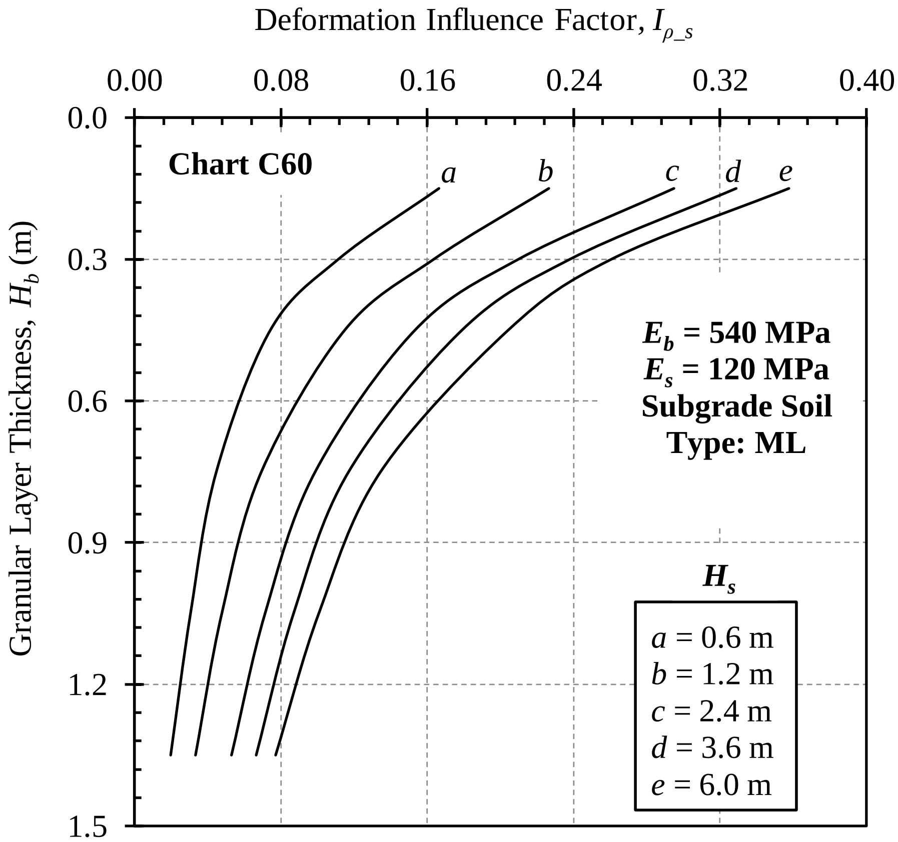

Deformation Influence Factor, I_{ρ_s}
0.00
0.08
0.16
0.24
0.32
0.40
0.0
0.3
0.6
0.9
1.2
1.5
Granular Layer Thickness, H_b (m)
Chart C60
a
b
c
d
e
E_b = 540 MPa
E_s = 120 MPa
Subgrade Soil
Type: ML
H_s
a = 0.6 m
b = 1.2 m
c = 2.4 m
d = 3.6 m
e = 6.0 m